

FIELD RELATIONS AND PETROLOGY OF THE RAINBOW RANGE  
SHIELD VOLCANO, WEST-CENTRAL BRITISH COLUMBIA

by

MARY LOU BEVIER

B.S. (Hons.), University of California, Santa Cruz, 1975

A THESIS SUBMITTED IN PARTIAL FULFILLMENT OF  
THE REQUIREMENTS FOR THE DEGREE OF  
MASTER OF SCIENCE

in

THE FACULTY OF GRADUATE STUDIES  
Department of Geological Sciences

We accept this thesis as conforming  
to the required standard

THE UNIVERSITY OF BRITISH COLUMBIA

April, 1978

In presenting this thesis in partial fulfilment of the requirements for an advanced degree at the University of British Columbia, I agree that the Library shall make it freely available for reference and study.

I further agree that permission for extensive copying of this thesis for scholarly purposes may be granted by the Head of my Department or by his representatives. It is understood that copying or publication of this thesis for financial gain shall not be allowed without my written permission.

Department of Geological Sciences

The University of British Columbia  
2075 Wesbrook Place  
Vancouver, Canada  
V6T 1W5

Date 28 April 1978

FIELD RELATIONS AND PETROLOGY OF THE RAINBOW RANGE SHIELD VOLCANO,  
WEST-CENTRAL BRITISH COLUMBIA

ABSTRACT

The Rainbow Range is a Late Miocene shield volcano (30 km diameter, 370 km<sup>3</sup>) whose stratiform flanks surround a complex central vent zone. Over a time span of 1-2 m.y., extrusion of highly fluid comendites and comenditic trachytes, along with minor mugearites and hawaiites, built up the gently sloping flanks. The viscosity of the peralkaline lavas was so low that their eruption produced a shield volcano rather than a composite cone.

Comenditic trachytes (65.5 percent SiO<sub>2</sub>) are the lowest flows exposed on the north flank of the Rainbow Range. Chemical traits include high Na<sub>2</sub>O + K<sub>2</sub>O (11 percent), moderately high Al<sub>2</sub>O<sub>3</sub> (15 percent), low total iron as Fe<sub>2</sub>O<sub>3</sub> (5 percent), and high Ba (300-1000 ppm). Thin flows of mugearite (54.9 percent SiO<sub>2</sub>) rest on the comenditic trachytes. Comendites (68.7 percent SiO<sub>2</sub>) unconformably overlie the mugearites and account for at least 75 percent of the volume of flows within the flank zone. These lavas are distinguished by lower Al<sub>2</sub>O<sub>3</sub> (13 percent), higher total iron as Fe<sub>2</sub>O<sub>3</sub> (7 percent), and extremely depleted Sr (1-10 ppm) and Ba (10-100 ppm). The termination of flank volcanic activity is recorded by the eruption of capping flows and related feeder dikes of hawaiite (50.1 percent SiO<sub>2</sub>).

Comenditic trachytes contain phenocrysts of anorthoclase (Or<sub>25-27</sub>), hedenbergite, and iron-titanium oxides in a groundmass of alkali feldspar, quartz, acmite, iron-titanium oxides, aenigmatite, and arfvedsonite. Comendites bear the phenocryst assemblage sanidine (Or<sub>34-37</sub>) + hedenbergite ± fayalite ± arfvedsonite set in a pilotaxitic groundmass of alkali feldspar, quartz, acmite, iron-titanium oxides, aenigmatite, and arfvedsonite.

Continuous variation in major and trace element trends and feldspar compositions suggests that the hawaiite-mugearite-comenditic trachyte-comendite suite was derived from an alkali basalt parent, tapped several times as it underwent prolonged fractional crystallization in an intracrustal magma chamber. A best-fit mathematical model for the origin of the suite involves step-wise derivation of the lavas in the order hawaiite → mugearite → comenditic trachyte → comendite, with the main phases precipitating out in the order olivine, clinopyroxene, plagioclase, iron-titanium oxide, and alkali feldspar. Strontium isotopic evidence indicates that the peralkaline lavas were erupted soon after differentiation.

The Rainbow Range and other peralkaline and alkaline volcanic centers of the Anahim volcanic belt are coeval with calc-alkaline volcanic centers of the Pemberton volcanic belt. Together these belts outline the orientation and extent of the subducted Juan de Fuca plate during Late Miocene time. Volcanic activity in the Anahim belt may be related to a) an "edge effect" of the subducted Juan de Fuca plate, b) movement of the North American plate over a mantle hot spot at a rate of 2-3 cm/year, or c) an east-west trending rift zone.

TABLE OF CONTENTS

	<u>Page</u>
ABSTRACT.....	ii
LIST OF TABLES.....	vii
LIST OF FIGURES AND PLATES.....	viii
ACKNOWLEDGEMENTS.....	x
INTRODUCTION.....	1
Location and Access.....	1
Purpose.....	1
Present Investigation.....	3
Previous Work.....	3
REGIONAL SETTING.....	4
Geology.....	4
Late Miocene Tectonic Setting of West-Central British Columbia.....	6
FIELD RELATIONS.....	8
North Flank of the Rainbow Range.....	9
Structure.....	9
Stratigraphy.....	9
Comenditic Trachyte Unit.....	9
Mugearite Unit.....	11
Comendite Unit.....	13
Hawaiite Unit.....	14

TABLE OF CONTENTS (Continued)

	<u>Page</u>
Anahim Peak.....	16
Structure.....	16
Stratigraphy.....	17
Flows.....	17
Plug Dome.....	18
Age of Volcanism.....	18
PETROGRAPHY.....	19
Hawaiite.....	19
Mugearite.....	20
Comenditic Trachyte.....	20
Comendite.....	22
Trachyte.....	23
MINERAL CHEMISTRY.....	23
Introduction.....	23
Methods.....	24
Olivine.....	24
Pyroxene Phenocrysts.....	26
Groundmass Pyroxene.....	28
Amphibole.....	30
Aenigmatite.....	31
Feldspar.....	32
Iron-Titanium Oxides.....	36
Other Accessory Minerals.....	37
WHOLE ROCK CHEMISTRY.....	40
Introduction.....	40

TABLE OF CONTENTS (Continued)

	<u>Page</u>
Normative Mineralogy.....	40
Rock Classification.....	41
Compositional Changes in Silicic Peralkaline Rocks as a Result of Post-Eruptive Processes.....	44
Chemical Variation Between Flows.....	45
Major Element Oxides.....	45
Trace Elements.....	47
Strontium Isotopic Data.....	50
MORPHOLOGY OF THE RAINBOW RANGE SHIELD VOLCANO.....	53
ORIGIN OF OVERSATURATED PERALKALINE ROCKS.....	55
ORIGIN OF LAVAS FROM THE RAINBOW RANGE AND ANAHIM PEAK.....	58
ORIGIN OF THE ANAHIM VOLCANIC BELT.....	61
CONCLUSIONS.....	65
Eruptive History of the Rainbow Range Shield Volcano.....	65
Origin of Rainbow Range Lavas and the Anahim Volcanic Belt.....	66
TABLES.....	68
REFERENCES.....	93

LIST OF TABLES

<u>Table</u>	<u>Page</u>
I. Potassium-argon analytical data for volcanic rocks from the Rainbow Range.....	68
II. Mineral assemblages of volcanic rocks from the Rainbow Range.....	69
III. Microprobe analyses of olivine phenocrysts.....	70
IV. Microprobe analyses of pyroxene phenocrysts and groundmass grains.....	71
V. Microprobe analyses of amphibole grains.....	73
VI. Microprobe analyses of aenigmatite.....	74
VII. Microprobe analyses of feldspar phenocrysts.....	75
VIII. Microprobe analyses of titanomagnetite.....	78
IX. Microprobe analyses of ilmenite.....	79
X. Whole rock major- and trace-element analyses and normative mineralogies.....	80
XI. Strontium isotopic data.....	84
XII. Calculated and observed viscosities.....	85
XIII. Least-squares mass balance calculation deriving mugearite from hawaiite.....	86
XIV. Least-squares mass balance calculation deriving comenditic trachyte from hawaiite.....	87
XV. Least-squares mass balance calculation deriving comendite from hawaiite.....	88
XVI. Least-squares mass balance calculation deriving comenditic trachyte from mugearite.....	89
XVII. Least-squares mass balance calculation deriving comendite from mugearite.....	90
XVIII. Least-squares mass balance calculation deriving comendite from comenditic trachyte.....	91
XIX. Least-squares mass balance calculation deriving Anahim Peak trachyte from Anahim Peak hawaiite.....	92

LIST OF FIGURES AND PLATES

<u>Figure</u>	<u>Page</u>
1. Location map.....	2
2. Generalized geologic map of the western part of the Anahim volcanic belt.....	5
3. Present day plate tectonic setting of southwestern British Columbia.....	7
4. Schematic stratigraphic section of volcanic rocks from the north flank of the Rainbow Range.....	10
5. Mugearite flows.....	12
6. Comendite flows.....	12
7. Hawaiite plugs near Tsitsutl Peak.....	15
8. Anahim Peak.....	15
9. Photomicrograph of anorthoclase in comenditic trachyte.....	21
10. Photomicrograph of phenocrysts phases in comendite.....	21
11. Triangular diagram for olivine showing Mn enrichment.....	25
12. Pyroxene phenocrysts plotted on the pyroxene quadrilateral.....	27
13. Triangular diagram showing acmite, diopside, and hedenbergite components of pyroxene phenocrysts and groundmass grains.....	29
14. Triangular diagram showing anorthite, albite, and orthoclase components of feldspar phenocrysts.....	33
15. Liquidus diagram for the system Q-Ab-Or plus different percentages of additional acmite and nosean.....	35
16. Compositions of titanomagnetites and ilmenites in molecular percent of FeO, Fe <sub>2</sub> O <sub>3</sub> , and TiO <sub>2</sub> .....	38
17. Log f <sub>O<sub>2</sub></sub> -T diagram in which are plotted coexisting iron-titanium oxide pairs from Rainbow Range lavas (using curves of Buddington and Lindsley, 1964).....	39
18. Classification schemes for oversaturated, peralkaline rocks.....	43

LIST OF FIGURES AND PLATES (Continued)

<u>Figure</u>	<u>Page</u>
19. Major element Harker diagrams for volcanic rocks from the north flank of the Rainbow Range.....	46
20. Trace element Harker diagrams for volcanic rocks from the north flank of the Rainbow Range.....	48
21. Trace element ratio Harker diagrams for volcanic rocks from the north flank of the Rainbow Range.....	49
22. $Sr^{87}/Sr^{86}$ versus $Rb^{87}/Sr^{86}$ isochron plot.....	52
23. Late Cenozoic volcanic belts of the Canadian Cordillera.....	62

Plate

- I. Geology of the North Flank of the Rainbow Range and Anahim Peak, British Columbia....(in back pocket)
- II. Map of Sample Localities.....(in back pocket)

ACKNOWLEDGEMENTS

I wish to thank Dr. Jack G. Souther of the Geological Survey of Canada for suggesting the project, and providing helicopter support during the fieldwork. I am grateful to Drs. Richard L. Armstrong and Jack G. Souther for helpful discussions, suggestions, and comments on the improvement of the final manuscript. In addition, I benefited greatly from discussions with other faculty members and graduate students of the Department of Geological Sciences at the University of British Columbia. Krista Scott was of invaluable assistance with strontium isotopic measurements, and I thank Joe Harakal for running the argon analyses. Brian Apland of the Department of Archaeology, Simon Fraser University, was of great help with the fieldwork and enlightened the author as to the archaeological significance of the Rainbow Range. My thanks go out to the many people we met in Anahim Lake and Bella Coola (especially Darcy Christiansen, Cam Moxon, Bob Cohen, Frances Wilmeth, Darryl Hodson, Hank Veelbehr, and Odd Knutsen) who unselfishly provided lodging and shared their knowledge on local terrain and folklore.

National Research Council of Canada Grant 67-8841 to Dr. R. L. Armstrong provided funding for the project.

## INTRODUCTION

### Location and Access

The Rainbow Range shield volcano lies in the southern part of Tweedsmuir Provincial Park (Figure 1), along the boundary between the Coast Mountains and the Interior Plateau in west-central British Columbia.

A good gravel road (Highway 20) that runs between Bella Coola and Anahim Lake comes within 20 km of the field area, but no adequate access for personnel and gear exists beyond this point. Helicopters provide the easiest means of entering the area. Transwest Airways maintains a small helicopter in Bella Coola during the summer months.

### Purpose

This project was undertaken as a combined field and laboratory study of the Late Miocene volcanic rocks of the Rainbow Range. Specific objectives were:

- 1) to map in detail the rock units comprising the north flank of the Rainbow Range shield volcano and work out the structure and eruptive history of the volcano,
- 2) to characterize the mineralogy and chemical composition of lavas from the Rainbow Range,
- 3) to determine the genetic relations between the lavas, and
- 4) to establish the connection, if any, between volcanism and plate tectonic setting.

The field work was conducted in collaboration with Brian Apland, a graduate student in Archaeology at Simon Fraser University, who was investigating,

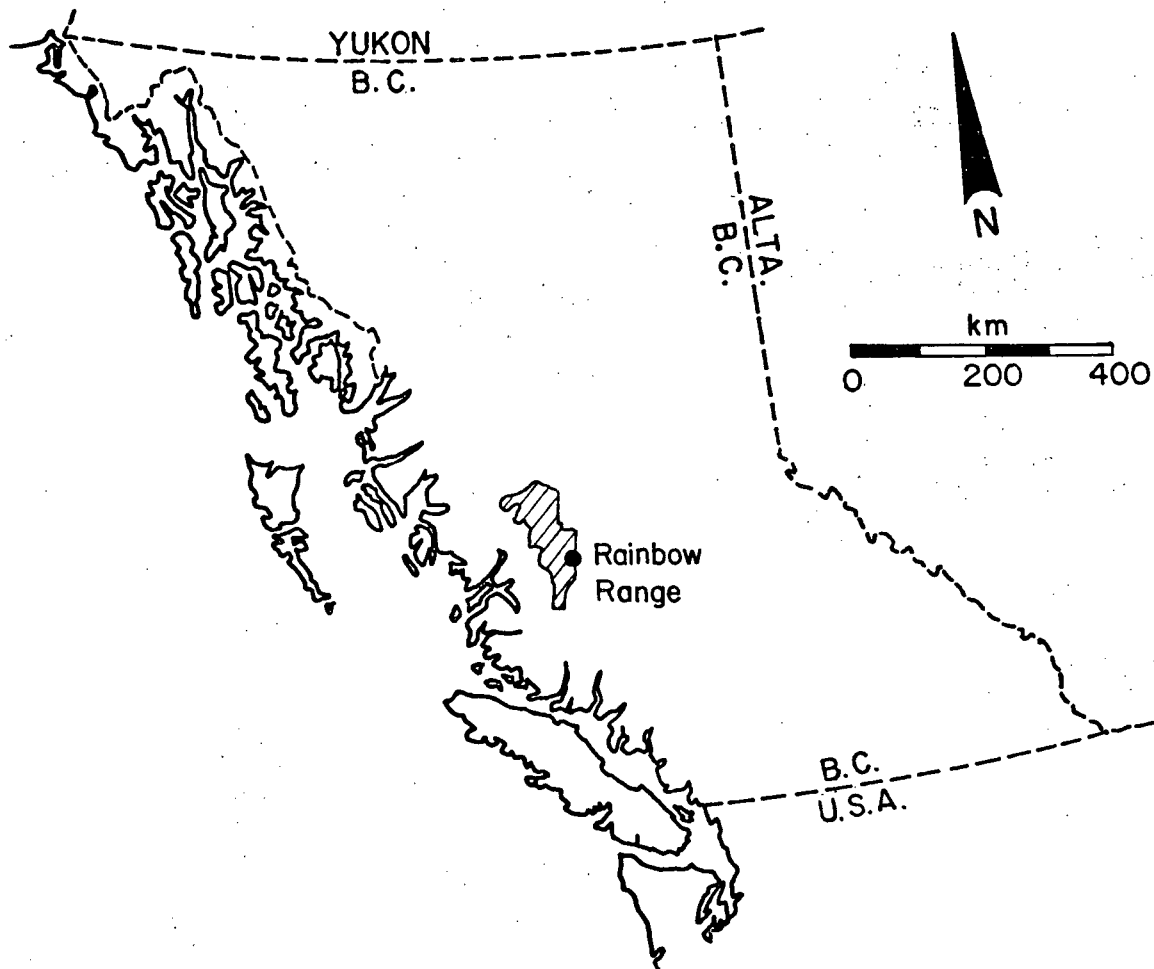


Figure 1. Map of British Columbia showing location of the Rainbow Range. Lined area is Tweedsmuir Provincial Park.

under contract to the National Museum of Canada, the nature and extent of obsidian sources in the region, as well as obtaining samples of source material used by prehistoric peoples (Apland, in press).

### Present Investigation

Field work was carried out during part of July and August, 1976. Four and one-half weeks were spent mapping flows exposed on the northern flank of the shield volcano on 1:50,000 scale National Topographic Map Series Maps (No. 93C/12 (Tusulko River) and No. 93C/13 (Ulkatcho)).

Laboratory work was done at the University of British Columbia. Whole-rock chemical analyses of major-element oxides and selected trace elements were obtained by X-ray fluorescence spectrometry, and mineral chemistry was determined by electron microprobe analysis. K-Ar dates and Sr isotopic ratios were determined by a combination of atomic absorption spectroscopy, X-ray fluorescence spectrometry, and mass spectrometry.

### Previous Work

Volcanic rocks of the Rainbow Range were first studied by H. W. Tipper (1969) of the Geological Survey of Canada as he mapped the (1<sup>0</sup> x 2<sup>0</sup>) Anahim Lake sheet at a scale of 1" = 4 miles. Descriptive notes published with the map state that the central part of the Rainbow Range is composed of vari-colored andesitic to dacitic flows and fragmental rocks, while the outer conical flanks are composed of later eruptions of basalt flows which flatten and merge with late Tertiary plateau lavas. Anahim Peak, a small isolated mountain on the northeast flank of the Rainbow Range, is described as a basaltic neck surrounded by flat-lying flows.

## REGIONAL SETTING

### Geology

Late Miocene volcanic rocks that make up the Rainbow Range are underlain on the west by Jurassic Hazelton Group and on the east by Miocene plateau lavas (Figure 2). The Hazelton Group consists mainly of volcanic breccias, waterlain tuffs, varicolored andesites and basalts, and rare sedimentary rocks derived from the volcanic rocks (Baer, 1973).

South and east of the Rainbow Range lie the extensive ( $>4750 \text{ km}^2$ ) Miocene plateau lavas. These consist of flat-lying basalts and basaltic andesites for which few vent areas are known. South of the Rainbow Range these flows have been upwarped to the west, indicating that the Coast Mountains were still rising after the Miocene (Tipper, 1963). The Rainbow Range is far enough east of the Coast Mountains that it has not been noticeably tilted or deformed.

Peralkaline rocks are also exposed west and east of the Rainbow Range. At Tanya Lakes and Sigutlat Lake, intrusive bodies of syenite ( $10\text{--}50 \text{ km}^2$ ) are exposed in north-east trending grabens. On King Island (100 km farther west), a  $13\pm 2$  m.y. syenite, east-west elongate, pluton is exposed. Numerous aegerine-augite and/or aenigmatite bearing dikes, along with small syenite bodies, and basaltic dikes, occur on islands west of King Island. Baer (1973) reports K-Ar age determinations of 14.5 and 12.5 m.y. for two of these dikes.

Two other large, peralkaline shield volcanoes (Ilgachuz Range and Itcha Range) lie east of the Rainbow Range. No detailed mapping has been done in the Ilgachuz Range; however, geomorphological evidence suggests that it is equivalent in age and composition to the Rainbow Range. K-Ar dates from

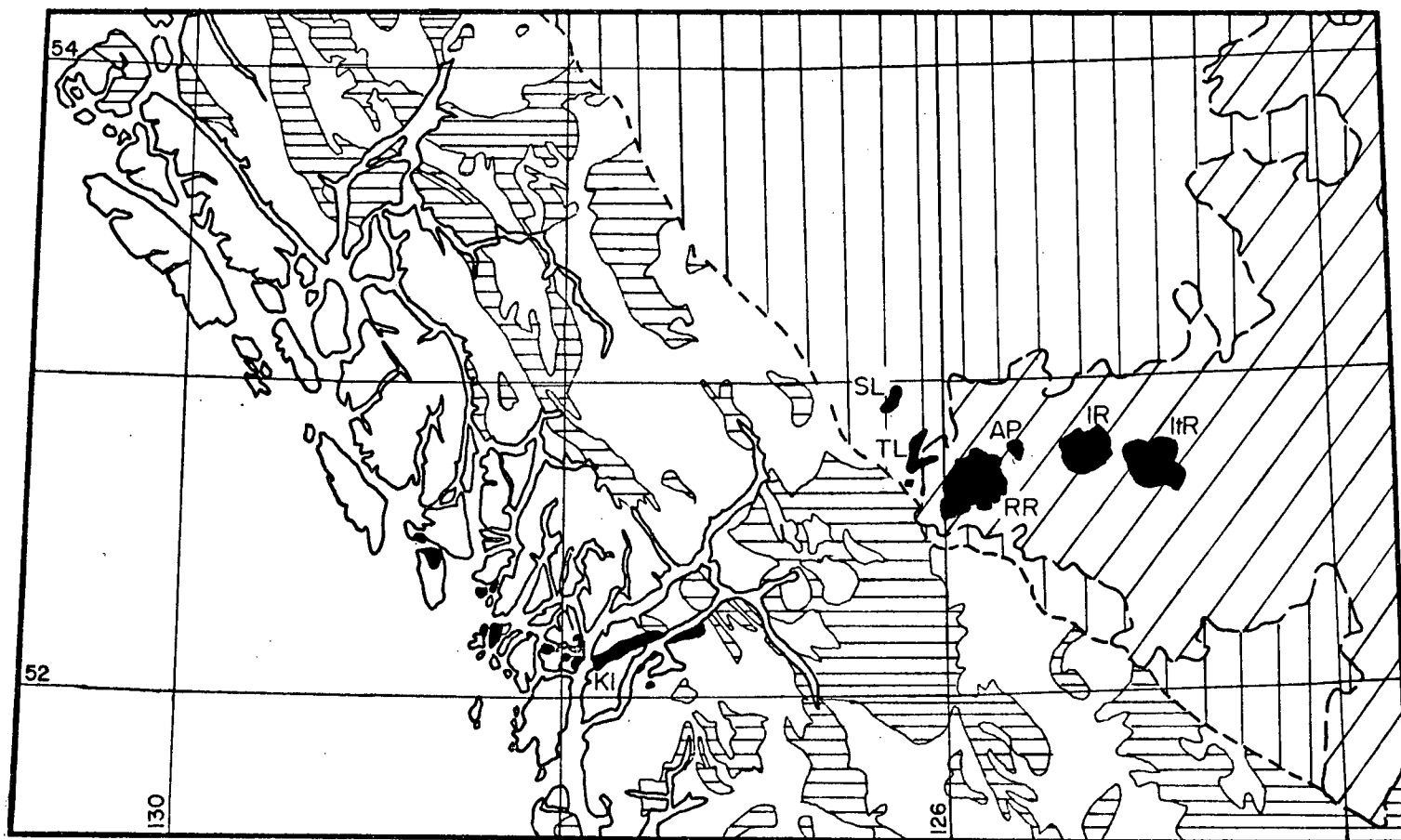


Figure 2. Generalized geologic map of the western part of the Anahim volcanic belt, showing distribution of Miocene-Quaternary volcanic centers (black), Coast Mountain plutonic rocks (uncolored), Mesozoic supracrustals (horizontal bars), Jurassic sedimentary rocks (vertical bars), and Miocene plateau lavas (diagonal bars). KI- King Island, RR- Rainbow Range, AP- Anahim Peak, IR- Ilgachuz Range, ItR- Itcha Range, TL- Tanya Lakes, SL- Sigutlat Lake.

the central part of the Itcha Range range from 3.2 to 0.78 m.y. (J.E. Hara-  
kal, unpublished determinations). The central part of the Itcha Range con-  
sists of flows, domes, breccias and tuff breccias, plugs, and shallow  
intrusions of alkaline and peralkaline phonolites, trachytes, trachyande-  
sites, and minor rhyolite, which have been strongly dissected by glacial  
erosion.(B. Proffett, personal communication, 1978). Cinder cones and flows  
of trachybasalt and basanite cap the differentiated volcanic suite.(Nicholls  
et. al., 1976). The basanites contain lherzolite nodules whereas the  
trachybasalts contain large plagioclase xenocrysts.

These three shield volcanoes, along with many isolated cinder cones  
and small flows, define a belt of Late Miocene-Quaternary volcanic centers  
known as the Anahim volcanic belt.(Souther, 1977) that runs east-west across  
British Columbia at approximately latitude  $52^{\circ}N$ . Glaciation has partially  
modified the form of all these volcanic centers.

Few documented faults are associated with these volcanic centers. Tipper  
(1969) mentions east-west faults in the Ilgachuz and Itcha Ranges and depicts  
northwest-trending faults in the southwestern quadrant of the Rainbow Range,

#### Late Miocene Tectonic Setting of West-Central British Columbia

During Late Miocene time, plate geometry off the coast of British  
Columbia was similar to the present configuration (Figure 3); however, some  
doubt exists as to the exact subdivisions between the Pacific, North American,  
and Juan de Fuca plates and position of the triple junction at that time. Re-  
views of the plate geometry of southwestern British Columbia have been given  
by Barr and Chase (1974), Chase, Tiffin, and Murray (1976), Riddihough and  
Hyndman (1976), and Riddihough (1977).

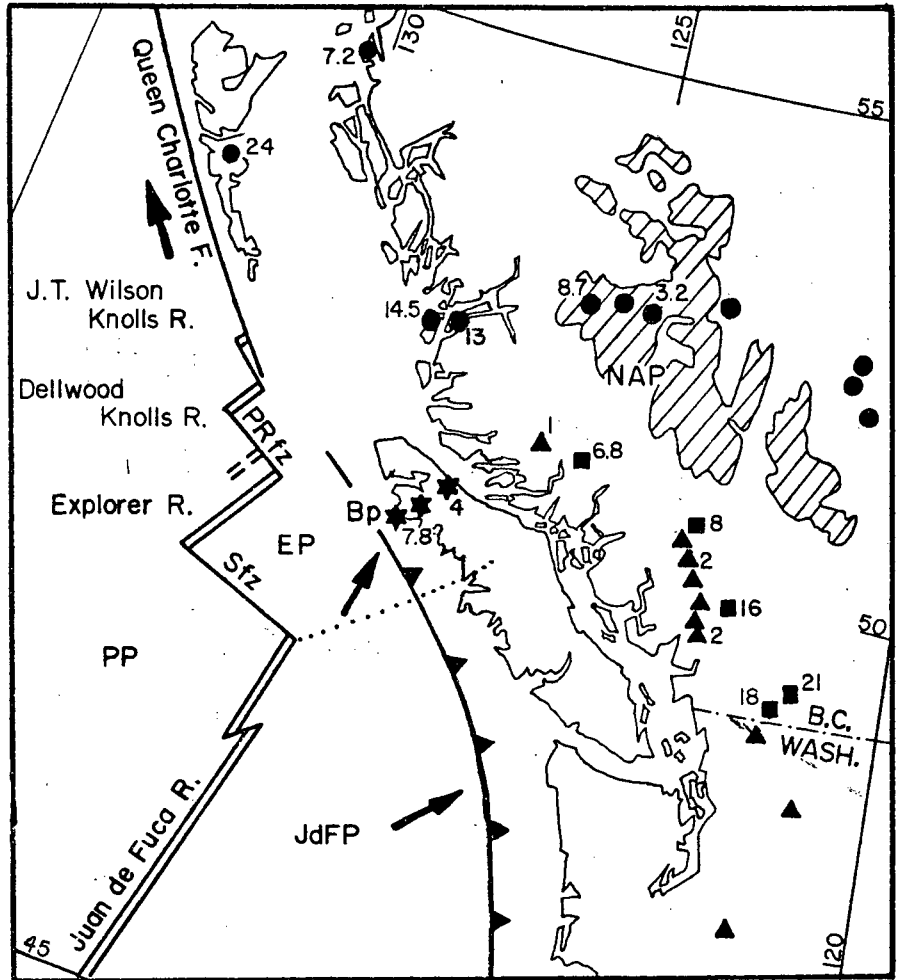


Figure 3. Present plate tectonic setting of southwestern British Columbia, showing extent of Anahim volcanic belt (circles), Pemberton volcanic belt (squares), Alert Bay volcanic belt (stars), Garibaldi volcanic belt (triangles), and K-Ar ages in m.y. Lined area is the extent of Miocene plateau lavas (Souther, 1977). PP- Pacific plate, EP- Explorer plate, NAP- North America plate, JdFP- Juan de Fuca plate, Bp- Brooks Peninsula, PRfz- Paul Revere fracture zone, Sfz- Sovanco fracture zone. Dashed line is possible EP-JdFP boundary (R. Hyndman, oral communication, 1978). Diagram modified from Riddihough and Hyndman (1976).

A right-lateral transform fault (Queen Charlotte fault) separates the Pacific and North American plates, while a subduction zone forms the boundary between the North American and Juan de Fuca plates. The Juan de Fuca-Pacific plate boundary is a spreading ridge system (Barr and Chase, 1974). Subduction of the Juan de Fuca plate beneath the North American plate gives rise to arc and back-arc volcanism. The Anahim volcanic belt lies near the projected trace of the northern edge of the subducted Juan de Fuca plate, the position of which is not well constrained during late Miocene time.

Movement in the position of the active spreading ridge makes magnetic anomaly patterns difficult to interpret, and it is these patterns which are used to determine relative motion between plates, and hence triple junction position. During the last 10 million years the active ridge between the Juan de Fuca and Pacific plates has repeatedly jumped between the Juan de Fuca, Explorer, Dellwood Knolls, and J. Tuzo Wilson Knolls sections (Riddihough and Hyndman, 1976; R. Hyndman, oral communication, 1978). The latest calculations (Riddihough, 1977) place the triple junction off Brooks Peninsula on northwestern Vancouver Island for the period 5 to 10 million years ago.

#### FIELD RELATIONS

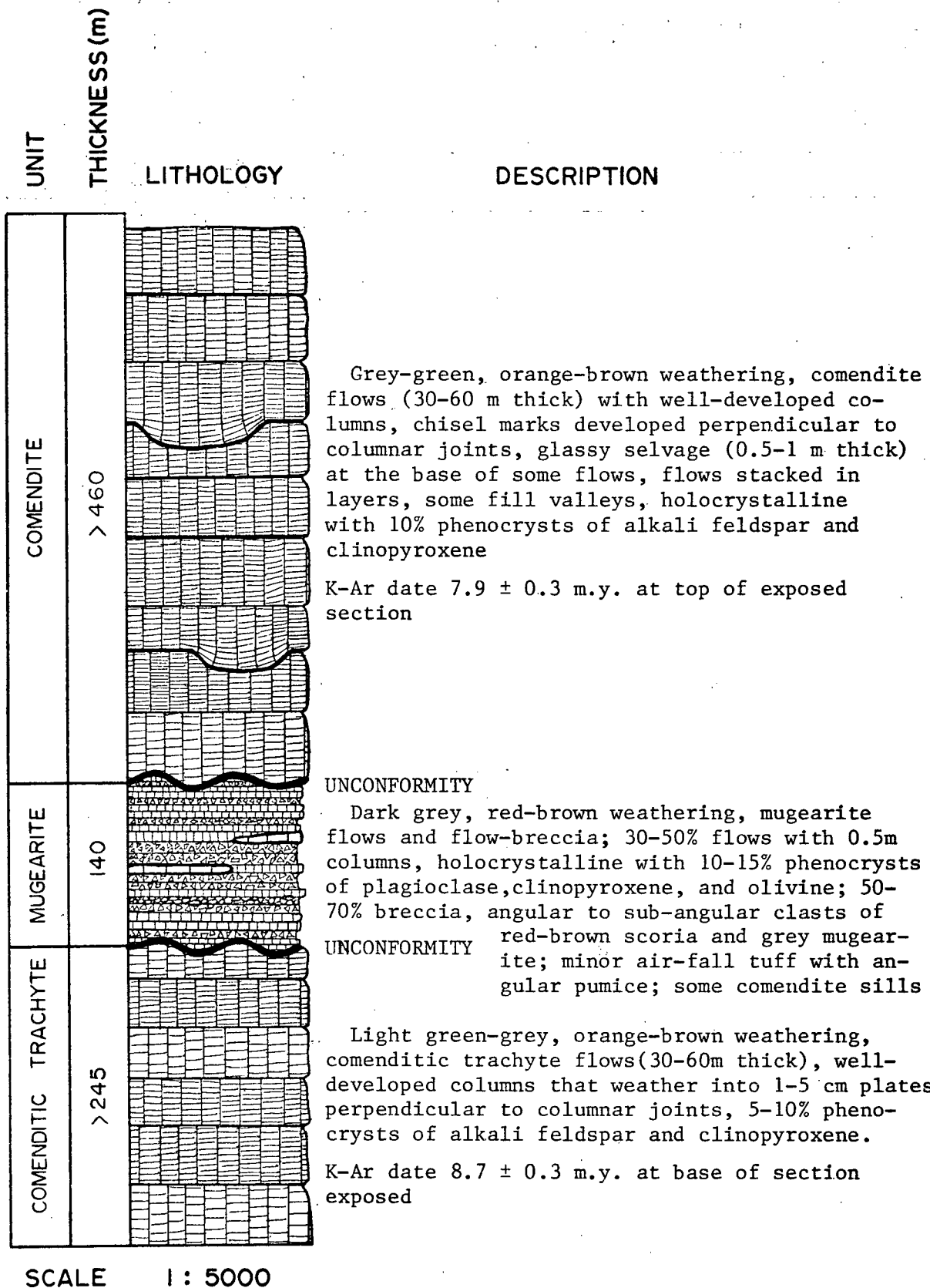
Approximately 30 km<sup>2</sup> of the northern flank of the Rainbow Range shield volcano was mapped in detail (Plate I). This area is dissected by radiating glacial valleys which afford excellent exposure of the internal structure of the volcano, and the terrain is suitable for backpacking. In addition, Anahim Peak, on the northeast flank of the volcano, can be reached on foot.

## North Flank of the Rainbow Range

Structure. The Rainbow Range shield volcano has a diameter of 30 km and volume of approximately 370 km<sup>3</sup>. Over a timespan of approximately 1 to 2 m.y., extrusion of highly fluid lavas built up the flanks of the shield volcano. Individual flows can be traced for up to 3 km. Primary dips range from 5° - 8°. Flow thickness is related to chemical composition: basic rocks form 1 - 4 m thick flows, while silicic flows range from 30 - 60 m thick. The stratiform flank zone surrounds a central complex of small domes, short, thick flows, and small intrusive bodies (Souther, 1977) that was not mapped in this study. No faulting or deformation has occurred on the north flank of the volcano since the cessation of volcanic activity. As with other peralkaline volcanic complexes in British Columbia, the morphology and structure of this volcano are similar to those of trachyte shield volcanoes in the South Turkana region of the Kenya rift valley (Webb and Weaver, 1975).

Stratigraphy. Alkaline and peralkaline lava flows from four volcanic episodes make up the 845 m section exposed on the north flank. They are informally divided into the comenditic trachyte unit, the mugearite unit, the comendite unit, and the hawaiite unit (Figure 4). With the exception of the hawaiite unit, no source vents are found within the map area.

Comenditic Trachyte Unit. Outcrops of the lowest unit exposed, the comenditic trachyte unit, are restricted to the sides of the westernmost valley in the field area. Much of the area of exposure is covered with talus, and individual flows can be traced from as little as 10 m to up to 2 km. A minimum of eight individual flows



SCALE 1 : 5000

Figure 4. Schematic stratigraphic section of volcanic rocks from the north flank of the Rainbow Range.

are present. The base of the >245 m section is not exposed. The unit consists of a sequence of 30 - 60 m thick flows of green-grey comenditic trachyte that display well-developed columnar jointing. Primary dips are  $5^{\circ}$  -  $8^{\circ}$  to the north. Columns are 1 - 2 m in diameter and they weather into thin (1 - 4 cm) plates that form perpendicular to the cooling joints. In many places up to 1 m of breccia is present at the base of each flow. Flows are holocrystalline throughout the unit. Phenocrysts of alkali feldspar (1 - 2 mm) and clinopyroxene (0.5 - 1 mm) make up 10 percent of the rocks.

Mugearite Unit. The second cycle of volcanic activity produced a 140 m thick series of thin (1 - 4 m) mugearite flows and discontinuous lenses of flow breccia that unconformably overlie the thicker comenditic trachyte flows (Figure 5). Dips range from  $15^{\circ}$  -  $25^{\circ}$  to the north. This unit is exposed only along the sides of the westernmost valley in the field area. Flow breccia accounts for up to 70 percent of the section. Individual flows are hard to follow for more than 0.5 km due to the large proportion of discontinuous breccia zones. Some breccia zones are incorporated within flows. All the flows are columnar-jointed. At 64 m above the base of the unit a 2.5 m thick, medium to dark yellow-grey, banded air-fall tuff is present. The layer is not traceable for more than 20 m in any direction; it lenses in and out and is therefore not suitable for use as a marker bed. The tuff is composed of sub-angular pumice fragments that range in size from 0.1 - 10 mm. Slight rounding of the pumice fragments is possibly due to abrasion during and after deposition.

The light to medium-grey mugearite lavas are characterized by their predominantly porphyritic nature. Phenocryst content increases up section from 10 to 25 percent, with plagioclase feldspar (0.5 -



Figure 5. A series of mugearite flows unconformably overlies comenditic trachyte flows in the westernmost part of the field area. Scale - 1 km across the photo



Figure 6. Thick (30-60 m) comendite flows crop out on a ridge northwest of Tsitsutl Peak. Scale - 1 km across the photo.

1 cm) greatly predominant over clinopyroxene (1 - 4 mm). The breccia consists of clasts of red scoria and pahoehoe fragments of mugearite that range in size from 5 - 20 cm.

Comendite Unit. Voluminous eruption of comendite lava flows was the next phase of volcanism on the north flank of the shield volcano (Figure 6). The stratigraphic section is a minimum of 460 m thick. These flows account for 75 percent of the volume of lava exposed within the flank zone. The flows spread out unconformably over the mugearite unit at slopes of  $5^{\circ}$  -  $8^{\circ}$  and build up the shield as it is seen today. Sills of comendite are found within the mugearite unit. The flows are relatively thick (30 - 60 m) compared to basic flows from the volcano. Even so, they were emplaced in a highly fluid condition compared to most silicic flows since individual flows as much as 1 km wide can be traced down a slope of  $5^{\circ}$  for at least 3 km. Forty comendite flows have been mapped on the north flank of the volcano, and more are thought to exist under talus. It is possible that some of the flows may be correlative across valleys, but since they are identical in morphology, mineralogy, and chemical composition, attempts at correlation have been unsuccessful. The maximum measurable section is 460 m thick and consists of approximately thirteen flows. Tsitsutl Peak (2973 m), the highest peak in the Rainbow Range, is at the top of this section. It is unknown how much of the stratigraphy has been stripped off by glaciers, but because the original shield-like shape of the volcano is still preserved, it appears that not much of the section is missing. Some flows as much as 90 m thick fill valleys, but for the most part the flows are stacked in layer-cake fashion. All of the flows show well-developed columnar jointing

(2 - 4 m wide) with chisel marks perpendicular to the jointing. At the base of most flows the contact with the underlying flow is abrupt, little brecciation is present, and a 1 m thick glassy selvage is well-developed. This black vitrophyre bears alkali feldspar and clinopyroxene phenocrysts.

The comendites are green-grey massive lavas, some vesicular in nature, that bear phenocrysts of alkali feldspar (1 - 3 mm) and red weathering clinopyroxene (0.1 - 0.5 mm). Except for lavas at the very base of the section, most comendites also contain sparse phenocrysts of olivine (0.1 - 0.5 mm).

Hawaiite Unit. During the waning stages of volcanic activity, hawaiite lavas erupted from at least five centers scattered across the north flank of the shield volcano. The hawaiites crop out as plugs, dikes, and flows that cap the comendite unit.

On the western slope of Tsitsutl Peak at least seven plugs appear as "hoodoos" or pinnacles (Figure 7). The plugs are spheroidal knobs approximately 20 m in diameter, composed of 1 m wide columns that fan out in all directions. At the base of these plugs are breccias consisting of angular to subangular fragments of hawaiite, comendite, and altered red, green, yellow, and grey volcanic rock fragments. The breccia does not show any bedding and it is poorly sorted, with fragments ranging in size from 0.5 - 500 cm. Underlying comendite lavas are altered for 0.5 km in all directions from these plugs. At two localities, hawaiites crop out as vertical to near vertical dikes traceable laterally for 10 - 20 m. One of these dikes contains vesicles filled with zeolites.

Erosional remnants of capping flows can be seen in two places.



Figure 7. Close-up view of hawaiite plugs that crop out on the west side of Tsitsutl Peak. The large plug on the right is 20 m across.



Figure 8. West side of Anahim Peak (2 km long), showing flat-lying flows and plug dome.

One 10 m thick flow crops out over an area of approximately 1 km<sup>2</sup>. At the base of the flow is a zone of oxidized lava 1 - 3 m in thickness. Columnar jointing is well-developed throughout the flow.

Most hawaiites are porphyritic, containing 15 percent euhedral plagioclase feldspar (0.3 - 1 cm long) and clinopyroxene (1 - 2 mm) phenocrysts in a dark grey aphanitic matrix. At the base of a plug situated one ridge west of Tsitsutl Peak, clots of xenocrystic plagioclase feldspar and orthopyroxene up to 8 cm across are present in the hawaiite.

### Anahim Peak

Structure. Anahim Peak (Plate I) is situated on the flank of the Rainbow Range shield volcano 10 km northeast of Tsitsutl Peak. Total area covered by the peak is slightly more than 2 km<sup>2</sup>.

The vent for the Anahim Peak flows appears to have opened up through a topographic high of older volcanic rocks. Below present tree-line on Anahim Peak, vegetation is dense and only where trees have been uprooted does one see pieces of a white flow-banded "rhyolite" that bears quartz and alkali feldspar phenocrysts. Tipper (1969) mapped this unit as being lithologically identical to the Cretaceous (?) - Tertiary Ootsa Lake Group that lies to the northwest.

Before the first flow erupted from the Anahim Peak vent, a friable volcaniclastic sandstone covered the white rhyolite. The altitude of this sandstone is not known. The contact between these two rock types is not exposed, and in fact it is not known if there are other units present. The presence of broken crystals of sodic hedenbergite (a clinopyroxene characteristic of peralkaline rocks from the Rainbow Range) in the sandstone indicates that erosion of the flanks of the shield volcano was

taking place before Anahim Peak became a center for volcanic activity.

At the beginning of the first eruption, cinders and spatter spewed out and disrupted the top 20 cm of the sandstone near the vent prior to a lava flow spreading out over the area. Subsequent to this flow at least six other flows were erupted from the vent, all preceded by spatter (and minor bombs) thrown from lava fountains. Near the vent, a layer of agglutinate up to 2 m thick is present at the base of most flows.

All the flows are flat-lying and appear to have been constrained in areal extent when erupted. Anahim Peak hawaiites are almost identical in chemical composition to Rainbow Range hawaiites (Table X) yet Anahim Peak flows are four to eight times as thick as Rainbow Range hawaiite flows. Examination of thin sections from the base and upper portion of several Anahim Peak hawaiite flows shows that the lower portions of flows have a significantly coarser-grained groundmass and higher percentage of phenocrysts than the upper portions of flows. These two lines of evidence suggest that the flows were ponded during eruption and cooling, probably as lava lakes within a pyroclastic cone, all trace of which has now been removed by erosion.

The volcanic conduit is plugged by a trachyte dome which brecciated and altered the immediately surrounding lavas.

### Stratigraphy.

Flows. Seven hawaiite flows with an outcrop area of approximately  $1 \text{ km}^2$  each make up the 335 m thick section exposed on Anahim Peak (Figure 8). Flows range in thickness from 30 - 80 m but an average thickness is 45 m. Columnar jointing is well-developed in all the flows. The joint faces commonly have chisel marks

on them. Spheroidal weathering is seen on the sides of some of the columns.

The hawaiites contain phenocrysts of plagioclase feldspar and clinopyroxene, both 0.1 - 0.8 mm long. The rocks are commonly coarser-grained than most basaltic lava flows. This characteristic, along with the fact that the flows are rather thick for basic lavas, suggests that the flows were ponded during cooling.

Plug Dome. The plug dome crops out over an area of about 1/8 km<sup>2</sup>. The plug is a light-grey metaluminous trachyte with sodic plagioclase feldspar and clinopyroxene phenocrysts. Thick, poorly developed columns (4 - 5 m diameter) are present and fan out toward the margins of the plug. Where the plug contacts the surrounding flows, there is a zone of alteration and brecciation. The breccia is yellow and contains angular to sub-angular fragments of massive hawaiite, scoria, white "rhyolite", and rare granite.

#### Age of Volcanism

Four lavas from the north flank of the Rainbow Range and Anahim Peak were dated by the potassium-argon method. Samples include a comenditic trachyte from the westernmost valley in the field area, a comendite from Tsitsutl Peak, a hawaiite from 2.5 km north-east of Tsitsutl Peak, and a hawaiite from Anahim Peak. Location of the samples and their calculated dates are given in Table I. Stratigraphically the comenditic trachyte represents the lowest flow that has been mapped on the north flank of the volcano, while the comendite from Tsitsutl Peak is topographically the highest flow exposed on the north flank. The hawaiite from 2.5 km northeast of Tsitsutl Peak is from a flow that caps the comendite unit. The hawaiite from Anahim Peak is

from the first flow that issued out of the vent.

Calculated K-Ar dates indicate that the Rainbow Range shield volcano was active during Late Miocene time. The hawaiite flows that were extruded from the Anahim Peak vent are younger than the flows on the north flank of the Rainbow Range.

#### PETROGRAPHY

Thin sections of samples from all units exposed on the north flank of the Rainbow Range shield volcano and Anahim Peak were examined. A summary of the mineral assemblages is given in Table II.

#### Hawaiite

Hawaiites from the north flank of the Rainbow Range and from Anahim Peak are petrographically similar. Most samples are highly porphyritic (15 percent phenocrysts) but a few from the shield volcano have only 1 - 2 percent phenocrysts. Plagioclase, pyroxene, and olivine are found as phenocrysts; microphenocrysts of magnetite, ilmenite, apatite, and biotite occur in trace amounts.

Plagioclase ( $An_{59}$ ) is found as fragments of euhedral crystals, some of which exhibit normal zoning. Most crystals are albite twinned but a few crystals have pericline and Carlsbad twins. Commonly the phenocrysts are poikilitic, enclosing small crystals of augite and opaque oxides. Glomeroporphyritic clots occur in most samples. Pink to pale brown phenocrysts of titan-augite have rims of opaque granules and fibrous orthopyroxene (?), showing that they are out of equilibrium with the rock. The clinopyroxene poikilitically encloses magnetite. In some samples (R-36, R-117), xenocrystic orthopyroxene is present as anhedral macrophenocrysts surrounded by a fibrous rim of clinopyroxene. Forsterite occurs as euhedral phenocrysts in the Anahim

Peak hawaiites but only as altered microphenocrysts in the Rainbow Range hawaiites.

The groundmass is a crystalline mosaic of twinned plagioclase laths with intergranular augite and opaque oxides. In some samples (R-36, R-117), the groundmass is hyalopilitic.

#### Mugearite

The mugearites contain 10 - 25 percent phenocrysts (plagioclase, olivine, and clinopyroxene) set in a pilotaxitic or trachytic groundmass of twinned plagioclase and alkali feldspar laths which enclose equant grains of augite and granules of opaque oxides. Plagioclase phenocrysts ( $An_{55}$ ) occur in glomeroporphyritic clots, olivine phenocrysts have been partially to totally altered, and pinkish augite occurs as rare subhedral phenocrysts. Magnetite and ilmenite phenocrysts are very scarce. One sample (R-107) has a trace of quartz in the groundmass.

#### Comenditic Trachyte

In a typical comenditic trachyte, phenocrysts of gridiron and Carlsbad twinned anorthoclase, and hedenbergite compose 5 - 10 percent of the rock, with anorthoclase by far the most abundant phenocryst type (Figure 9). Hedenbergite phenocrysts are weakly pleochroic ( $\alpha$  = green;  $\beta$  = pale green;  $\gamma$  = brownish-yellow). Sparse ilmenite and magnetite grains are also present.

The groundmass consists of sub-parallel laths of alkali feldspar and varying proportions of intergranular acmitic pyroxene, opaque oxide, aenigmatite, arfvedsonite, and quartz. In some samples, acmitic pyroxene occurs as poikilitic grains. Aenigmatite (pleochroic dark-brown to opaque) is found



Figure 9. Photomicrograph of gridiron twinned anorthoclase phenocryst in comenditic trachyte. Groundmass is mainly alkali feldspar laths with ferromagnesian minerals and quartz in the interstices. Scale - 3 mm across the photo.

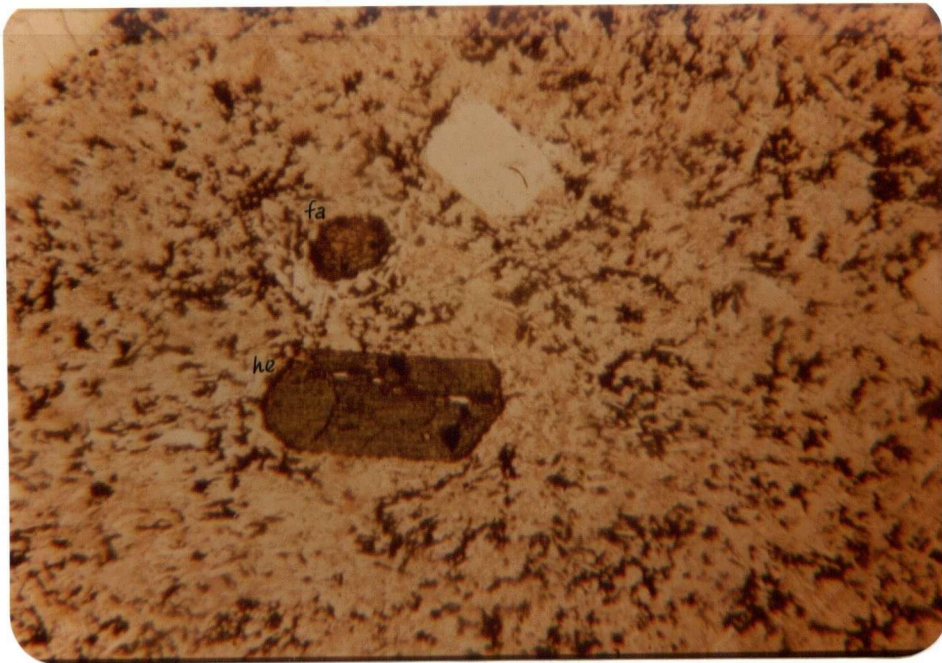


Figure 10. Photomicrograph of hedenbergite, fayalite and sanidine phenocrysts in comendite. Groundmass is composed of alkali feldspar and quartz with acmitic pyroxene, arfvedsonite, and aenigmatite filling the interstices between grains. Scale - 3 mm across the photo.

in clots surrounding magnetite and ilmenite grains where it has grown as a reaction product of these oxides. Sparse clusters of arfvedsonite ( $\alpha$  = deep green - blue;  $\beta$  = greyish violet;  $\gamma$  = blue green) are present in some samples.

### Comendite

Comendites from the north flank of the Rainbow Range are holocrystalline and contain approximately 10 percent phenocrysts. Groundmass mineralogy and textures remain constant whereas two phenocryst assemblages are found. Sanidine and hedenbergite phenocrysts are found in all comendites while fayalite and arfvedsonite are found in comendites from the top two-thirds of the stratigraphic section (Figure 10).

Sanidine phenocrysts are generally euhedral and commonly exhibit Carlsbad twinning. Glomeroporphyritic clots of sanidine are present. Euhedral to subhedral hedenbergite phenocrysts ( $\alpha$  = green;  $\beta$  = pale green;  $\gamma$  = pale yellow-green) are included within sanidine laths and mechanically included within the clots. In the lavas that contain arfvedsonite phenocrysts, some hedenbergite crystals are mantled by arfvedsonite. Ilmenite and magnetite phenocrysts are rare. Most fayalite ( $\alpha = \gamma$  = pale yellow;  $\beta$  = yellow) has an opacite rim or is surrounded by a thick corona of arfvedsonite. Rare arfvedsonite phenocrysts ( $\alpha$  = deep green-blue;  $\beta$  = greyish-white;  $\gamma$  = brown-blue) are always corroded.

Laths of alkali feldspar and patches of anhedral quartz grains form over half the groundmass. Ferromagnesian minerals (acmitic pyroxene, aenigmatite, and arfvedsonite) in the felted groundmass occur as mossy, fern-like aggregates that envelope alkali feldspar and quartz.

## Trachyte

Trachyte (AP-12) that forms a plug dome at Anahim Peak contains 8 - 10 percent phenocrysts of plagioclase and pyroxene. Calcic oligoclase ( $An_{29}$ ) occurs as poikilitic phenocrysts that show patchy extinction and enclose hedenbergitic pyroxene and opaque oxides. Titan-augite phenocrysts are pink to pale brown, show hourglass zoning, and are encircled by opacite rims.

Augite, magnetite, and ilmenite are found in the interstices between plagioclase and alkali feldspar microlites of the intergranular groundmass. Rare, light blue hexagonal grains of an isotropic mineral with streaks of minute inclusions, probably h a yne, are found in the trachyte.

## MINERAL CHEMISTRY

### Introduction

Along the north flank of the Rainbow Range shield volcano, four distinct stratigraphic episodes of volcanic activity produced a suite of lavas ranging in composition from hawaiiite to comendite. These lavas can be distinguished on the basis of mineralogy and chemical composition. In the oversaturated peralkaline rocks most phases are high in Na and Fe and low in Ca and Mg, whereas mineral phases found in the basic rocks do not show such extremes in composition. The minerals are examined with respect to the insight they provide into petrogenesis of the lavas.

Reviews of the mineralogy of oversaturated peralkaline rocks include those by Carmichael (1962), Nicholls and Carmichael (1969), Sutherland (1974), and Bryan (1976).

## Methods

An ARL-SEMQ electron microprobe was used for approximately eighty analyses of minerals from fourteen rocks. The accelerating voltage used was 15 KV; the sample current was about 40 nannoamperes. Spot size was 10 - 15 micrometers for phenocryst analyses and 1 - 3 micrometers for groundmass grain analyses. The correction procedure was that of Bence and Albee (1968) and Albee and Ray (1970). Ferric iron contents of pyroxenes and amphiboles were calculated following Papike et. al. (1974).

## Olivine

Fayalitic olivine is present in minor amounts as phenocrysts in the comendites, while forsteritic olivine occurs as phenocrysts in mugearites and microphenocrysts in hawaiites. Representative analyses of olivines are presented in Table III.

Fayalite has been reported as phenocrysts in many peralkaline, silicic rocks (e.g. Carmichael, 1962; Becker, 1976; Bryan, 1976). Compositionally, the fayalite that occurs in comendites from the Rainbow Range is extremely iron-rich,  $Fa_{94.5}$ . The manganese oxide content of the fayalite averages about 3 weight percent (Figure 11) which is much higher than the whole-rock manganese oxide content. Becker (1976, Table II) reports fayalite from a comendite in Big Bend National Park, Texas, that is almost identical in composition to that from the Rainbow Range.

Forsterite from hawaiites and mugearites has an average composition of  $Fo_{63}$ . Phenocrysts are usually zoned, have half the calcium and one-tenth the manganese of the fayalites, and the range of compositions probed is from  $Fo_{78}$ - $Fo_{54}$ . Basaltic rocks associated with oversaturated peralkaline rocks on Isla Socorro in the east Pacific (Bryan, 1976, Table 5) contain forsterite

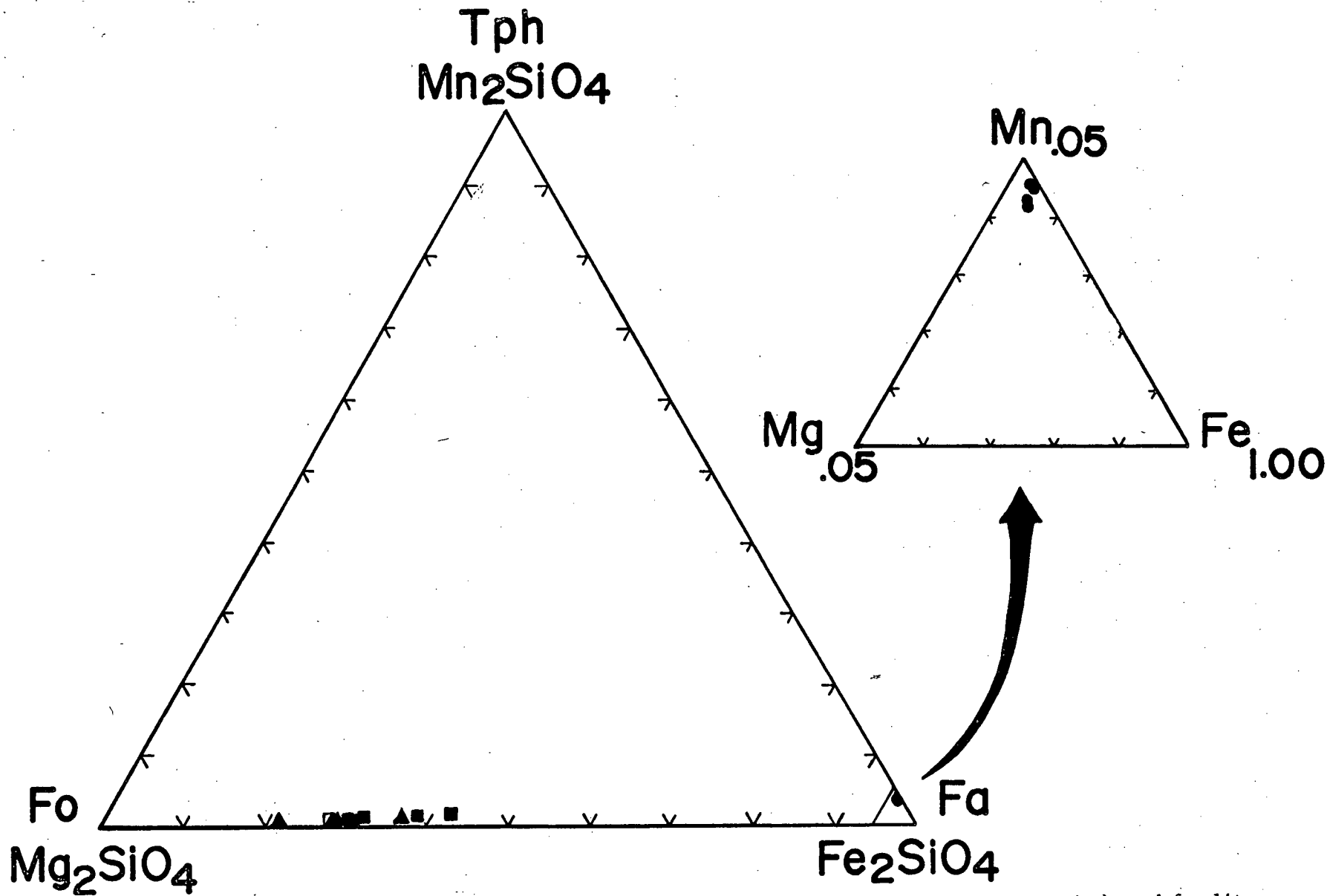


Figure 11. Triangular diagram for olivine with end members tephroite (Tph), forsterite (Fo), and fayalite (Fa) (mol. %), showing Mn enrichment of fayalite. Symbols: hawaiite-■, mugearite-▲, Anahim Peak trachyte-◼, comendite-●.

similar in composition. One forsterite crystal (1 mm diameter) analyzed from the trachyte plug at Anahim Peak shows an extreme compositional variation, from Fo<sub>72</sub>-Fo<sub>37</sub> (normal zoning). The crystal occurs in a clotted plagioclase and pyroxene microlites that appears foreign in origin.

### Pyroxene Phenocrysts

Calcic pyroxenes are typical of the Rainbow Range lavas, and range from aluminous augite through ferro-augite to hedenbergite and sodic hedenbergite (Table IV). When plotted in the pyroxene quadrilateral (Figure 12) they lie on a trend of iron-enrichment close to that of Nandewar volcano in Australia, a center of mildly alkaline lavas with associated oversaturated differentiation products (Abbott, 1969). Bryan (1976) also reports a suite of pyroxenes from Isla Socorro in the east Pacific that embodies the same compositional range as those from the Rainbow Range.

Diopsidic augites from the hawaiites are distinguished by their moderately high TiO<sub>2</sub> (1.61-2.45 percent), Na<sub>2</sub>O (0.39-0.65 percent), and Al<sub>2</sub>O<sub>3</sub> (3.02-5.68 percent) contents. Comparatively, ferro-augite (found only in the Anahim Peak trachyte) is lower in these elements and contains about 5 weight percent more total iron.

Highly aluminous (6.72 weight percent Al<sub>2</sub>O<sub>3</sub>) hypersthene (En<sub>70</sub>) is found as megacrysts in some hawaiites. Most orthopyroxene megacrysts reported in the literature are aluminous bronzite (En<sub>80</sub>-En<sub>90</sub>) (Binns, et. al., 1970). High aluminum content in orthopyroxene is a phenomenon that is favored at high pressure (Boyd and England, 1960, 1963). Experimental studies of basaltic compositions (for example, Green and Ringwood, 1967; Green and Hibberson, 1970) have shown that orthopyroxene ± clinopyroxene with compositions similar to those of megacrysts are near-liquidus phases at pressures of approximately

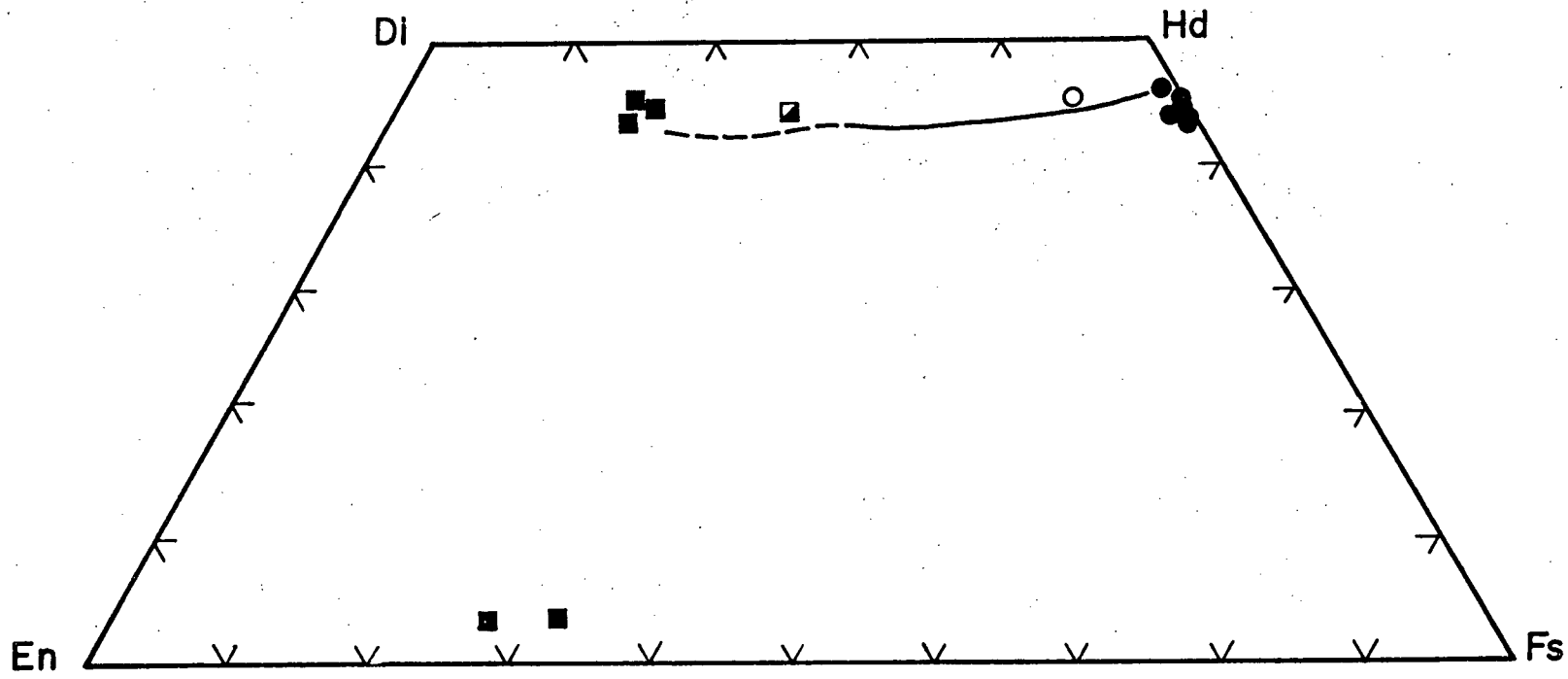


Figure 12. Compositions of pyroxene phenocrysts plotted on the pyroxene quadrilateral (mol. %). Trend from Nandewar volcano shown for comparison (Abbott, 1969). Symbols: hawaiite-■, mugarite-▲, Anahim Peak trachyte-□, comenditic trachyte-○, comendite-●.

10 - 20 kb. The Rainbow Range orthopyroxene megacrysts have a vitreous appearance in hand sample, a tendency toward conchoidal fracture rather than cleavage, and an absence of exsolution lamellae, typical of megacrysts (Irving, 1974). Reaction of megacryst rims with the host rock indicates that the orthopyroxene and host rock were not in equilibrium at the time of extrusion.

Clinopyroxenes found as phenocrysts in the peralkaline rocks are sodic hedenbergites, with compositions close to  $Wo_{45.5}Fs_{47.5}En_7$  in comenditic trachytes and  $Wo_{44}Fs_{55}En_1$  in comendites. Variation in composition of pyroxenes from comenditic trachytes and comendites parallels trends seen in whole-rock composition of these rocks:  $Na_2O$  and  $Fe_2O_3$  are high while  $MgO$  and  $CaO$  are low. Compared to augitic pyroxenes found in basic alkaline rocks, the sodic hedenbergites are high in  $Na_2O$  and total iron, and low in  $TiO_2$ ,  $Al_2O_3$ , and  $MgO$ .

#### Groundmass Pyroxene

Groundmass pyroxenes from the peralkaline rocks are near pure end-member acmite ( $NaFe^{+3}Si_2O_6$ ) in composition, with small amounts of hedenbergite in solid solution. They are chemically distinct from the pyroxene phenocrysts, being higher in  $Fe_2O_3$  and  $Na_2O$ , and lower in  $CaO$  (Figure 13). The pyroxene crystallization trend in these rocks is toward extreme iron enrichment before sodium becomes enriched. Because the groundmass pyroxenes are very small, reliable analyses were difficult to obtain. For comparison, one analysis of a groundmass pyroxene from the Burro Mesa "Riebeckite" Rhyolite (Becker, 1976), a crystalline comendite flow from Big Bend National Park, Texas, is listed in Table IV and plotted in Figure 13. One qualitative analysis of a groundmass pyroxene from a Rainbow Range comendite shows the same relative amounts

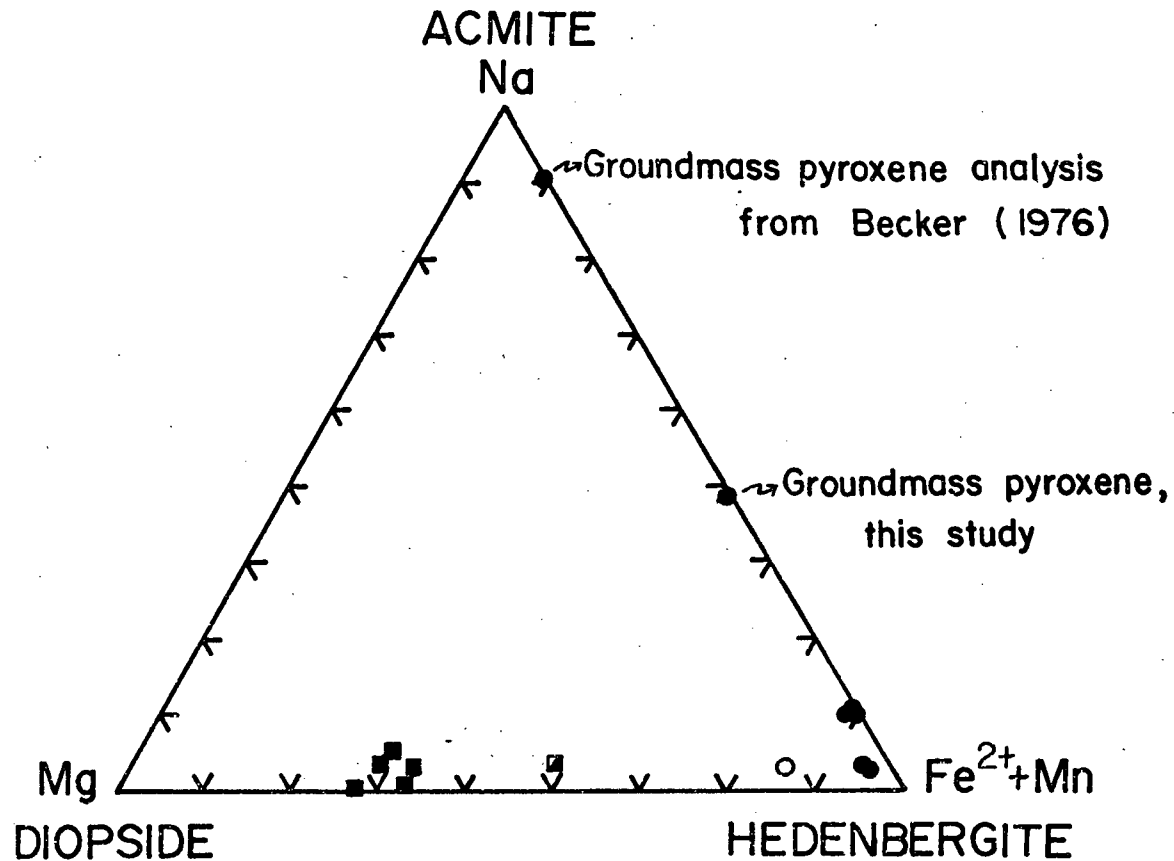


Figure 13. Triangular diagram for pyroxene in terms of acmite, diopside, and hedenbergite (mol. %). One groundmass pyroxene analysis from the Rainbow Range is only semi-quantitative; one analysis from Becker (1976) is shown for comparison. Symbols as in Figure 12.

of oxide components.  $TiO_2$  and  $Al_2O_3$  contents are higher in the groundmass pyroxenes, while MnO is higher in the phenocrysts. Nicholls and Carmichael (1969) note the same inverse relationship between Ti and Mn in pyroxenes from New Zealand comendites.

The poikilitic habit of the acmitic pyroxene is evidence for a low pressure origin, i.e. after extrusion of the lava, at 1 atm. pressure. Experimental work shows that acmite has a low thermal stability with respect to other silicate minerals. Bailey and Schairer (1966) found that pure acmite melts at  $975^\circ \pm 5^\circ C$  at 1 atm.

The presence of acmite does indicate that the liquid was highly peralkaline at the time of extrusion. In the system  $Na_2O-Al_2O_3-Fe_2O_3-SiO_2$ , Bailey and Schairer (1966) found that acmite crystallizes in the presence of quartz + liquid only from a liquid bearing normative sodium silicate.

### Amphibole

Amphibole is found only in peralkaline silicic rocks from the Rainbow Range. It occurs primarily as a groundmass mineral and rarely as phenocrysts or as mantles around fayalite phenocrysts. Microprobe analyses show that two amphiboles are present: arfvedsonite  $[(Na_{0.8}K_{0.2})(Ca_{0.5}Na_{1.5})(Mn_{0.2}Fe_{4.6}^{+2}Fe_{0.2}^{+3}Ti_{0.1})Si_8O_{22}(OH,F)_2]$  and katophorite  $[(Na_{0.9}K_{0.1})(Ca_{1.5}Na_{0.5})(Mn_{0.1}Fe_{2.8}^{+2}Fe_{1.6}^{+3}Al_{0.5}Ti_{0.1})Si_8O_{22}(OH,F)_2]$  (Table V). The one analyzed katophorite is from the groundmass. Arfvedsonite is the amphibole expected in peralkaline silicic volcanic rocks because it is stable to a higher temperature than riebeckite (Ernst, 1962). Arfvedsonite has been reported as a groundmass component in many peralkaline silicic volcanic rocks (e.g. Nicholls and Carmichael, 1969; Sutherland, 1974; Becker, 1976).

The amphibole forms irregular patches of poikilitic grains in the

groundmass, suggesting that it formed after extrusion, as did the acmite. Hydroxyl amphibole is not stable as magmatic liquidus temperatures and low pressure, but fluorine has been found to stabilize amphibole at low pressure (Troll and Gilbert, 1974). Although fluorine was not determined in Rainbow Range amphiboles, it has been reported in most arfvedsonites from peralkaline silicic volcanic rocks (e.g. Nicholls and Carmichael, 1969; Sutherland, 1974; Becker, 1976), and it seems likely that fluor-arfvedsonite is the amphibole present in the Rainbow Range peralkaline lavas.

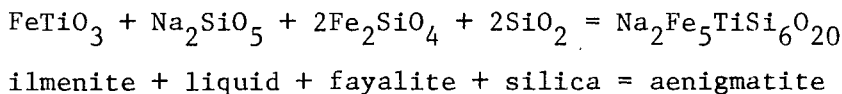
#### Aenigmatite

Aenigmatite ( $\text{Na}_2\text{Fe}_5\text{TiSi}_6\text{O}_{20}$ ) is a common constituent of the comenditic trachyte and comendite lavas from the Rainbow Range, where it is found exclusively as an interstitial groundmass phase. The mineral has been found in a number of peralkaline volcanic rocks (e.g. Abbott, 1967; Nash et. al., 1969; Nicholls and Carmichael, 1969; Sutherland, 1974; Yagi and Souther, 1974; Marsh, 1975; Becker, 1976; Self and Gunn, 1976; Barker and Hodges, 1977; and Larsen, 1977).

Two analyses of groundmass aenigmatite grains from Rainbow Range comendites are given in Table VI. One of these (R-44-1) was provided by B. Profett of the University of Calgary. An analysis of aenigmatite from Mt. Edziza (Yagi and Souther, 1974, Table 4, #2) is shown for comparison. Because the mineral grains are very small reliable analysis were difficult to obtain. The composition of the Rainbow Range aenigmatite is similar to those reported for groundmass aenigmatite in other peralkaline volcanic rocks (e.g. Nicholls and Carmichael, 1969).

In the Rainbow Range peralkaline lavas aenigmatite crystallized after extrusion, as evidenced by its interstitial nature. This indication of late

stage formation is consistent with experimental results (Lindsley, 1971) that show the maximum thermal stability of synthetic aenigmatite to be below 900°C. Aenigmatite always surrounds small grains of Fe-Ti oxide, and appears to have formed by a reaction that consumed the oxide phase. This petrographic feature has been observed by Lindsley et. al. (1971), Marsh (1975), and Becker (1976). Becker (1976) suggests that a possible reaction for the formation of aenigmatite is:



Fayalite is not necessarily specifically involved in the reaction; however, the liquid reacting with ilmenite must be rich in iron and silica.

### Feldspar

Feldspar is the most prevalent phenocryst phase found in Rainbow Range lavas. A suite of analyzed feldspar phenocrysts ranges from plagioclase in basic rocks to alkali feldspar in peralkaline silicic rocks (Figure 14). The compositional range covered by these feldspar phenocrysts is similar to that of analyzed feldspar suites from two oceanic islands, Isla Socorro (Bryan, 1976) and Terceira in the Azores (Self and Gunn, 1976).

Microprobe analyses of 17 feldspar phenocrysts are given in Table VII. Labradorite is the plagioclase feldspar most often found in hawaiites and mugearites, although one hawaiite (AP-11) contains calcic andesine. The trachyte plug at Anahim Peak bears large phenocrysts of oligoclase. Zoning in plagioclase phenocrysts can be either normal or reverse, and nowhere exceeds 3 mol. percent. Anorthoclase from comenditic trachytes ranges from Or<sub>22</sub>-Or<sub>28</sub> (mol. percent) which is slightly more sodic than the range for

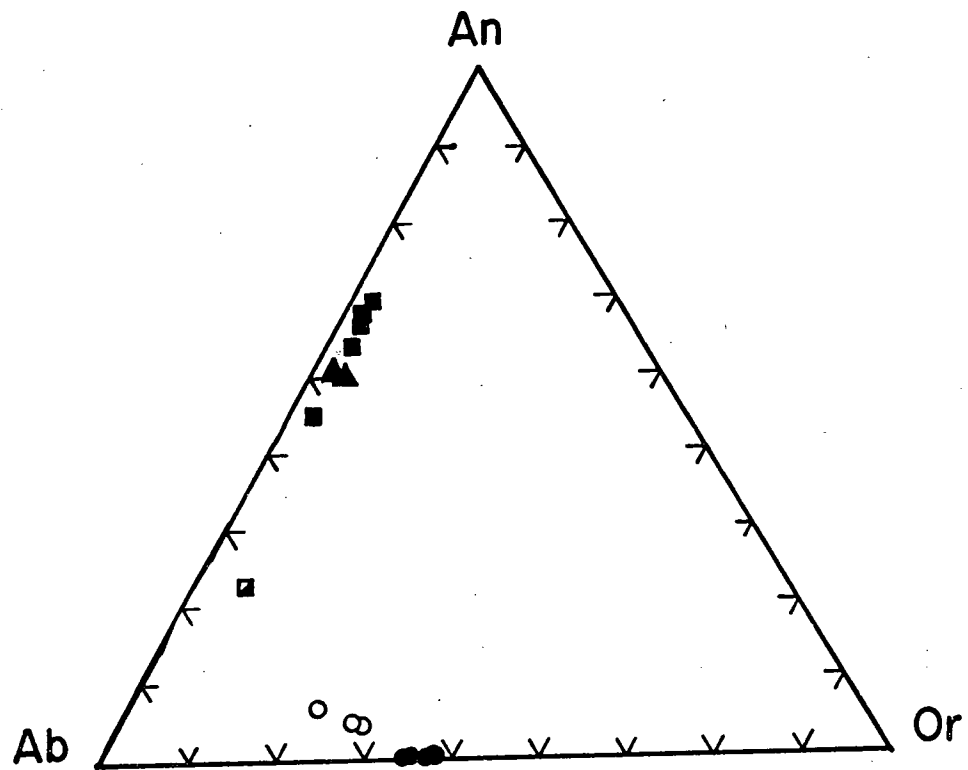


Figure 14. Triangular diagram for feldspar in terms of albite (Ab), anorthite (An), and orthoclase (Or). (mol. %). Symbols as in Figure 12.

peralkaline trachytes cited in Sutherland (1974), but corresponds well to one analysis from Pantelleria (Villari, 1970, p. 361). Alkali feldspar from Rainbow Range comendites ranges from  $Or_{34}$ - $Or_{37}$ , within the observed range from other reported localities (Sutherland, 1974). All alkali feldspars analyzed have less than 1 weight percent CaO. The maximum zonation found between end members in any crystal is 1 mol. percent.

Experimental work on alkali feldspar in peralkaline liquids has concentrated on determination of the location of the thermal valley under varying experimental conditions (e.g. Carmichael, 1962; Carmichael and MacKenzie, 1963; Bailey and Schairer, 1964; Thompson and MacKenzie, 1967; Bailey and Macdonald, 1969; and Roux and Varet, 1975). Bailey (1974) presents an overview of experimental work on feldspars in oversaturated, peralkaline systems.

Alkali feldspar phenocrysts from Rainbow Range peralkaline lavas are presumed to represent the first feldspar to precipitate from a liquid of the rock composition, because there is little range in composition of alkali feldspar from any one rock, and the phenocrysts are not obviously xenocrystic.

In order to determine where the Rainbow Range peralkaline liquids and feldspars lie with respect to a "thermal valley" and a quartz-feldspar field boundary, the normative constituents  $Q + Ab + Or$  were recalculated to 100 percent and plotted, along with coexisting feldspar compositions, on Carmichael and MacKenzie's (1963, Figure 4) composite liquidus diagram for the system  $NaAlSi_3O_8$ - $KAlSi_3O_8$ - $SiO_2$ - $H_2O$  with different percentages of additional acmite and nosean (Figure 15). The absence of quartz phenocrysts in the rocks indicates that the intersection of the thermal valley with the quartz-feldspar field boundary was not reached by the liquids while phenocrysts were still crystallizing. The bulk rock compositions must have been near the bottom of the thermal valley to produce the restricted range of feldspar

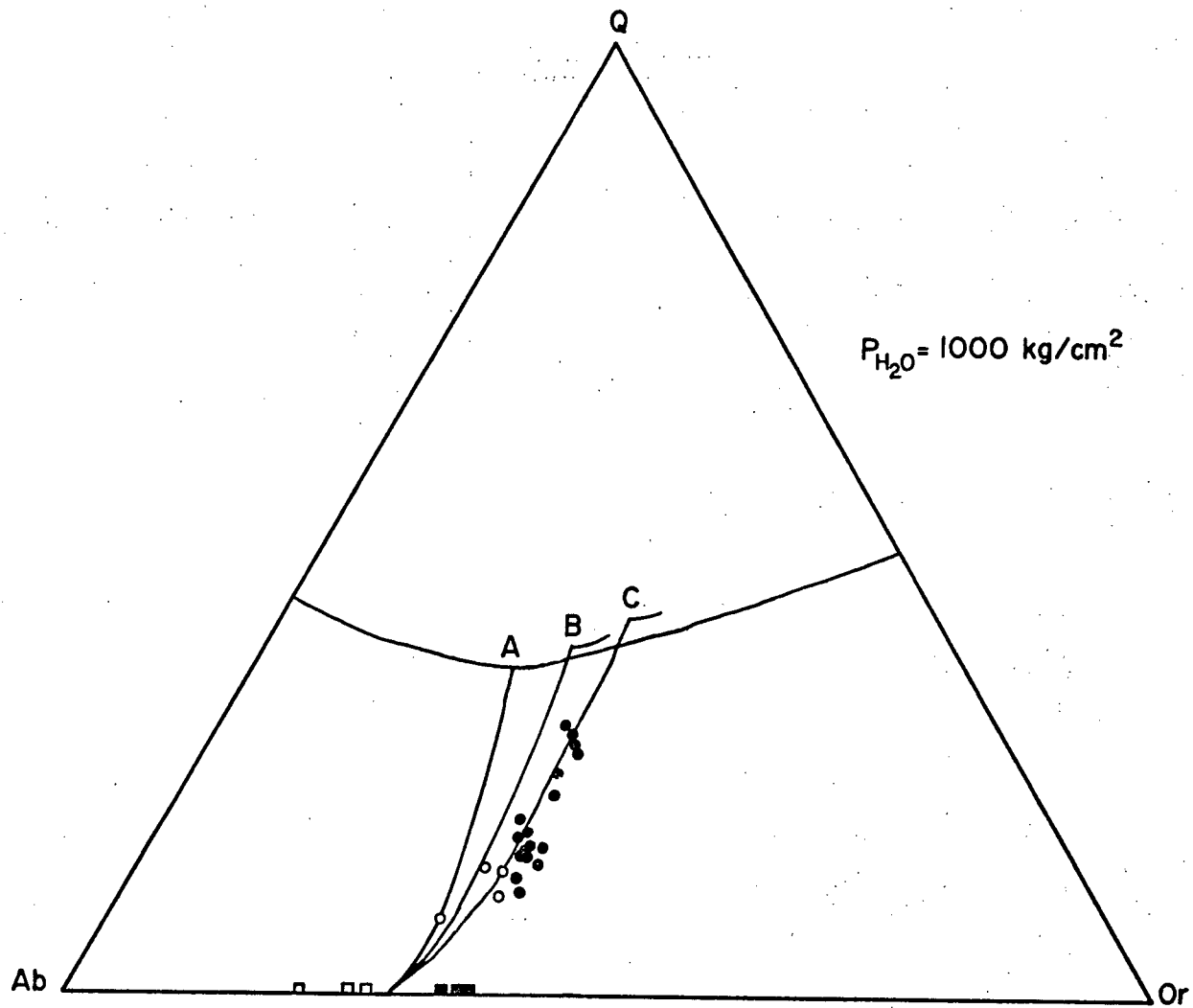


Figure 15. Compositions of Rainbow Range comenditic trachytes (open circles) and comendites (solid circles) and their coexisting feldspars (open and solid squares, respectively) (mol. %), plotted on Carmichael and MacKenzie's (1963, Figure 4) composite liquidus diagram for the system  $\text{NaAlSi}_3\text{O}_8\text{-KAlSi}_3\text{O}_8\text{-SiO}_2\text{-H}_2\text{O}$  plus different percentages of additional acmite and nosean. A, B, and C represent the thermal minimum for A- no acmite or nosean, B- 4.5% acmite + 4.5% nosean, and C- 8.3% acmite + 8.3% nosean.

compositions.

Experimentally, the minimum has been seen to move towards the Or-Q join with increased peralkalinity (Carmichael, 1962). The Rainbow Range comendite trend lies parallel to Carmichael and MacKenzie's curve C for 8.3 percent nosean. Rainbow Range comendites have about 5 percent normative acmite and 1 percent normative nosean. While the Rainbow Range comenditic trachyte trend is not as distinct, it is displaced towards a lower Or content. The comenditic trachytes have approximately 1 percent normative acmite and lack normative nosean.

Carmichael and MacKenzie's data are for  $P_{H_2O} = 1$  kb, yet oversaturated, peralkaline rocks are generally thought to be dry (anhydrous) and rich in halogens (Nicholls and Carmichael, 1969; Roux and Varet, 1975). The variations of the liquidus surface under varying confining pressures and vapor compositions are not known. Preliminary experiments by J. T. Iiyama (see Roux and Varet, 1975) show that the minimum is shifted towards K-rich compositions in the presence of an alkali chloride vapor at 1 kb. The Rainbow Range data are consistent with this observation.

#### Iron-Titanium Oxides

Iron-titanium oxides are found in all Rainbow Range lavas. In hawaiites, mugearites, and the Anahim Peak trachyte, titanomagnetite and ilmenite are found as discrete phenocrysts, microphenocrysts, groundmass granules, and occasionally as inclusions in plagioclase and clinopyroxene. Titanomagnetite and ilmenite in the comenditic trachytes and comendites occur primarily as groundmass granules and microphenocrysts; in comendites the oxide phase has always partially reacted to form aenigmatite.

Analyses are given in Tables VIII and IX. Composition of the oxide

phases varies with rock type. MgO is enriched in oxide phases from the basic lavas and depleted in oxide phases from the peralkaline lavas, while MnO displays the opposite trend. Analysed oxide phases from peralkaline acid lavas in Pantelleria and eastern Australia also show high MnO and low MgO concentrations (Carmichael, 1967; Ewart et. al., 1976). Analyses have been recalculated according to the method described by Carmichael (1967), and plotted in terms of FeO, Fe<sub>2</sub>O<sub>3</sub>, and TiO<sub>2</sub> in Figure 16. Ulvospinel content in titanomagnetites ranges from 50 to 87 percent, while coexisting ilmenites contain 2 to 7 percent R<sub>2</sub>O<sub>3</sub>. Iron-titanium oxides from Rainbow Range lavas vary in composition with coexisting ferromagnesian silicates, a characteristic noted by Carmichael (1967). Oxide phases from Rainbow Range peralkaline lavas are lower in R<sub>2</sub>O<sub>3</sub> and higher in ulvospinel than oxide phases from Rainbow Range alkaline lavas.

The temperature and log  $f_{O_2}$  of equilibration of coexisting titanomagnetite and ilmenite can be obtained using the methods of Buddington and Lindsley (1964). The analyzed oxide phases are all from the groundmass and hence equilibration temperatures should represent solidus temperatures. In Figure 17, coexisting oxide pairs from six Rainbow Range lavas ranging from hawaiite to comenditic trachyte are plotted on a log  $f_{O_2}$ -T diagram according to the curves of Buddington and Lindsley (1964). Estimated temperatures and oxygen fugacities of Rainbow Range lavas fall along or close to the QFM buffer. This is consistent with the mineralogy of the rocks.

#### Other Accessory Minerals

Apatite is commonly present as small needles in the matrix of all Rainbow Range lavas, whereas stout microphenocrysts filled with parallel inclusion trains occur in the Anahim Peak hawaiites. Rare groundmass red-brown biotite

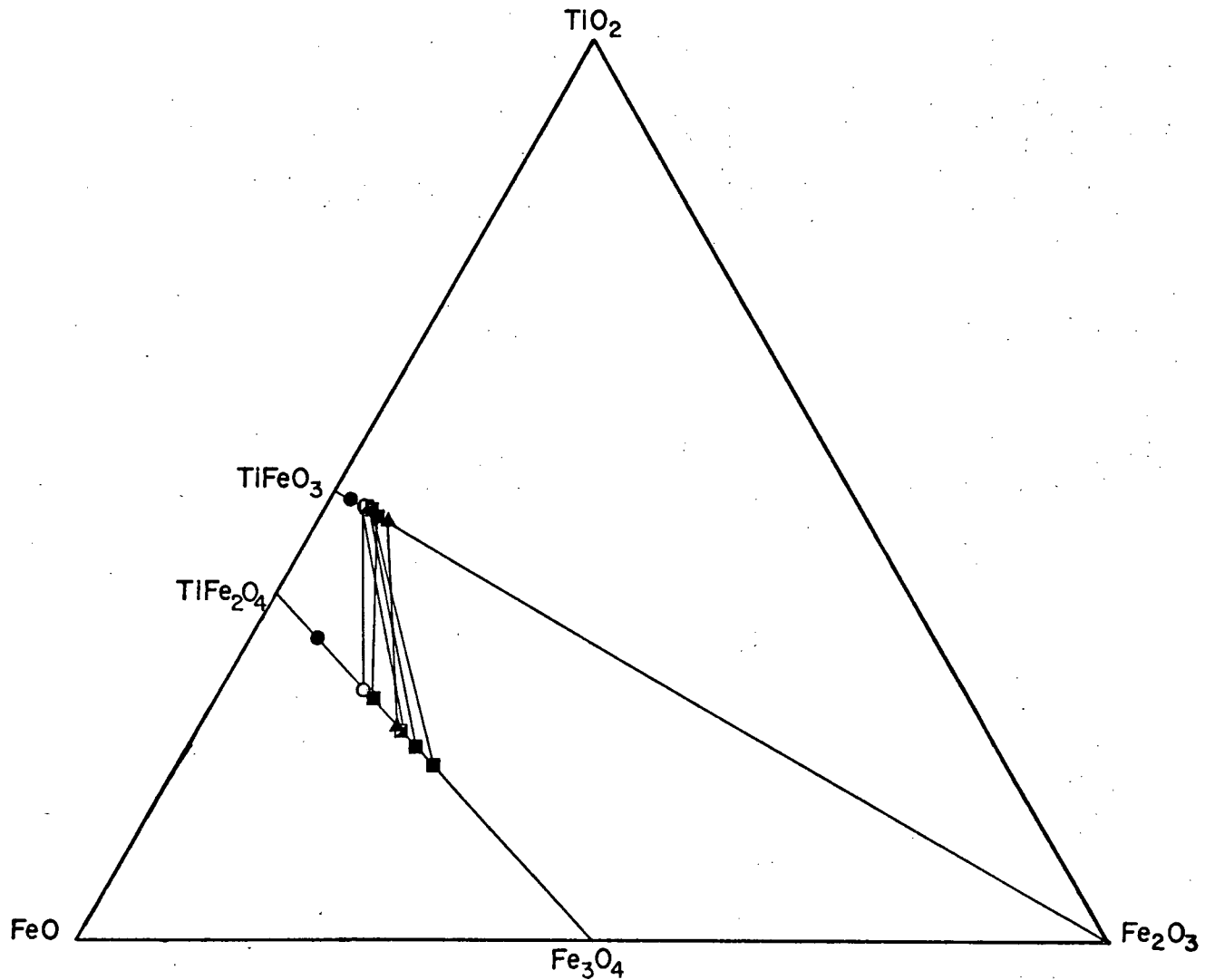


Figure 16. Compositions of titanomagnetite and ilmenite (mol. %) plotted in terms of  $\text{TiO}_2$ ,  $\text{FeO}$ , and  $\text{Fe}_2\text{O}_3$ . Tie-lines connect coexisting oxide pairs. Symbols as in Figure 12.



and light blue haüyne (?) are also present in the Anahim Peak trachyte. Quartz occurs as minute anhedral grains throughout the groundmass of the comendites and comenditic trachytes.

## WHOLE ROCK CHEMISTRY

### Introduction

Major and trace element data are used to interpret the nature of source rocks for the Rainbow Range lavas, and the role of various processes in magma genesis and differentiation. Thirty-two samples of Late Miocene volcanic rocks from the Rainbow Range and Anahim Peak (Plate II) were analyzed by X-ray fluorescence for major element oxides  $\text{SiO}_2$ ,  $\text{TiO}_2$ ,  $\text{Al}_2\text{O}_3$ ,  $\text{Fe}_2\text{O}_3$ ,  $\text{MnO}$ ,  $\text{MgO}$ ,  $\text{CaO}$ ,  $\text{Na}_2\text{O}$ ,  $\text{K}_2\text{O}$ , and  $\text{P}_2\text{O}_5$ , and the trace elements Nb, Rb, Sr, Ba, and Ni. Anhydrous analyses, recalculated to 100 percent, are presented in Table X.

Samples were prepared following the method of Norrish and Hutton (1969). Concentrations of major element oxides, except  $\text{Na}_2\text{O}$ , were determined from glasses diluted with a commercially prepared flux (Chemplex Grade III, #925, composition: 16 percent lanthanum oxide, 47 percent lithium tetraborate, and 37 percent lithium carbonate); trace elements and  $\text{Na}_2\text{O}$  concentrations were determined from undiluted pressed powder pellets. Data were reduced using the procedures of Watters (1976):

### Normative Mineralogy

Normative minerals (Table X) for all samples were calculated using a computer program. The  $\text{Fe}_2\text{O}_3/\text{FeO}$  ratio of the volcanic rocks has not been determined analytically. In order to calculate normative mineral compositions,

iron was partitioned according to the method of Carman et. al. (1975). A factor (R) for each rock type was determined from  $Fe_2O_3/FeO$  ratios in the same rock types found in the literature. The formulas used for the partition of iron are  $Fe_2O_3' = Fe_2O_3/(1+1.1113R)$  and  $FeO' = Fe_2O_3'/R$ , where  $R = Fe_2O_3/FeO$  of the same rock type. The R values used were: .32 for hawaiites (Nockolds, 1954), .38 for mugearites, metaluminous trachytes, and comenditic trachytes (Irvine and Baragar, 1971; Macdonald, 1974), and .43 for comendites (Macdonald, 1974).

The proportions of ferromagnesian minerals in the norm are dependent on the oxidation state of the iron. For example, when all the iron in a peralkaline rock is in the +3 state, sodium is used to form acmite, and sodium metasilicate is absent. Ferrosilite and nosean become important phases when ferrous iron is added, and hematite and sphene disappear while ilmenite increases.

### Rock Classification

Lava flows from the Rainbow Range represent a compositionally bimodal suite of basic alkaline and silicic peralkaline rocks. Peralkaline rocks account for at least 80 volume percent of the rocks exposed on the north flank of the shield volcano.

Basic to intermediate rocks are classified according to Thompson et. al. (1972) using the Thornton and Tuttle (1960) differentiation index (D.I.). Alkali olivine basalts have D.I. < 35, hawaiites 35-45, mugearites 45-65, benmoreites 65-75, and trachytes > 75.

By definition (Shand, 1951), peralkaline rocks have a molecular excess of  $(Na_2O+K_2O)$  over  $Al_2O_3$ . Oversaturated peralkaline rocks have been divided

into two groups, pantellerites and comendites. The two types differ mainly in chemistry and not in mineralogy. Comendites are mildly peralkaline, while pantellerites are more extremely peralkaline. Originally the distinction was based on the fact that pantellerites have a higher proportion of femic minerals. Lacroix (1927) chose 12.5 percent normative femic minerals as his division between the two, aware that since a complete chemical transition existed between the two groups any division would be arbitrary. A classification scheme based on normative femic minerals and normative quartz was used by Macdonald and Bailey (1973). This scheme included the peralkaline trachytes as those rocks with less than 10 percent normative quartz. Subsequently Macdonald (1974) proposed a classification scheme based on iron and aluminum contents. These elements were chosen because they appeared to be largely unaffected by post-eruptive devitrification and hydration. In Figure 18, oversaturated, peralkaline volcanic rocks from the Rainbow Range are plotted on both of the classification schemes. Macdonald and Bailey's (1973) scheme separates the lower unit and upper unit of Rainbow Range lava flows into comenditic trachytes and comendites, respectively. In Macdonald's later scheme, analyses that previously plotted as comendites are scattered around the intersection of the field boundaries, plotting as comenditic trachytes, comendites, and pantellerites.

Peralkaline volcanic rocks from the Rainbow Range do not fit unambiguously into either classification scheme. They are high in  $Al_2O_3$  (indicating trachytic affinities) and low in normative femic minerals compared to crystalline pantellerites (Macdonald, 1974). Based on a combination of petrographic and chemical variations, volcanic rocks from the lower unit are named comenditic trachytes, and volcanic rocks from the upper unit are named comendites.

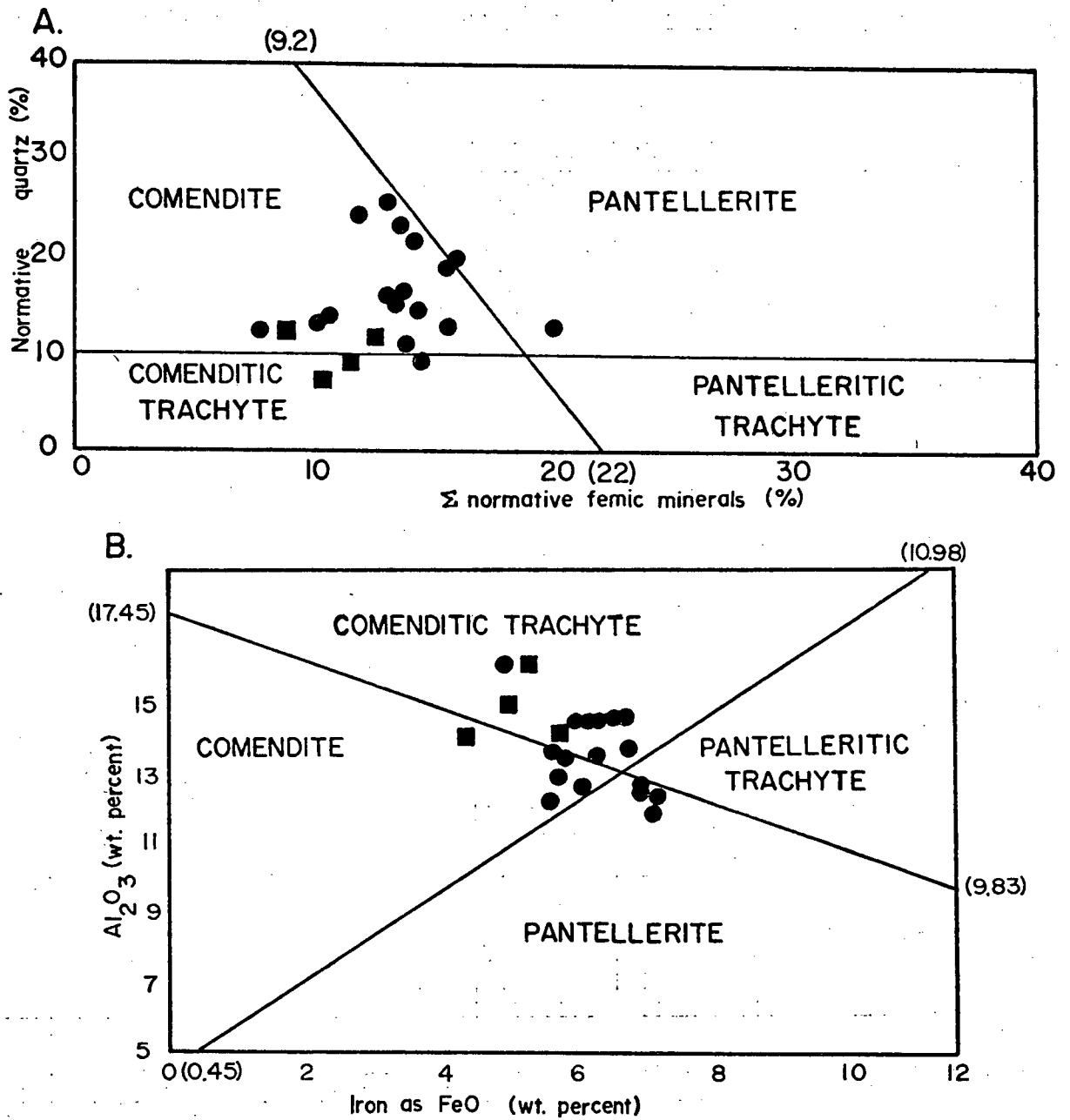


Figure 18. Classification schemes for silicic peralkaline volcanic rocks.

A. From Macdonald and Bailey (1973).

B. From Macdonald (1974).

Symbols: comenditic trachyte- ■, comendite- ●.

Compositional Changes in Silicic Peralkaline Rocks as a Result of Post-Eruptive Processes

Silicic peralkaline volcanic rocks are particularly susceptible to changes in chemical composition due to a variety of post-eruptive processes, because of their peralkaline nature. The most common change is a loss of sodium from crystalline rocks or hydrated glasses. This has been attributed to devitrification (Lipman, 1965; Noble, 1965; Ewart et. al., 1968), primary crystallization (Noble, 1968; Macdonald and Bailey, 1973), and ground water leaching (Lipman, 1965; Macdonald and Bailey, 1973). Macdonald and Bailey (1973) show that 2 wt. percent  $\text{Na}_2\text{O}$  can be lost from the crystalline interior of a flow.  $\text{K}_2\text{O}$  is usually lost or gained (Lipman, 1965; Noble et. al., 1967).

Halogens can be lost during primary crystallization, devitrification, and hydration (Noble, 1965, 1968; Noble et. al., 1967; Macdonald and Bailey, 1973). In fact Noble et. al. (1967) report that half the fluorine and four-fifths of the chlorine in peralkaline volcanic rocks can be lost during primary crystallization. Fluorine and chlorine contents of Rainbow Range peralkaline volcanic rocks were not determined; however, their presence has been well documented in many silicic, peralkaline volcanic rocks (Nicholls and Carmichael, 1969; Macdonald and Bailey, 1973) and it is probable that some halogens were lost from Rainbow Range peralkaline lavas after eruption.

It has been suggested that only non-hydrated obsidians represent the true composition of the original peralkaline liquid (Noble, 1966; Macdonald and Bailey, 1973). All analyzed peralkaline volcanic rocks from the Rainbow Range are from holocrystalline lava flows. None of the samples analyzed are significantly hydrated (maximum loss on ignition was 1.88 weight percent). There is good agreement between sodium and potassium contents from analyzed

samples of any one rock type, indicating that alkalis were not lost in great amounts. Rainbow Range peralkaline lavas do not appear to have changed enough in chemical composition since extrusion to have originally been pantellerites.

#### Chemical Variation Between Flows

Major Element Oxides. Concentrations of major element oxides are shown in Harker diagrams (Figure 19). These diagrams show important chemical variations between different rock types from the Rainbow Range. All oxides except  $\text{Na}_2\text{O}$  and  $\text{K}_2\text{O}$  decrease with increasing silica content. Although iron displays a decreasing trend, it is enriched in the most silicic rocks. For lavas from the Rainbow Range there is a complete gap in silica content between 56.30 and 64.80 weight percent. Only the Anahim Peak trachyte has a silica content within this gap.

Comenditic trachyte and comendite analyses from the Rainbow Range are similar in major element chemistry to Macdonald's (1974, Table 1) "average crystalline comenditic trachyte" and "average crystalline comendite." These silicic, peralkaline rocks have higher contents of total iron and  $\text{Na}_2\text{O}$ , and extremely lower contents of  $\text{MgO}$  and  $\text{CaO}$  than the average calc-alkaline rhyolite (Carmichael et. al., 1974).

Suites of volcanic rocks with similar major element oxide trends include those from Aden (Cox et. al., 1970), Erta Ale in the northern Afar (Barberi and Varet, 1974), Mt. Edziza in northwestern British Columbia (Souther and Symons, 1974), eastern Australia (Ewart et. al., 1976), Isla Socorro in the eastern Pacific (Bryan, 1976), Terceira in the Azores (Self and Gunn, 1976), and the Trans-Pecos of west Texas and Kenya (Gregory) rift in east Africa (Barker, 1977).

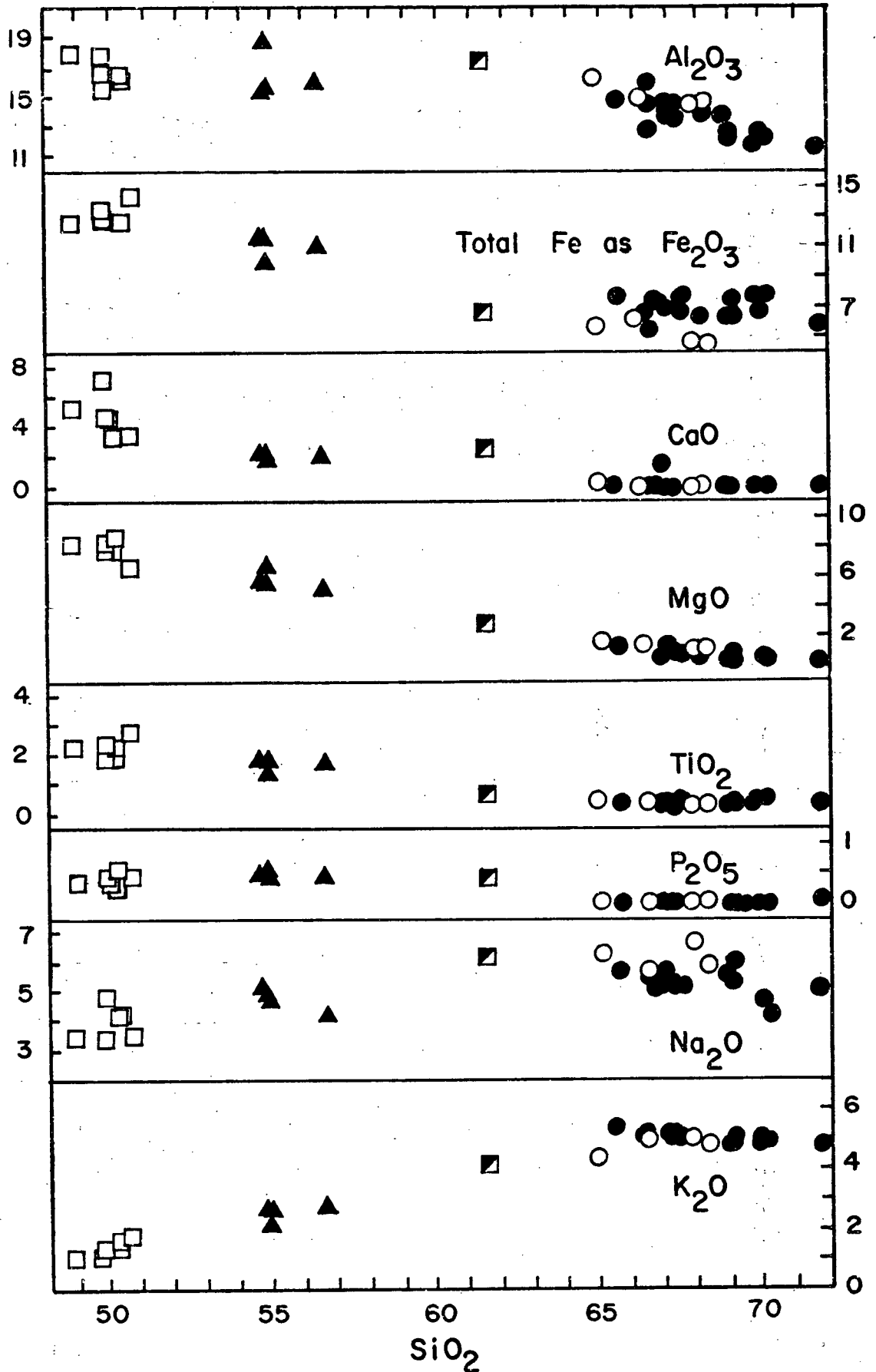


Figure 19. Major-element Harker diagrams for volcanic rocks from the Rainbow Range and Anahim Peak. Symbols: hawaiite- $\square$ , mugearite- $\blacktriangle$ , Anahim Peak trachyte- $\square$ , comenditic trachyte- $\circ$ , comendite- $\bullet$ .

Trace Elements. Samples from the Rainbow Range volcanic suite were analyzed for five trace elements- Nb, Rb, Sr, Ba, and Ni (Table X). The five show a variety of trends and serve to emphasize the relevance of trace element data to problems of magma genesis. Trace elements and trace element ratios are plotted in Harker diagrams (Figures 20 and 21) analogous to those used for major element oxides.

Rainbow Range peralkaline rocks have trace element contents within the range of values compiled by Macdonald and Bailey (1973) for peralkaline oversaturated obsidians, although rubidium contents are somewhat low. In addition, the trace element contents of the Rainbow Range peralkaline rocks show the characteristic pattern of extreme enrichment in some trace elements and particularly low contents of others.

Nickel content decreases with increasing silica content. This is an expected trend, indicating incorporation of Ni into the lattices of pyroxene, olivine, ilmenite, and magnetite in the more basic rocks. Niobium is concentrated in the siliceous peralkaline rocks where it is thought to follow zirconium (Cox et. al., 1970).

Rubidium, strontium, and barium are all related and will be discussed together. These three elements have large ionic radii ( 1.16Å) and are partitioned into the feldspar phase. Rb/Sr ratios increase radically with differentiation. Rubidium steadily increases with increasing acidity, following calcium. Strontium values for comendites are extremely low, ranging from 1.4 to 10.9 ppm, significantly lower than the 450 ppm average for mugearites. This may indicate a different parent magma for the comendites, although a common primary magma is implied by the smooth rubidium trend (Self and Gunn, 1976). K/Rb ratios appear unaffected by differentiation, except at the silica-rich end where they show a slight decrease. The average K/Rb ratio.

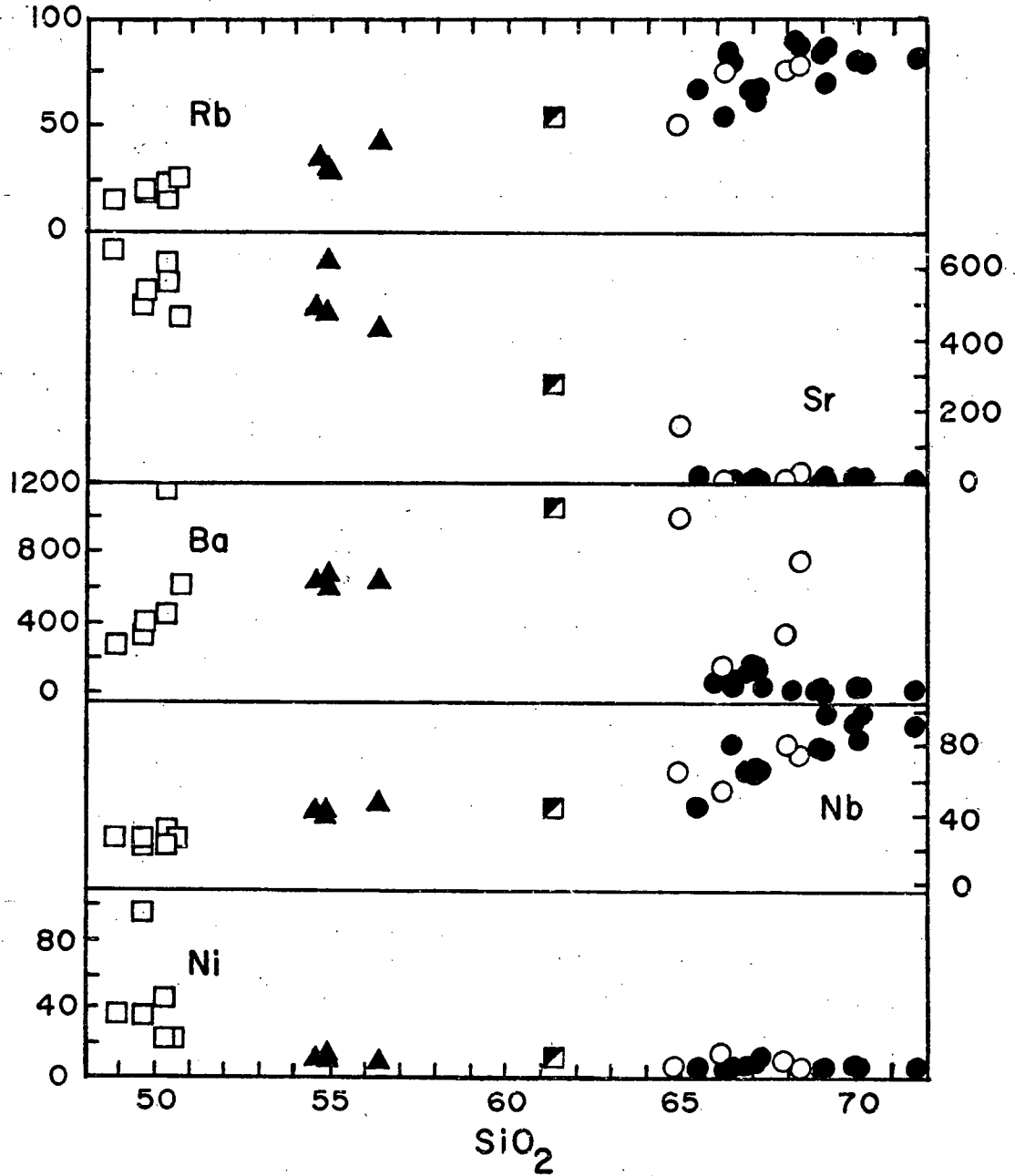


Figure 20. Trace element Harker diagrams for volcanic rocks from the Rainbow Range and Anahim Peak. Symbols as in Figure 19.

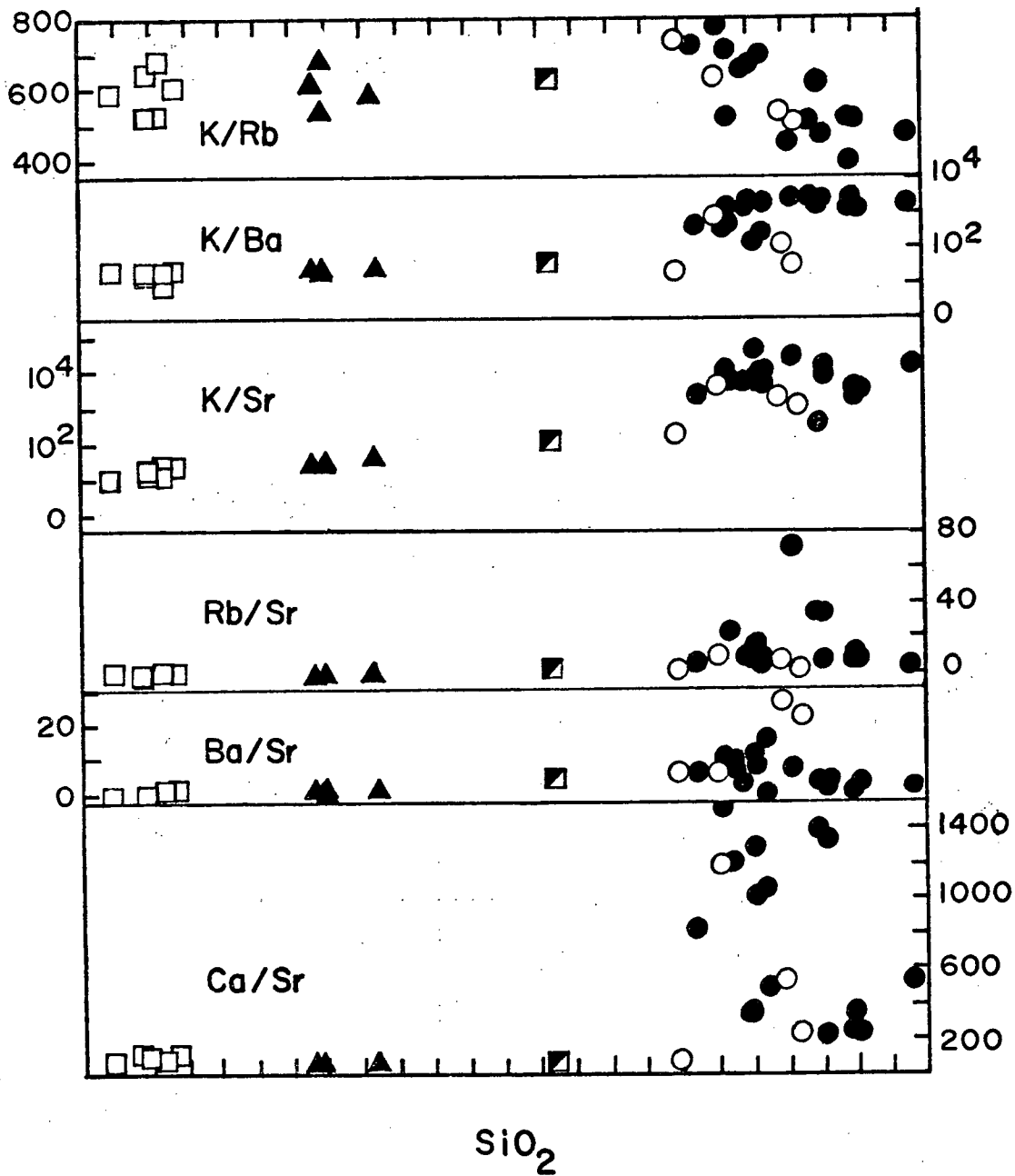


Figure 21. Trace-element ratio Harker diagrams for volcanic rocks from the Rainbow Range and Anahim Peak. Symbols as in Figure 19.

of Rainbow Range comendites is 594, unusually high for salic igneous rocks (Ferrara and Treuil, 1974). Korringa and Noble (1972) noted similar high K/Rb ratios and (and low Rb contents) in silicic peralkaline rocks from Pantelleria.

Barium builds up to a maximum and falls sharply off in the most silicic members of the suite. This inflection point in the barium trend is due to the onset of alkali feldspar crystallization (Ferrara and Treuil, 1974). Enormous increases in K/Ba and Rb/Ba at the inflection point also support this conclusion.

Other basic alkaline-silicic peralkaline volcanic rock suites that show these same trends are from San Pietro and Pantelleria (Barberi, et. al., 1970), eastern Australia (Ewart et. al., 1976). and Isla Socorro (Bryan, 1976).

#### Strontium Isotopic Data

$Sr^{87}/Sr^{86}$  ratios for eight Rainbow Range volcanic rocks, covering the range of compositions described from the shield volcano and including two samples from Anahim Peak, range from .7031 to .727 (Table XI). The ratios fall into two distinct groups: ratios from basic rocks cluster around .7032 (Rb/Sr = .028 to .204) while ratios from silicic peralkaline rocks range from .7042 to .727 (Rb/Sr = 2.28 to 74.4). Other basic alkaline-silicic peralkaline suites that display similar spreads in strontium isotopic ratios include those from Aden (.7038-.7072), Cox et. al., 1970; Erta Ale (.702-704), Barberi and Varet, 1970; eastern Australia (.7038->.71), Ewart et. al., 1976; the Trans-Pecos field of west Texas (.7032-.7254), Barker et. al., 1977; and the Stikine volcanic belt of northwestern British Columbia (.7026->.714), Armstrong et. al., 1977.

An isochron plot of all eight samples (Figure 22) shows a very good correlation between  $\text{Sr}^{87}/\text{Sr}^{86}$  and  $\text{Rb}^{87}/\text{Sr}^{86}$  ratios, and regression of the data according to the method of York (1967) gives an age of  $6.9 \pm 1.0$  m.y. and initial  $\text{Sr}^{87}/\text{Sr}^{86}$  ratio of  $.7032 \pm .0001$  for the suite. The age is in good agreement with K-Ar age determinations from the shield volcano (Table I). The calculated initial ratio is equivalent to that of the most primitive lavas known from the shield volcano, hawaiites, whose  $\text{Sr}^{87}/\text{Sr}^{86}$  ratios have not changed significantly since eruption because of their low Rb/Sr ratios.

Many explanations have been given for the differences in  $\text{Sr}^{87}/\text{Sr}^{86}$  ratios in suites of cogenetic volcanic rocks. The first is that the isotopic variations reflect variations in the Rb/Sr and  $\text{Sr}^{87}/\text{Sr}^{86}$  ratios of magma source material in the mantle. Mantle Rb/Sr ratio may vary laterally and with depth. A second explanation is that different  $\text{Sr}^{87}/\text{Sr}^{86}$  ratios will be generated as a result of different Rb/Sr ratios in different portions of a long-lived magma chamber (Artemov and Yaroshevskiy, 1965). The third explanation is that the isotopic variations were caused by contamination of the magmas with radiogenic strontium by bulk assimilation or wall-rock reaction (Green and Ringwood, 1967).

In order to assess which of these explanations appears to account for the high strontium isotopic ratios of the differentiated members of the Rainbow Range volcanic suite, initial  $\text{Sr}^{87}/\text{Sr}^{86}$  ratios were calculated (Table XI) using measured  $\text{Sr}^{87}/\text{Sr}^{86}$  and Rb/Sr ratios and known K-Ar ages or estimated ages based on relative stratigraphic position. With the exception of one sample (R-29), calculated initial  $\text{Sr}^{87}/\text{Sr}^{86}$  ratios are, within 1 $\sigma$  error limits, equal to the initial ratio calculated for the isochron, and all agree within 2 $\sigma$ . Decay of  $\text{Rb}^{87}$  to  $\text{Sr}^{87}$  since the time of eruption can account for the higher  $\text{Sr}^{87}/\text{Sr}^{86}$  ratios of the peralkaline lavas.

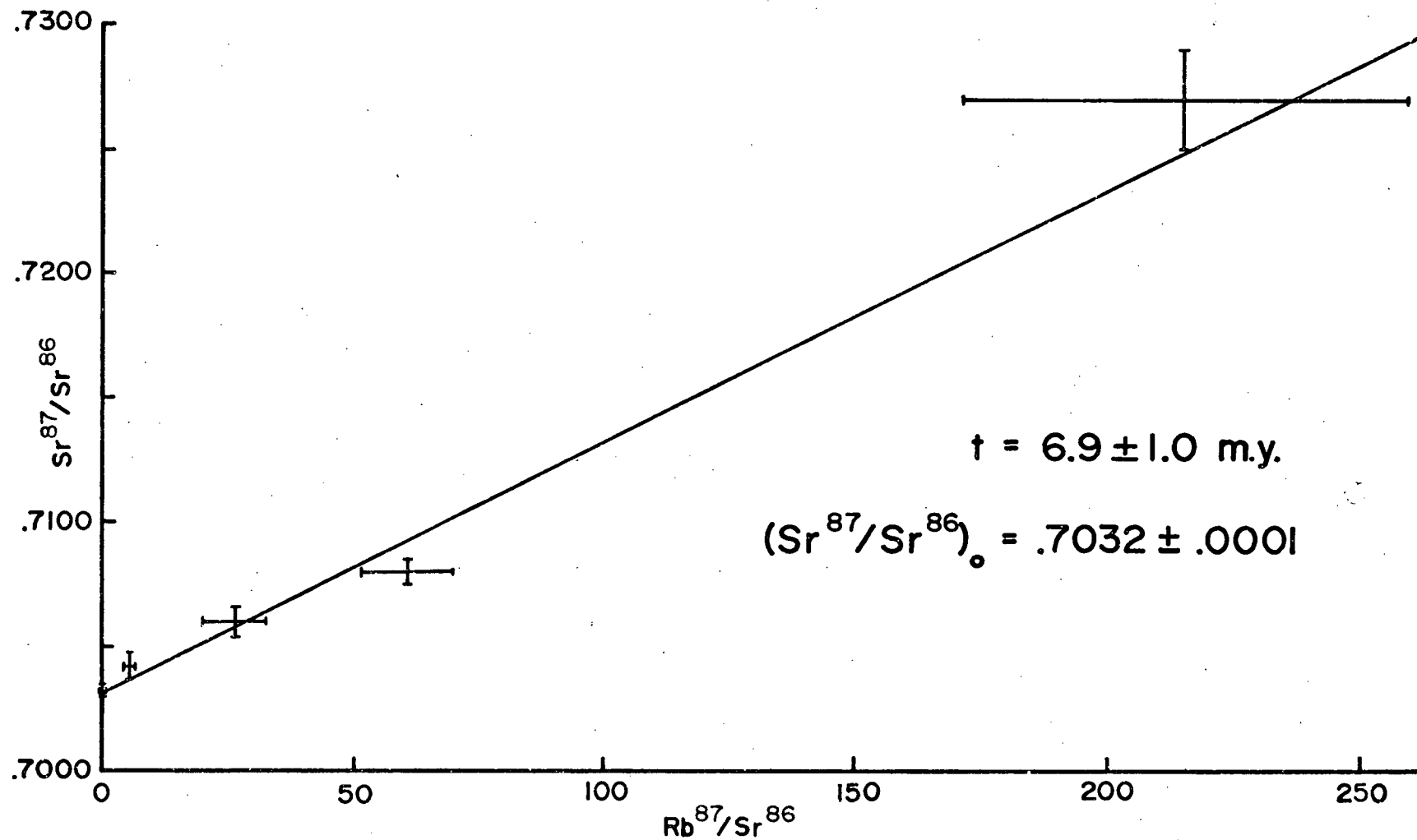


Figure 22. Rb/Sr whole rock isochron for volcanic rocks from the Rainbow Range and Anahim Peak. See Table XI for meaning of error bars.

MORPHOLOGY OF THE RAINBOW RANGE SHIELD VOLCANO

The Rainbow Range shield volcano is unique in that even though a high proportion of the lava is silicic, ranging from 64 to 71 weight percent  $\text{SiO}_2$ , the volcanic edifice is a shield volcano, intermediate in size between Icelandic and Hawaiian shield volcanoes. The broad, low slopes of the volcano indicate that the viscosity of these lavas was unusually low during eruption. Lavas with the same silica content and average viscosity would normally build a composite cone. Peralkaline shield volcanoes have been reported in the literature only from one other locality outside of British Columbia - the South Turkana region of the Kenya rift valley (Webb and Weaver, 1975).

The viscosity of a silicate liquid is dependent on the extent of development of chains and networks of silica tetrahedra (Ringwood, 1955; Barth, 1962). Networking forming ions (e.g.  $\text{Si}^{+4}$ ,  $\text{Al}^{+3}$ ,  $\text{Ti}^{+4}$ ) increase polymerization of silica tetrahedra in the magma if oxygen atoms are available to bond with them. When present in large quantities, network modifying ions (e.g.  $\text{Na}^+$ ,  $\text{K}^+$ ) free oxygen atoms so that silica tetrahedra form independently from one another. An increase in independent silica tetrahedra corresponds to a decrease in viscosity.

Schminke (1974) discusses the factors influencing the viscosity of peralkaline magmas and proposes that the combination of peralkaline composition and high temperature together reduce the viscosity of peralkaline silicic lavas below that of an average calc-alkaline silicic lava. Peralkaline lavas are high in  $\text{Na}^+$ ,  $\text{K}^+$ ,  $\text{Fe}^{+3}$ , and  $\text{F}^-$  (silicate network modifiers) and low in  $\text{Al}^{+3}$  (a silicate network former). Many peralkaline lavas are reported to have low viscosities (Schminke and Swanson, 1967; Walker and Swanson, 1968; Schminke, 1974; Scarfe, 1977). Liquidus temperatures calculated for silicic

peralkaline lavas range from 900°C to 1050°C (Carmichael, 1967; Bailey et. al., 1974; Barberi et. al., 1975). In contrast, Carmichael et. al. (1974) report extrusion temperatures for "rhyolites" ranging from 735°C to 925°C.

Using the method of Shaw (1972), viscosities were calculated for peralkaline lavas from the Rainbow Range and compared with calculated and experimentally determined viscosities of calc-alkaline rhyolite, pantellerite, tholeiitic basalt, and alkali basalt (Table XII). Results show that Rainbow Range peralkaline lavas are 10 to 30 times less viscous than calc-alkaline rhyolite at the same temperature and water content. In addition, the results are in agreement with experimentally determined viscosities of a pantellerite from Fantale in Ethiopia (Scarfe, 1977). Tholeiitic and alkalic basalts are 1000 times less viscous than peralkaline silicic lavas at 1200°C (approximate liquidus temperature of basalt).

During eruption, the actual viscosity of the Rainbow Range peralkaline lavas would have differed from the calculated values for a number of reasons. The presence of crystals in a melt would raise its viscosity (Shaw, 1965, 1969; Murase and McBirney, 1973), whereas dissolved volatiles would reduce its viscosity (Shaw, 1963, 1972). Rainbow Range peralkaline lavas contain 5 - 10 percent crystals, the presence of which would be unlikely to increase the viscosity of the melt more than a factor of 1.3 - 1.8 (Shaw, 1965). Peralkaline lavas are known to be rich in halogens (Nicholls and Carmichael, 1969; Bailey and Macdonald, 1975). The effect of F<sup>-</sup> and Cl<sup>-</sup> on the viscosity of melts of geologic interest is not known, but studies of glass systems suggest that F<sup>-</sup> is an important melt depolymerizer (Hirayama and Camp, 1969). Therefore, the possibility exists that upon eruption, Rainbow Range peralkaline lavas were considerably less viscous than the calculated values.

ORIGIN OF OVERSATURATED, PERALKALINE VOLCANIC ROCKS

Several theories have been proposed for the origin of oversaturated, peralkaline volcanic rocks. The most common of these are partial fusion of lower crustal material and fractional crystallization or partial fusion of a basic parent. Another process currently being discussed in the literature is the modification of the above mechanisms by volatile transfer in an open system.

In a study of non-hydrated, aphyric, peralkaline obsidians (i.e. rocks most representative of peralkaline liquid compositions) from different continental and oceanic localities, Bailey and Macdonald (1970) found that continental obsidians clustered in composition around the quartz-feldspar minima, while oceanic obsidians scattered along the thermal valley between Ab and Or. They concluded that continental peralkaline magmas must form by partial melting of lower crustal material in order to have such tightly clustered compositions at the quartz-feldspar minima, while oceanic peralkaline magmas form from fractional crystallization of trachytes.

However, initial  $\text{Sr}^{87}/\text{Sr}^{86}$  ratios of peralkaline lavas indicate that these rocks are mantle-derived. Peralkaline volcanic rocks from Pantelleria have strontium isotopic ratios ranging from .7029 to .7032 (Korringa and Noble, 1972). Ferrara and Treuil (1974) report a range of .703 to .707 for most young peralkaline volcanic rocks from the Kenya rift.

In his classic paper, Yoder (1973) showed that hydrous melting of a rock composed of olivine and clinopyroxene at high pressure (10-15 kb) could produce contemporaneous basalt and "rhyolite". This "rhyolite" could differentiate towards peralkaline composition by alkali feldspar fractionation.

The most commonly invoked mechanism for origin of oversaturated, peralka-

line magmas is by fractional crystallization of an alkalic basalt. Lindsey and others (1971) showed unequivocally that a peralkaline residuum could form from fractional crystallization of basalt, in their study of pegmatitic segregations found in a flow of Columbia River basalt. Indeed, alkalic basalts are often spatially related to areas of peralkaline volcanic activity (Barberi and Varet, 1970; Barberi et. al., 1975; Bryan, 1976; Self and Gunn, 1976).

This process is envisaged in several steps. Fractionation of plagioclase and ferromagnesian minerals depletes the residual liquid in Ca, Mg, Al, Fe, Cr, Sc, V, and Sr, and enriches the residual liquid in Si, alkalis, Nb, Th, Y, and Zr. When the magma becomes low in Ca, continued crystallization of plagioclase (the "plagioclase effect" of Bowen, 1945) drives the liquid toward peralkaline compositions by depleting the aluminum content of the magma with respect to alkali content. Subsequent crystallization of alkali feldspar increases the excess of alkalis over aluminum. The Na/K ratio of alkali feldspar is lower than that of the liquid, so alkali feldspar fractionation raises the Na/K ratio of the residual liquid (the "orthoclase effect" of Bailey and Schairer, 1964).

Experimental studies (Carmichael and MacKenzie, 1963; Bailey, 1967; Bailey and Macdonald, 1969; Roux and Varet, 1975) also support the theory that oversaturated peralkaline magmas are derived by feldspar fractionation. Numerous experiments document that peralkaline rock compositions lie in the low temperature thermal valley between Ab and Or in the system Q-Ab-Or, indicating that the magmas were derived by feldspar fractionation from liquids of trachytic composition.

Many field and petrologic studies also point towards fractional crystallization of an alkalic basalt parent for the derivation of oversaturated, peralkaline lavas. Barberi et. al. (1975) describe a most convincing example - a basalt to pantellerite suite with continuous variation in major and trace

element composition, from the Boina Center in Ethiopia. Noble (1965, 1968) argues for prolonged fractional crystallization based on the radically enriched and extremely depleted trace element contents found in oversaturated, peralkaline rocks. Similar reasoning is employed by Gass and Mallick (1968), Noble et al. (1969), Barberi and Varet (1970), Ewart et. al. (1976), and Self and Gunn (1976).

As more precise trace element data become available for oversaturated, peralkaline rocks, increasing evidence suggests that crystal fractionation or partial fusion cannot totally explain observed trace element trends. Presence of an alkali and/or halogen-rich volatile phase is claimed necessary for the deviation of trace element contents from those predicted by crystal-liquid equilibria (Bailey and Macdonald, 1969, 1975; Bailey, 1973; Bailey et. al, 1975).

In a study of peralkaline obsidians from Eburru volcano in Kenya. Bailey and Macdonald (1975) found that trace element abundances were not compatible with a closed system evolutionary process controlled by crystal-liquid equilibria. However, they found high correlation of F with Zr and Rb, and Cl with Nb and Yt, and suggested that in an open system partitioning of metal-halogen complexes between a volatile phase and silicate melt would depend on conditions at the time of differentiation, such as volume of vapor and melt, variations in composition of vapor and melt, pressure, and temperature.

Martin (1970) showed experimentally that the presence of water as a volatile phase was responsible for the separation of a peralkaline liquid fraction from a basaltic parent, especially through the mobilization of silica and alkalis. Orville (1963) also demonstrated alkali transfer between alkali feldspars and alkali chloride-water solutions experimentally.

The derivation of oversaturated, peralkaline volcanic rocks is by no

means a simple process. Their close association in space and time with basic alkaline rocks indicates that fractional crystallization or partial fusion of a mafic parent is almost assuredly necessary for their genesis. Several studies show the importance of a volatile phase in altering the final composition of these rocks, and emphasize the need for additional experiments in the presence of a volatile phase to determine the extent of its influence on evolution of the peralkaline condition.

#### ORIGIN OF LAVAS FROM THE RAINBOW RANGE AND ANAHIM PEAK

Continuous variation in major and trace element trends and feldspar compositions for the hawaiite-mugearite-comenditic trachyte-comendite suite from the Rainbow Range suggests that the differentiated rocks were derived from the same parent magma, tapped several times as it was undergoing fractional crystallization in a high-level magma chamber. In addition, the magma chamber may have been compositionally zoned prior to eruption to produce the sequence of alternating basic and silicic, peralkaline lava flows. The Rainbow Range shield volcano lies near the western edge of the Late Miocene plateau basalt province of south-central British Columbia, suggesting that these basalts are perhaps the ultimate source for the differentiated suite seen in the Rainbow Range.

Least squares mass balance equations were made using the computer program MAGMIX (modified from Bryan and others, 1969) in order to determine whether the major element composition of one lava could be derived from the composition of another by fractionation of the phenocryst phases present. Compositions of fractionated phases are actual phenocryst compositions from the parent lavas. Mass balance calculations for trace elements were made using the results of major element models and equation 1 of Gast (1968) for

Rayleigh (surface) equilibrium. Data of Drake and Weill (1975), Ringwood (1975), and Arth (1976) have been used to estimate partition coefficients for trace elements.

Because no obsidians were found within the field area compositions of porphyritic volcanic rocks were used in the models. It is not known whether the phenocrysts (1 to 2 percent in basic rocks and up to 10 percent in silicic rocks) represent cumulate material or whether they crystallized from the differentiated liquid. Disequilibrium features such as reaction rims are rarely seen in the rocks, suggesting that the phenocrysts are in equilibrium with the bulk rock composition.

Seven models were tested. Hawaiite, the most primitive rock type found on the north flank of the Rainbow Range, was used as parental material to all the more differentiated rock types. It is presumed to have been derived from approximately 30 percent fractional crystallization of alkali olivine basalt in a manner similar to that discussed by Fiesinger and Nicholls (1977, pages 34-35). Mugearite was tested as parental material to comenditic trachyte and comendite, and comenditic trachyte was evaluated as a possible parent of comendite. In addition, hawaiite from Anahim Peak was modelled as a parent to the Anahim Peak trachyte. The phases subtracted from basic parents were olivine, plagioclase, augite, magnetite, ilmenite, and apatite, while anorthoclase and hedenbergite were subtracted from comenditic trachyte. Results of calculations yielding the lowest residuals are shown in Tables XIII through XIX.

Increasing degrees of crystallization (71, 86, and 87 percent) of a hawaiite parent can account for the major element composition of mugearite, comenditic trachyte, and comendite, respectively. Major element compositions of comenditic trachyte and comendite can also be matched by fractional

crystallization of a mugearite parent. However, trace element calculations bring to light serious defects in some of these models. If hawaiite or mugearite are used as parental liquid for the derivation of comendite, calculated Ba concentrations are unreasonable. There is no satisfactory way to resolve this discrepancy except by the fractionation of a Ba-rich phase, presumably alkali feldspar. Comendite can be derived from comenditic trachyte by crystallization of 40 percent of the parent as anorthoclase and hedenbergite, and the Ba discrepancy is reduced.

A small center on the northeast flank of the shield volcano, Anahim Peak, produced seven hawaiite flows before a metaluminous trachyte plug filled the vent. Major and trace element contents of the trachyte, except for Sr, can be derived by 59 percent crystallization of hawaiite. The strontium discrepancy can be rectified by assuming a  $K_D$  of 6.0 for strontium in plagioclase.

Mathematically, the series of models which most accurately reproduce the compositions of the more differentiated lavas is hawaiite  $\rightarrow$  mugearite  $\rightarrow$  comenditic trachyte  $\rightarrow$  comendite. In order of appearance, the main phases crystallizing are olivine, clinopyroxene, plagioclase, iron-titanium oxides and alkali feldspar. In this manner, crystallization of alkali feldspar from a liquid of comenditic trachyte composition can account for the trace element contents of comenditic liquid, for they are incompatible with fractionation of phases found in more basic lavas. The same crystallization sequence was reported by Barberi et. al. (1975) for the Boina center in Ethiopia.

From oldest to youngest, the stratigraphic sequence of lavas erupted from the Rainbow Range center is comenditic trachyte-mugearite-comendite-hawaiite. Unfortunately the base of the section is not exposed within the study area. Two explanations are offered for the production of this sequence:

a) each pulse of basic magma introduced beneath the volcano differentiated for a different amount of time before erupting, or b) a zoned magma chamber existed beneath the volcano, and liquids at different depths were tapped at different times.

Derivation by crystal fractionation provides a simple and reasonable model for generation of the differentiated rock suite found in the Rainbow Range. However, trace element contents become harder to model as the rocks grow progressively more differentiated. This is partly due to the lack of accurately known distribution coefficients. It may also indicate open system behavior of trace elements by a volatile transfer mechanism when only small amounts of residual liquid remain. Data on halogen contents of the differentiated lavas and the relationship of residual trace elements (Rb, Nb, Zr, Y, Zr) to halogens are needed to examine this process.

#### ORIGIN OF THE ANAHIM VOLCANIC BELT

The Anahim volcanic belt runs east-west along approximately latitude 52° N. and consists of at least 37 Quaternary volcanic centers plus some Miocene and Pliocene centers (Souther, 1977). Compositionally the volcanic rocks range from alkali basalts through peralkaline, silicic differentiates. This east-west trend of highly alkaline volcanic centers is at a high angle to the Pemberton volcanic belt, a group of middle to late Miocene sub-volcanic plutons of calc-alkaline composition which parallel the continental margin of southwestern British Columbia. Together these belts outline the orientation and extent of the subducted Juan de Fuca plate in middle to Late Miocene time (Figure 3).

This pattern of paired volcanic belts of contrasting chemical types is repeated two other times within the late Cenozoic record in the Canadian Cordillera (Figure 23). The calc-alkaline Wrangell volcanic belt, generated

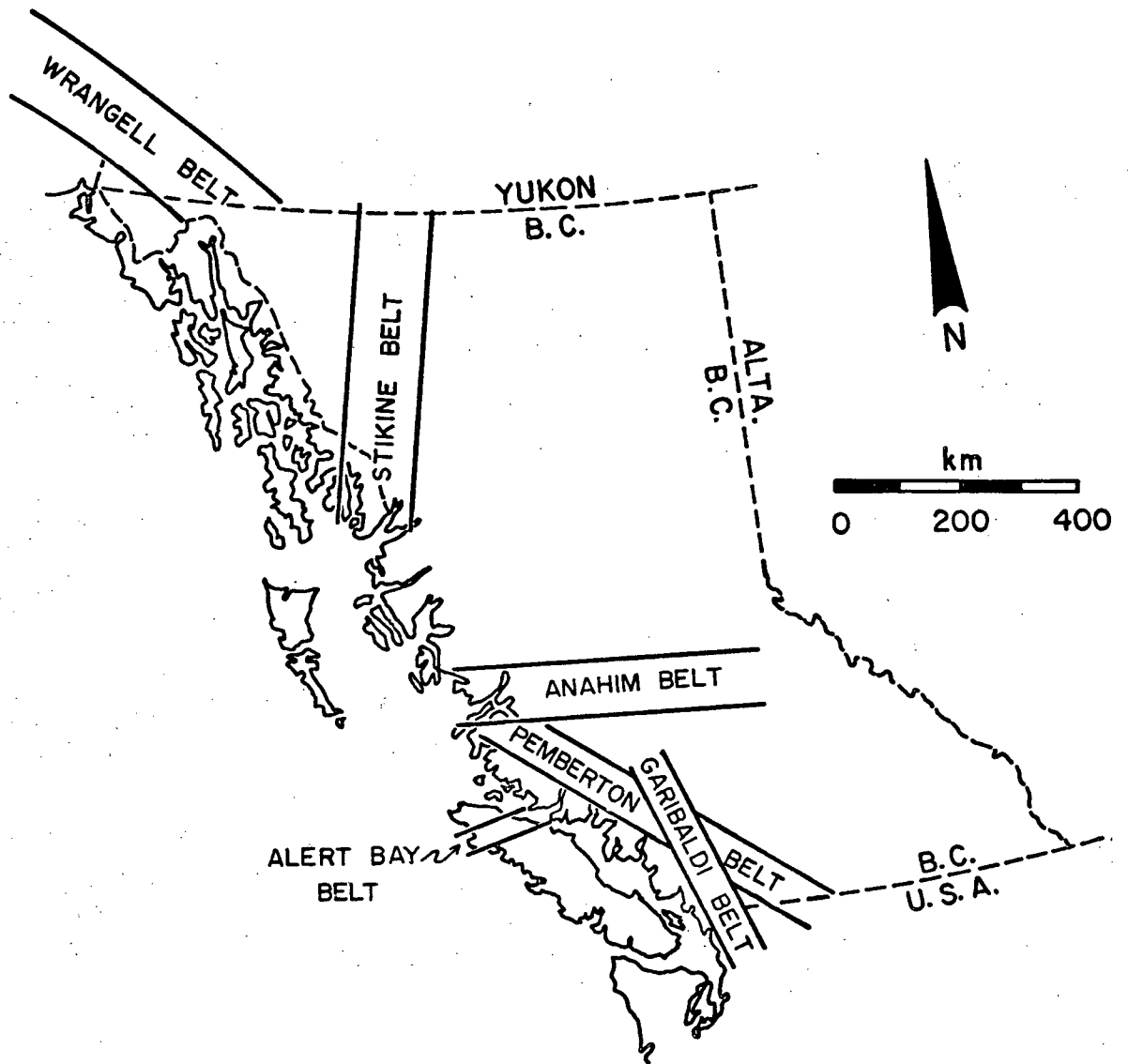


Figure 23. Late Cenozoic volcanic belts of the Canadian Cordillera. The Wrangell, Pemberton, and Garibaldi belts were the site of calc-alkaline volcanism, whereas the Stikine, Anahim, and Alert Bay belts were the site of alkaline to peralkaline volcanism.

by subduction of the Pacific plate beneath Alaska, is at an acute angle to, and separated from the alkaline to peralkaline Stikine volcanic belt of northwestern British Columbia. Volcanoes from both of these belts range in age from Miocene through Quaternary. The calc-alkaline Garibaldi volcanic belt, formed from subduction of the Juan de Fuca plate beneath southwestern British Columbia (Riddihough and Hyndman, 1976; Green, 1977), lies at a high angle to the Alert Bay volcanic belt on Vancouver Island, and the Anahim volcanic belt.

Continental alkaline to peralkaline volcanic suites are found in tensional settings, for example, the Stikine volcanic belt of northwestern British Columbia (Souther, 1970, 1977), the East Africa rift, Great Basin of the western United States, and Trans-Pecos of west Texas. There is little evidence for major faulting and offset along the trace of the Anahim volcanic belt, although east-west trending normal faults have been documented from the Ilgachuz Range (Tipper, 1969) and Itcha Range (Tipper, 1957).

Souther (1970, 1977) proposed that volcanic rocks of the Anahim volcanic belt were erupted from magma rising in deep fractures along the northern edge of the subducted Juan de Fuca plate. In Late Miocene time, while calc-alkaline volcanism was occurring in a belt parallel to the ancient continental margin (Pemberton volcanic belt) and indicating subduction of the Juan de Fuca plate beneath the North American plate, the northern edge of the subducted Juan de Fuca plate was sufficiently competent to disrupt the upper mantle, causing diapirism and subsequent partial melting of peridotite to produce alkali basalt. Thus, volcanic activity along the Anahim volcanic belt is an "edge effect" related to subduction of the Juan de Fuca plate. The tectonic setting is similar in many ways to that of the Samoan islands in the southwest Pacific, in which the Pacific plate is being buckled beneath the Australian plate along a transform fault at right angles to the Tonga trench.

The Samoan islands are constructed of alkaline lavas (thought to be derived from viscous shear melting of the upper mantle) which are erupted along the trace of this transform fault (Hawkins and Natland, 1975).

A second possible tectonic origin for the Anahim volcanic belt involves the movement of the North American plate over a mantle hot spot. Available dates from the Anahim belt (Figure 3) record eastward time transgression of volcanic activity, suggesting that volcanism in the Anahim volcanic belt is related to a mantle hot spot beneath British Columbia. Using the oldest date known from various volcanic centers in the belt, one can calculate that volcanic activity has moved eastward with time at a rate of 2.0 - 3.3 cm/year. This compares well with the 2.7 cm/year rate calculated for movement of hot spots beneath Yellowstone, Wyoming, and Raton, New Mexico (Minster et. al., 1974). In addition, the trend of the Anahim volcanic belt along approximately latitude  $52^{\circ}$  N. is a trend consistent with its being along a small circle to Minster et. al.'s (1974) pole to the other North American hot spot traces.

The common association of continental alkaline to peralkaline volcanic rocks with tensional environments leads one to speculate that lavas of the Anahim volcanic belt may have originated in a rift zone. The lack of normal faulting (such as is well documented in the Stikine belt (Souther, 1970, 1977)) casts some doubt on this possibility. Furthermore, it is difficult to relate an east-west trending rift zone with the probable tectonic setting at the time the Anahim volcanic rocks were being erupted.

Field relations show that along the entire length of the Anahim volcanic belt, basalt rose rapidly to the surface (as evidence by its primitive composition) through narrow conduits (as evidenced by the abundance of small one-pulse centers) (Souther, 1977). Where batches of alkali basalt were

trapped in long-lived magma reservoirs, salic differentiates had time to develop. This resulted in an evolutionary trend towards the establishment of more complex central volcanoes, built up of strongly differentiated lavas.

As a whole, the age, petrologic, and isotopic variations along the belt have not been systematically studied and are not well known. Alkali basalts are found along the length of the belt, while salic differentiates are reported only from the larger volcanic centers. In addition to oversaturated peralkaline volcanic rocks found in the Rainbow Range shield volcano, undersaturated varieties have been reported from the central part of the Itcha Range (B. Proffett, personal communication, 1977). Other peralkaline rocks are found on King, Lake, Campbell, Price, and Bardswell Islands, and near Tanya and Sigutlat Lakes.

Strontium isotopic studies suggest that the origin of these lavas is related to upper mantle processes. In fact, strontium isotopic studies combined with petrologic data show that volcanic rocks from the Anahim volcanic belt are consistent with an origin by partial melting of the upper mantle to produce the alkali basalts (Fiesinger and Nicholls, 1977), while modification by low pressure crystal fractionation of the alkali basalt magma, trapped in intracrustal magma chambers, produced the salic differentiates.

## CONCLUSIONS

### Eruptive History of the Rainbow Range Shield Volcano

Four petrologically distinct units make up the exposed stratigraphic section on the north flank of the Rainbow Range shield volcano:

- (1) Comenditic trachyte unit, characterized by thick greenish-grey flows, slightly peralkaline chemistry, and phenocrysts of grid-twinned anorthoclase ( $Or_{25-27}$ ), and hedenbergite.

- (2) Mugearite unit, distinguished by thin dark flows with intercalated flow breccia, and phenocrysts of plagioclase, olivine, and augite.
- (3) Comendite unit, the most voluminous unit on the north flank of the shield volcano, characterized by thick greenish-grey flows, peralkaline chemistry (including strongly enriched or depleted trace element contents), and phenocrysts of sanidine ( $Or_{34-37}$ ) and hedenbergite,  $\pm$  fayalite and arfvedsonite.
- (4) Hawaiite unit, notable for its restricted occurrence as capping flows and related feeders, primitive chemistry, and sparse phenocrysts of plagioclase, olivine, and augite.

The Anahim Peak lava flows are hawaiites which erupted from a vent now plugged by trachyte. These lavas are younger than those from the north flank of the shield volcano.

Basaltic lavas found along the Anahim volcanic belt typically were fissure-fed. A major constructional volcanic edifice formed only when a long-lived magma reservoir was established at depth. Magma stagnating in the reservoir had time to differentiate, and repeated eruption of evolved lavas in one area built the Rainbow Range shielded volcano. Oversaturated, peralkaline lavas are less viscous than calc-alkaline silicic lavas; hence the volcano has a shield-like morphology.

#### Origin of Rainbow Range Lavas and the Anahim Volcanic Belt

Lava flows that built up the north flank of the Rainbow Range likely originated by fractional crystallization of alkali basalt, a rock type common along the entire length of the Anahim volcanic belt. Data on volatile and other residual trace element (e.g. Zr, Y) contents are needed to evaluate the influence of a volatile phase on the distribution of trace elements between

cumulate and residual liquid, when the mass of the liquid is very small.

The Anahim and Pemberton volcanic belts outline the extent of the subducted Juan de Fuca plate during Late Miocene time. The Pemberton volcanic belt parallels the continental margin of southwestern British Columbia, whereas the Anahim volcanic belt lies along the probable trace of the northern edge of the subducted Juan de Fuca plate.

Three possible models have been suggested for the origin of the Anahim volcanic belt. These are:

- 1) the volcanic rocks are derived from magmas generated along the northern edge of the subducting Juan de Fuca plate.
- 2) the belt represents a surface trace marking the passage of the North American plate over a mantle hot spot.
- 3) the magmas were generated in an east-west trending rift zone.

Insufficient data is available at present to favor any one of these models.

TABLE I. POTASSIUM-ARGON ANALYTICAL DATA FOR VOLCANIC ROCKS FROM THE RAINBOW RANGE.

Sample	Location	Rock Type	% K <sup>a</sup>	<sup>40</sup> Ar <sub>rad</sub> <sup>b</sup> (x10 <sup>-6</sup> cc/g)	$\frac{100 \text{ } ^{40}\text{Ar}_{\text{rad}}}{\text{ } ^{40}\text{Ar}_{\text{total}}}$	Calculated Date (m.y.)
R-97	52 44'N, 125 52'W Northwest flank, Rainbow Range	comenditic trachyte	4.20, 4.24	1.461	60.0	8.7 ± 0.3
R-29	52 47'N, 125 43'W Tsitsutl Peak	comendite	4.21, 4.26	1.224	30.6	7.2 ± 0.3
R-25	52 45'N, 125 45'W Northeast flank, Rainbow Range	hawaiite	1.26, 1.28	0.402	68.0	7.9 ± 0.3
AP-15	52 45'N, 125 38'W Anahim Peak	hawaiite	1.37, 1.37	0.368	53.5	6.7 ± 0.3

a. Potassium analyses by M.L. Bevier using atomic absorption techniques; duplicate analyses are listed.

b. Argon analyses by J. Harakal and M.L. Bevier using MS10 spectrometer; constants used in calculations are:

$$\lambda_{\epsilon} = 0.585 \times 10^{-10} / \text{year}; \lambda_{\beta} = 4.72 \times 10^{-10} / \text{year}; \text{}^{40}\text{K}/\text{K} = 1.19 \times 10^{-4} \text{ (atom. ratio).}$$

TABLE II. MINERAL ASSEMBLAGES OF VOLCANIC ROCKS FROM THE RAINBOW RANGE.

Sample Number	Phenocrysts							Groundmass Phases							
	Plag.	Aug.	Fo.	Fa.	Hed.	Alk. Fs.	Opauques	Plag.	Aug./Ac.	Arf.	Aenig.	Alk. Fs.	Qtz.	Opauques	Glass
<u>Hawaiite</u>															
R-25	X	X	tr				X	X	tr						X
R-36	X	X	X				X	X	x						X
R-73	X	X	tr				X	X	x						X
R-77	X	X	X				X	X	x						X
<u>Mugearite</u>															
R-99	X	X	X				X	X	x			X			X
R-107	X	tr	X				X	X	x			X	tr		X
R-108	X	X	X				X	X	x			X			X
R-109	X	X	X				X	X	x			X			X
<u>Comenditic Trachyte</u>															
R-96					X	X	X		x	tr	X	X	X		X
R-97					X	X	tr		x		X	X	X		X
R-102					X	X	tr		x		X				X
R-106					X	X	tr		x		X				X
<u>Comendite</u>															
R-23					X	X	X		x	X	X	X	X		X
R-29					X	X	X		x	X	X	X	X		X
R-44				X	X	X	X		x	X	X	X	X		X
R-54					X	X	X		x		X	X	X		X
R-68				X	X	X	X		x	X	X	X	X		X
<u>Anahim Peak</u>															
<u>Hawaiite</u>															
AP-11	X	X	X				X	X	x						X
AP-15	X	X	X				X	X	x						X
<u>Anahim Peak Trachyte</u>															
AP-12	X	X	tr		tr	tr	X	X	x			tr			X

TABLE III. MICROPROBE ANALYSES OF OLIVINE PHENOCRYSTS.

	AP-11 8	R-25 14	AP-12 11	R-108 16	R-44 9	R-68 9	R-68 12
SiO <sub>2</sub>	37.04	37.10	37.52	37.42	26.43	28.77	29.28
TiO <sub>2</sub>	-	0.02	0.04	0.05	0.07	0.06	-
Al <sub>2</sub> O <sub>3</sub>	0.06	0.08	0.05	0.04	0.05	0.03	0.02
FeO	27.73	29.90	25.08	27.20	65.69	66.15	65.92
MnO	0.37	0.41	0.30	0.36	3.03	2.89	2.80
MgO	33.84	32.57	36.02	35.59	0.05	0.15	0.15
CaO	0.18	0.27	0.20	0.25	0.54	0.52	0.52
Na <sub>2</sub> O	0.02	0.02	0.02	0.01	0.02	0.05	0.06
K <sub>2</sub> O	-	0.01	0.01	-	0.03	0.03	-
SUM	99.24	100.38	99.24	100.92	95.91	98.65	98.75
Cations based on 4 oxygens							
Si	0.9987	0.9985	0.9983	0.9889	0.9503	0.9895	1.0015
Ti	-	0.0004	0.0008	0.0009	0.0019	0.0015	-
Al	0.0020	0.0026	0.0015	0.0013	0.0022	0.0011	0.0009
Fe <sup>2+</sup>	0.6253	0.6731	0.5580	0.6012	1.9755	1.9030	1.8858
Mn	0.0085	0.0094	0.0068	0.0080	0.0923	0.0842	0.0811
Mg	1.3600	1.3066	1.4282	1.4018	0.0026	0.0077	0.0077
Ca	0.0052	0.0077	0.0058	0.0070	0.0209	0.0190	0.0191
Na	0.0011	0.0013	0.0009	0.0007	0.0012	0.0034	0.0039
K	-	0.0003	0.0003	0.0002	0.0012	0.0013	-
ΣY	2.0021	2.0010	2.0015	2.0202	2.0959	2.0197	1.9985
ΣZ	0.9987	0.9989	0.9991	0.9898	0.9522	0.9910	1.0015
(atomic.%)							
Fo	68.03	65.43	71.45	69.46	0.12	0.38	0.39
Fa	31.28	33.71	27.92	29.79	94.46	94.49	94.59
Tph	0.43	0.47	0.34	0.40	4.41	4.18	4.07
La	0.26	0.39	0.29	0.35	1.00	0.94	0.96
Mg	68.21	65.69	71.66	69.70	0.12	0.38	0.39
Fe <sup>2+</sup>	31.36	33.84	28.00	29.89	95.42	95.40	95.50
Mn	0.43	0.47	0.34	0.40	4.45	4.22	4.11

TABLE IV. MICROPROBE ANALYSES OF PYROXENE PHENOCRYSTS AND GROUNDMASS GRAINS.

	R-79 3	R-36 9	R-25 22	AP-11 5	AP-15 21	AP-12 29	R-97 12
SiO <sub>2</sub>	51.85	51.65	51.62	49.21	49.79	50.97	48.30
TiO <sub>2</sub>	0.64	0.61	1.61	1.91	1.71	0.49	0.52
Al <sub>2</sub> O <sub>3</sub>	3.36	6.72	3.02	5.68	3.89	1.35	0.54
Fe <sub>2</sub> O <sub>3</sub> *	-	-	-	0.08	0.72	0.42	0.76
FeO	19.04	15.52	10.52	9.43	9.80	15.88	26.10
MnO	0.34	0.22	0.28	0.16	0.20	0.56	0.95
MgO	22.00	23.18	12.12	12.26	13.11	9.22	2.28
CaO	1.82	1.58	20.24	20.37	20.00	20.56	20.22
Na <sub>2</sub> O	0.09	0.12	0.39	0.65	0.52	0.50	0.37
K <sub>2</sub> O	0.02	0.01	0.03	0.02	0.02	0.03	0.01
SUM	99.16	99.61	99.83	99.77	99.76	99.98	100.05
Cations based on 6 oxygens							
Si	1.9236	1.8706	1.9331	1.8434	1.8741	1.9677	1.9718
Al	0.0764	0.1294	0.0669	0.1566	0.1259	0.0323	0.0260
Al	0.0704	0.1574	0.0663	0.0942	0.0466	0.0293	-
Ti	0.0179	0.0165	0.0454	0.0539	0.0484	0.0142	0.0160
Fe <sup>3+</sup>	-	-	-	0.0021	0.0203	0.0122	0.0232
Fe <sup>2+</sup>	0.5909	0.4700	0.3294	0.2955	0.3083	0.5129	0.8912
Mn	0.0106	0.0067	0.0090	0.0050	0.0064	0.0182	0.0329
Mg	1.2164	1.2514	0.6767	0.6847	0.7354	0.5306	0.1387
Ca	0.0725	0.0614	0.8123	0.8177	0.8065	0.8506	0.8845
Na	0.0062	0.0084	0.0282	0.0475	0.0378	0.0376	0.0292
K	0.0007	0.0064	0.0015	0.0007	0.0009	0.0013	0.0006
ΣX+Y	1.9856	1.9782	1.9688	2.0013	1.9640	1.9776	2.0163
ΣZ	2.0000	2.0000	2.0000	2.0000	2.0000	2.0000	1.9978
(atomic %)							
Ca	3.84	3.43	44.45	45.35	43.44	44.48	45.42
Mg	64.35	69.93	37.03	37.98	39.61	27.75	7.12
Fe <sup>2+</sup> + Mn	31.82	26.64	18.52	16.67	16.95	27.77	47.46
Na	0.34	0.48	2.70	4.60	3.47	3.42	2.67
Mg	66.68	72.06	64.86	66.30	67.60	48.27	12.70
Fe <sup>2+</sup> + Mn	32.98	27.45	32.44	29.10	28.93	48.31	84.62

\* Iron partitioned according to the method of Papike et. al. (1974).

TABLE IV. CONTINUED

	R-23 15	R-44 18	R-44 20	R-54 16	R-100b 14	Groundmass	
						R-44 2	1504**
SiO <sub>2</sub>	47.84	47.29	48.67	48.13	47.94	62.15	52.58
TiO <sub>2</sub>	0.60	0.39	0.40	0.46	0.60	0.72	4.56
Al <sub>2</sub> O <sub>3</sub> *	0.38	0.09	0.13	0.14	0.35	0.93	0.70
Fe <sub>2</sub> O <sub>3</sub>	0.59	3.52	2.88	3.01	1.47	6.16	25.46
FeO*	28.45	27.49	27.81	27.83	28.08	12.16	2.89
MnO	1.17	1.10	1.05	1.01	1.15	0.31	0.42
MgO	0.35	0.03	0.04	0.05	0.48	0.06	0.04
CaO	20.06	17.60	18.37	17.57	19.06	4.84	0.18
Na <sub>2</sub> O	0.47	1.61	1.51	1.61	0.50	3.51	13.65
K <sub>2</sub> O	0.01	0.02	0.01	-	-	0.41	-
SUM	99.92	99.14	100.87	99.81	99.63	91.25	100.48
Cations based on 6 oxygens							
Si	1.9802	1.9930	2.0043	2.0048	1.9885	2.4691	1.99
Al	0.0185	0.0044	-	-	0.0115	-	0.01
Al	-	-	0.0065	0.0069	0.0055	0.0436	0.03
Ti	0.0188	0.0123	0.0125	0.0143	0.0187	0.0215	0.13
Fe <sup>3+</sup>	0.0185	0.1116	0.0892	0.0942	0.0092	0.1841	0.73
Fe <sup>2+</sup>	0.9849	0.9691	0.9577	0.9692	1.0113	0.4039	0.10
Mn	0.0411	0.0391	0.0365	0.0356	0.0404	0.0103	0.01
Mg	0.0185	0.0016	0.0024	0.0034	0.0299	0.0036	-
Ca	0.8895	0.7949	0.8106	0.7841	0.8472	0.2060	0.01
Na	0.0376	0.1318	0.1207	0.1297	0.0406	0.2707	1.00
K	0.0004	0.0011	0.0003	-	-	0.0206	-
ΣX+Y	2.0093	2.0615	2.0364	2.0374	2.0028	1.1643	2.01
ΣZ	1.9987	1.9974	2.0043	2.0048	2.0000	2.4691	2.00
(atomic %)							
Ca	45.99	44.05	44.85	43.75	43.92	33.02	8.33
Mg	0.96	0.09	0.13	0.19	1.55	0.58	8.33
Fe <sup>2+</sup> + Mn	53.05	55.87	55.01	56.06	54.53	66.40	83.33
Na	3.47	11.55	10.80	11.40	3.62	39.32	90.09
Mg	1.71	0.14	3.27	0.30	2.66	0.52	-
Fe <sup>2+</sup> + Mn	94.82	88.31	88.98	88.30	93.72	60.16	9.91

\* Iron partitioned according to the method of Papike et. al. (1974).

\*\* Analysis from Becker (1976).

TABLE V. MICROPROBE ANALYSES OF AMPHIBOLE GRAINS.

	R-54 23	R-54 24	R-54 28	R-68 19
SiO <sub>2</sub>	46.57	47.62	49.80	48.85
TiO <sub>2</sub>	0.57	0.46	0.46	0.33
Al <sub>2</sub> O <sub>3</sub>	0.15	0.18	2.01	0.17
Fe <sub>2</sub> O <sub>3</sub> *	-	1.42	10.29	1.25
FeO*	35.04	33.76	16.08	34.04
MnO	1.23	1.20	0.53	1.14
MgO	0.10	0.08	0.06	0.05
CaO	2.09	2.07	8.27	2.44
Na <sub>2</sub> O	7.64	6.65	7.59	7.06
K <sub>2</sub> O	1.48	1.32	0.72	1.23
SUM	94.87	94.76	95.81	96.56
Cations based on 23 oxygens				
Si	7.9144	8.0407	8.0516	8.0721
Al	0.0305	-	-	-
Al	-	0.0352	0.3838	0.0339
Ti	0.0724	0.0586	0.0561	0.0407
Fe <sup>3+</sup>	-	0.1847	1.2515	0.1552
Fe <sup>2+</sup>	4.9799	4.7676	2.1747	4.7036
Mn	0.1765	0.1713	0.0730	0.1601
Mg	0.0251	0.0193	0.0140	0.0117
Ca	0.3809	0.3746	1.4321	0.4326
Na	1.4175	1.3996	0.4809	1.3956
Na	1.0988	0.7785	1.8970	0.8656
K	0.3202	0.2840	0.1495	0.2595
ΣZ	7.9449	8.0407	8.0516	8.0721
ΣX	5.0523	5.0109	3.8660	4.9334
ΣY	2.0000	2.0000	2.0000	2.0000
ΣW	1.4190	1.0625	2.0465	1.1251
(atomic %)				
Mg	0.86	0.75	0.37	0.43
Ca	13.03	14.56	37.45	15.99
Na	86.11	84.69	62.18	83.58

\*Iron partitioned according to the method of Papike et. al. (1974).

TABLE VI. MICROPROBE ANALYSES OF AENIGMATITE.

	R-44 *	R-54	2 **
	1	26	
SiO <sub>2</sub>	40.92	39.59	41.70
TiO <sub>2</sub>	8.18	7.91	6.95
Al <sub>2</sub> O <sub>3</sub>	0.23	0.40	0.29
FeO	42.30	39.93	42.30
MnO	0.79	1.10	0.71
MgO	-	0.06	0.11
CaO	0.16	0.23	0.32
Na <sub>2</sub> O	7.67	4.78	7.20
K <sub>2</sub> O	-	-	0.11
SUM	100.08	94.00	99.69
Cations based on 20 oxygens			
Si	5.827	6.0409	5.97
Ti	0.876	0.9072	0.75
Al	0.040	0.0718	0.05
Fe <sup>2+</sup>	4.952	5.0955	5.01
Mn	0.096	0.1422	0.09
Mg	-	0.0131	0.03
Ca	0.025	0.0374	0.05
Na	2.119	1.4153	2.00
K	-	-	0.02
(atomic %)			
$\frac{100 \times \text{Ti}}{\text{Fe} + \text{Ti}}$	15.03	15.11	13.02

\* Analysis supplied by B. Proffett (University of Calgary).

\*\* Analysis from Yagi and Souther (1974).

TABLE VII. MICROPROBE ANALYSES OF FELDSPAR PHENOCRYSTS.

	AP-11 1	AP-15 5	R-25 1b	R-25 7	R-36 5	R-108 1	R-108 3
SiO <sub>2</sub>	57.96	53.02	54.21	55.65	55.86	56.09	54.78
TiO <sub>2</sub>	0.06	0.12	0.14	0.11	0.09	0.06	0.10
Al <sub>2</sub> O <sub>3</sub>	26.45	29.62	29.86	28.20	27.95	27.76	27.94
FeO	0.26	0.55	0.56	0.57	0.32	0.50	0.52
MnO	0.04	-	-	0.03	-	0.03	-
MgO	0.03	0.05	0.08	0.09	0.07	0.06	0.07
CaO	9.03	12.45	11.24	11.26	10.49	10.31	10.58
Na <sub>2</sub> O	5.87	4.40	4.27	4.58	4.68	5.31	5.47
K <sub>2</sub> O	0.46	0.36	0.27	0.35	0.41	0.37	0.41
SUM	100.16	100.57	100.63	100.84	99.87	100.49	98.87
Cations based on 8 oxygens							
Si	2.5942	2.3971	2.4309	2.4915	2.5148	2.5162	2.4822
Ti	0.0019	0.0041	0.0046	0.0039	0.0031	0.0022	0.0034
Al	1.3955	1.5785	1.5780	1.4884	1.4829	1.4680	1.4919
Fe	0.0097	0.0209	0.0209	0.0212	0.0119	0.0189	0.0197
Mn	0.0017	0.0001	-	0.0013	-	0.0012	-
Mg	0.0022	0.0003	0.0056	0.0059	0.0048	0.0041	0.0049
Ca	0.4330	0.6021	0.5339	0.5400	0.5060	0.4955	0.5138
Na	0.5099	0.3853	0.3712	0.3976	0.4083	0.4618	0.4810
K	0.0262	0.0206	0.0156	0.0199	0.0234	0.0212	0.0239
ΣZ	3.9916	3.9797	4.0135	3.9838	4.0008	3.9864	3.9775
ΣX	0.9827	1.0293	0.9472	0.9859	0.9544	1.0027	1.0433
(atomic %)							
An	44.68	59.73	57.99	56.40	53.96	50.64	50.44
Ab	52.62	38.22	40.32	41.52	43.54	47.19	47.22
Or	2.70	2.04	1.69	2.08	2.50	2.17	2.35

TABLE VII. CONTINUED

	AP-12 9	R-97 1	R-97 3	R-97 7	R-44 3	R-44 4	R-54 5
SiO <sub>2</sub>	62.17	67.46	66.64	66.41	69.17	68.98	67.64
TiO <sub>2</sub>	0.01	-	-	0.02	0.01	-	-
Al <sub>2</sub> O <sub>3</sub>	22.90	19.36	18.76	19.45	17.54	17.25	18.29
FeO	0.56	0.22	0.20	0.20	0.44	0.70	0.31
MnO	0.01	-	0.03	-	0.02	-	-
MgO	0.01	-	-	-	0.02	-	-
CaO	4.61	0.89	0.85	1.35	-	-	0.15
Na <sub>2</sub> O	8.22	8.12	7.96	8.24	7.37	7.32	7.19
K <sub>2</sub> O	0.96	4.66	4.91	3.73	6.00	5.98	6.11
SUM	99.45	100.71	99.35	99.40	100.57	100.23	99.69
Cations based on 8 oxygens							
Si	2.7807	2.9794	2.9885	2.9645	3.0615	3.0662	3.0246
Ti	0.0004	-	-	0.0007	0.0004	0.0001	-
Al	1.2074	1.0079	0.9913	1.0232	0.9147	0.9037	0.9641
Fe	0.0208	0.0081	0.0074	0.0074	0.0164	0.0262	0.0116
Mn	0.0003	-	0.0011	0.0002	0.0009	0.0001	-
Mg	0.0009	-	0.0003	-	0.0015	0.0002	-
Ca	0.2208	0.0421	0.0408	0.0645	-	0.0002	0.0073
Na	0.7129	0.6953	0.6918	0.7130	0.6325	0.6310	0.6230
K	0.0547	0.2627	0.2811	0.2125	0.3386	0.3393	0.3484
ΣZ	3.9885	3.9873	3.9798	3.9884	3.9766	3.9700	3.9887
ΣX	1.0104	1.0082	1.0225	0.9976	0.9899	0.9971	0.9903
(atomic %)							
An	22.34	4.21	4.02	6.52	-	0.02	0.75
Ab	72.13	69.52	68.25	72.02	63.22	65.02	63.66
Or	5.53	26.27	27.73	21.46	34.87	34.96	35.60

TABLE VII. CONTINUED

	R-68 1	R-68 5	R100b 6
SiO <sub>2</sub>	68.46	67.56	68.27
TiO <sub>2</sub>	0.04	0.04	0.03
Al <sub>2</sub> O <sub>3</sub>	18.39	18.33	17.54
FeO	0.46	0.24	0.29
MnO	-	0.02	-
MgO	-	-	-
CaO	0.11	0.02	0.17
Na <sub>2</sub> O	7.15	7.02	7.05
K <sub>2</sub> O	6.00	6.28	6.41
SUM	100.61	99.51	99.76
Cations based on 8 oxygens			
Si	3.0300	3.0254	3.0513
Ti	0.0014	0.0015	0.0008
Al	0.9591	0.9675	0.9240
Fe	0.0171	0.0009	0.0108
Mn	-	0.0007	-
Mg	-	0.0001	-
Ca	0.0052	0.0009	0.0082
Na	0.6139	0.6098	0.6110
K	0.3389	0.3590	0.3655
ΣZ	3.9905	3.9944	3.9761
ΣX	0.9751	0.9714	0.9955
(atomic %)			
An	0.54	0.09	0.83
Ab	64.08	62.89	62.05
Or	35.38	37.02	37.12

TABLE VIII. MICROPROBE ANALYSES OF TITANOMAGNETITE.

	AP-11 12	AP-15 24	R-117 20	R-108 21	AP-12 18	R-97 17	R-23 9
SiO <sub>2</sub>	0.07	0.14	0.34	0.11	0.12	0.24	0.27
TiO <sub>2</sub>	17.26	19.50	24.53	21.32	21.30	23.67	28.39
Al <sub>2</sub> O <sub>3</sub>	1.79	2.73	3.81	2.09	0.46	0.20	0.06
FeO	73.79	70.29	65.10	70.83	74.29	67.45	61.50
MnO	0.38	0.48	0.41	0.54	0.88	1.07	1.25
MgO	1.32	2.13	3.23	1.01	0.28	0.06	0.01
CaO	0.06	0.01	0.04	-	0.05	-	-
SUM	94.66	95.25	97.46	95.91	97.38	92.70	91.48
Recalculated Analyses, Ulvospinel basis							
FeO	44.37	45.62	49.30	48.76	49.74	50.54	54.14
Fe <sub>2</sub> O <sub>3</sub>	32.70	27.97	17.56	24.53	27.28	18.79	8.17
TOTAL	97.94	98.55	99.22	98.36	100.11	94.58	92.29
Mol. % Usp	50.08	56.08	69.86	61.62	60.71	71.61	87.46

TABLE IX. MICROPROBE ANALYSES OF ILMENITE.

	AP-11 11	AP-15 26	R-117 14	R-108 22	AP-12 20	R-97 16	R-54 9
SiO <sub>2</sub>	0.03	0.09	0.08	-	0.08	0.08	0.04
TiO <sub>2</sub>	49.81	50.97	46.81	48.18	50.28	46.55	51.04
Al <sub>2</sub> O <sub>3</sub>	0.14	0.17	1.43	0.33	0.05	0.12	0.01
FeO	47.75	44.53	42.08	47.47	48.08	44.22	46.48
MnO	0.48	0.61	0.58	0.37	0.63	1.10	2.05
MgO	2.00	3.47	3.41	2.87	0.92	0.05	0.01
CaO	0.05	-	0.23	0.03	0.03	0.88	0.02
SUM	100.28	99.85	94.81	99.25	100.08	93.00	99.65
Recalculated Analyses, Ilmenite basis							
FeO	43.12	41.02	38.18	41.18	44.68	41.21	44.72
Fe <sub>2</sub> O <sub>3</sub>	5.14	3.91	4.33	6.99	3.74	3.34	1.96
TOTAL	100.79	100.25	95.24	99.95	100.42	93.33	99.85
Mol. % R <sub>2</sub> O <sub>3</sub>	4.89	3.74	5.32	6.76	3.55	3.49	1.87

TABLE X. WHOLE ROCK MAJOR-ELEMENT VOLATILE-FREE ANALYSES RECALCULATED TO 100 PERCENT, VOLATILE-INCLUDED ORIGINAL SUMS, TRACE-ELEMENT ANALYSES, AND NORMATIVE MINERALOGIES.

	Precision *	Hawaiite						Mugearite	
		AP-11	AP-15	R-25	R-36	R-73	R-77	R-99	R-107
SiO <sub>2</sub>	±1%	49.74	50.33	50.30	48.85	50.62	49.83	54.92	56.30
TiO <sub>2</sub>	±2%	1.76	2.29	1.98	2.18	2.79	2.37	1.71	1.63
Al <sub>2</sub> O <sub>3</sub>	±1%	15.29	16.17	16.54	17.90	15.76	16.45	15.69	16.02
Fe <sub>2</sub> O <sub>3</sub>	±1%	12.91	12.84	12.89	12.60	14.61	13.25	11.41	11.00
MnO	±1%	0.15	0.14	0.19	0.14	0.17	0.15	0.14	0.13
MgO	±4%	7.03	4.32	3.18	5.18	3.51	4.87	2.69	2.14
CaO	±1%	8.19	8.01	8.52	8.12	6.79	7.68	5.75	5.35
Na <sub>2</sub> O	±5%	3.41	4.16	4.43	3.51	3.52	3.58	4.57	4.21
K <sub>2</sub> O	±5%	1.13	1.57	1.46	1.15	1.80	1.42	2.60	2.80
P <sub>2</sub> O <sub>5</sub>	±30%	0.38	0.17	0.51	0.36	0.44	0.40	0.52	0.44
L.O.I. **		1.23	0.74	0.00	0.00	0.00	0.90	1.88	1.97
ORIGINAL SUM		98.83	100.29	99.40	98.73	102.88	101.19	99.03	102.67
Rb	±5%	18.4	24.9	17.5	15.9	25.5	18.4	31.1	40.5
Sr	±5%	497.0	568.2	619.1	649.1	451.8	527.7	468.7	432.7
Ba	±5%	329.0	431.9	1154.4	290.0	613.3	397.9	663.3	618.6
Nb	±15%	24.7	33.5	23.8	26.9	27.6	28.2	42.7	46.0
Ni	±5%	96.1	47.0	21.5	39.2	21.7	36.6	10.9	10.0
Rb/Sr		0.037	0.044	0.028	0.024	0.056	0.035	0.066	0.094
K/Rb		504	522	686	594	601	648	681	587
K/Ba		28.2	30.1	10.4	32.6	25.0	30.0	32.0	38.4
K/Sr		18.8	22.9	19.5	14.7	33.0	22.3	45.9	53.6
Ba/Sr		0.7	0.8	1.9	0.5	1.4	0.8	1.4	1.4
Ca/Sr		117.8	100.8	98.4	89.4	107.4	104.0	87.7	88.4
Q		-	-	-	-	-	-	1.66	5.22
Or		6.68	9.28	8.63	6.80	8.39	8.39	15.36	16.55
Ab		28.85	34.62	35.61	29.70	29.79	30.29	38.67	35.62
An		23.08	20.81	20.93	29.69	23.01	24.62	14.62	16.55
Ne		-	0.31	1.02	-	-	-	-	-
Ac		-	-	-	-	-	-	-	-
Ns		-	-	-	-	-	-	-	-
Di { Wo		6.29	7.44	7.52	3.44	3.37	4.54	4.39	2.97
En		3.62	3.68	3.12	1.84	1.44	2.33	1.87	1.14
Fs		2.39	3.62	4.43	1.49	1.93	2.10	2.53	1.88
Hy { En		6.37	-	-	4.73	7.30	6.54	4.83	4.19
Fs		4.20	-	-	3.84	9.82	5.89	6.55	6.91
Ol { Fo		5.27	4.96	3.36	4.44	-	2.28	-	-
Fa		3.83	5.38	5.26	3.98	-	2.27	-	-
Mt		4.19	4.16	4.18	4.09	4.74	4.29	4.22	4.06
Ilm		3.34	4.35	3.76	4.14	5.30	4.50	3.25	3.10
Ap		0.88	0.39	1.18	0.83	0.93	0.93	1.20	1.02
Cor		-	-	-	-	-	-	-	-

\* Precision is based on replicate analyses of U.S.G.S. rock standard AGV-1.

\*\* Loss on ignition at 1000°C.

TABLE X. CONTINUED

	Mugearite		Trachyte	Comenditic Trachyte			
	R-108	R-109	AP-12	R-96	R-97	R-102	R-106
SiO <sub>2</sub>	54.93	54.64	61.33	67.81	68.32	66.07	64.82
TiO <sub>2</sub>	1.44	1.92	0.64	0.32	0.34	0.39	0.45
Al <sub>2</sub> O <sub>3</sub>	18.69	15.25	17.31	14.51	14.97	15.00	16.25
Fe <sub>2</sub> O <sub>3</sub>	9.03	11.62	6.39	4.63	4.39	6.16	5.79
MnO	0.12	0.15	0.11	0.10	0.07	0.14	0.14
MgO	1.86	2.46	0.56	0.00	0.03	0.00	0.01
CaO	6.71	5.80	2.83	0.95	1.00	1.27	1.82
Na <sub>2</sub> O	4.66	5.04	6.18	6.61	5.88	5.70	6.19
K <sub>2</sub> O	2.14	2.61	4.24	5.00	4.92	5.20	4.43
P <sub>2</sub> O <sub>5</sub>	0.42	0.50	0.42	0.07	0.07	0.08	0.10
L.O.I.	0.00	0.00	0.00	0.00	0.75	1.15	0.54
ORIGINAL							
SUM	98.34	97.95	99.07	97.13	96.92	100.43	97.92
Rb	32.5	34.7	54.7	75.7	78.4	68.1	49.2
Sr	624.7	491.1	267.9	13.0	34.4	7.4	155.5
Ba	579.1	616.0	1050.9	346.9	781.8	46.9	1002.5
Nb	39.0	42.3	44.5	79.9	73.6	55.5	65.6
Ni	13.5	11.1	12.6	10.7	8.9	15.0	9.0
Rb/Sr	0.052	0.071	0.204	5.823	2.279	9.203	0.316
K/Rb	535	611	635	532	504	635	730
K/Ba	30.0	34.4	33.1	116.0	50.5	921.6	35.9
K/Sr	28.4	44.0	131.1	3184.6	1184.2	5818.4	235.9
Ba/Sr	0.9	1.3	3.9	26.7	22.7	6.3	6.5
Ca/Sr	76.8	84.4	75.5	522.3	207.8	1226.6	83.7
Q	1.91	-	1.80	11.66	12.48	9.09	6.82
Or	12.65	15.42	25.06	29.55	29.07	30.73	26.18
Ab	39.43	42.65	52.29	46.80	49.61	48.21	52.38
An	23.76	11.28	6.97	-	-	-	3.47
Ne	-	-	-	-	-	-	-
Ac	-	-	-	3.41	0.13	0.02	-
Ns	-	-	-	1.22	-	-	-
Di {	2.83	5.94	1.81	1.78	1.88	2.41	2.05
En {	1.13	2.43	0.38	-	0.04	-	0.01
Fs {	1.73	3.56	1.55	2.02	2.09	2.74	2.31
Hy {	3.50	3.13	1.01	-	0.04	-	0.01
Fs {	5.34	4.58	4.11	3.33	1.99	3.17	3.11
Ol {	-	0.40	-	-	-	-	-
Fa {	-	0.64	-	-	-	-	-
Mt	3.33	4.29	2.36	-	1.56	2.26	2.15
Ilm	2.73	3.65	1.22	0.61	0.65	0.74	0.85
Ap	0.97	1.16	0.97	0.16	0.16	0.19	0.23
Cor	-	-	-	-	-	-	-



TABLE X. CONTINUED

	Comendite							
	R-48	R-51	R-54	R-71	R-76	R-81	R-88	R-116
SiO <sub>2</sub>	69.00	67.02	69.03	68.79	65.43	66.34	68.12	71.66
TiO <sub>2</sub>	0.41	0.41	0.37	0.36	0.40	0.41	0.39	0.41
Al <sub>2</sub> O <sub>3</sub>	12.25	14.07	12.77	13.56	14.49	16.15	13.67	11.83
Fe <sub>2</sub> O <sub>3</sub>	7.69	7.00	6.29	6.16	7.48	5.32	6.47	6.00
MnO	0.13	0.15	0.12	0.12	0.13	0.10	0.13	0.08
MgO	0.00	0.00	0.00	0.00	0.00	0.00	0.00	0.00
CaO	0.35	0.71	0.51	0.49	1.17	1.26	0.50	0.25
Na <sub>2</sub> O	5.31	5.48	5.89	5.60	5.51	5.05	5.77	5.04
K <sub>2</sub> O	4.82	5.11	4.96	4.85	5.31	5.29	4.90	4.68
P <sub>2</sub> O <sub>5</sub>	0.06	0.06	0.06	0.05	0.08	0.08	0.06	0.05
L.O.I.	1.48	0.92	0.45	0.38	1.15	1.68	0.49	0.00
ORIGINAL SUM	100.42	100.59	98.94	103.06	98.36	102.15	101.26	99.95
Rb	70.1	62.8	87.0	81.6	59.8	61.3	85.4	81.5
Sr	10.5	3.8	2.7	2.5	10.3	7.4	1.2	3.3
Ba	15.8	30.3	11.4	9.7	65.5	61.3	10.3	14.3
Nb	98.3	62.7	77.5	79.8	42.4	53.7	83.5	90.4
Ni	8.7	9.5	7.5	8.4	8.7	8.5	9.2	8.3
Rb/Sr	6.676	16.526	32.222	32.640	5.806	8.284	74.430	24.697
K/Rb	572	678	467	507	723	729	481	475
K/Ba	2536.4	1404.6	3566.2	4268.0	659.9	729.4	3987.3	2709.8
K/Sr	3800.9	11134.	15211.	559.3	4268.6	5919.1	34250.	11743.
Ba/Sr	1.5	8.0	4.2	3.9	6.4	8.3	8.6	4.3
Ca/Sr	238.2	1335.4	1350.0	1400.8	811.8	1216.9	2977.9	541.4
Q	19.61	12.87	18.17	16.27	9.41	12.14	14.70	25.09
Or	28.48	30.20	29.31	28.66	31.38	31.26	28.96	27.66
Ab	36.18	43.92	38.07	42.75	44.97	42.73	43.03	34.80
An	-	-	-	-	-	5.73	-	-
Ne	-	-	-	-	-	-	-	-
Ac	6.22	2.16	5.06	4.09	1.46	-	5.10	4.83
Ns	0.39	-	1.40	-	-	-	-	0.55
Wo	0.56	1.31	0.89	0.88	2.21	-	0.87	0.38
Di {	-	-	-	-	-	-	-	-
En	-	-	-	-	-	-	-	-
Fs	0.64	1.48	1.01	1.00	2.50	-	0.99	0.43
Hy {	-	-	-	-	-	-	-	-
En	-	-	-	-	-	-	-	-
Fs	8.09	5.46	6.09	5.72	4.67	4.62	6.28	6.18
Ol {	-	-	-	-	-	-	-	-
Fo	-	-	-	-	-	-	-	-
Fa	-	-	-	-	-	-	-	-
Mt	-	1.75	-	0.45	2.30	2.15	0.07	-
Ilm	0.78	0.78	0.70	0.68	0.76	0.78	0.74	0.78
Ap	0.14	0.14	0.14	0.12	0.19	0.19	0.14	0.12
Cor	-	-	-	-	-	0.02	-	-

TABLE XI. STRONTIUM ISOTOPIC DATA.<sup>d</sup>

Sample	SiO <sub>2</sub> <sup>a</sup> (wt.%)	Rb <sup>a</sup> (ppm)	Sr <sup>a</sup> (ppm)	Rb/Sr	Sr <sup>87</sup> /Sr <sup>86</sup> <sup>b</sup>	Sr <sup>87</sup> /Sr <sup>86</sup> <sub>o</sub>	K-Ar Date (m.y.)
AP-12	60.76	54.7	267.9	0.204±3%	.7032 ± .00015	-	-
AP-15	50.48	24.9	568.2	0.044±3%	.7032 ± .00015	-	-
R-25	50.00	17.5	619.1	0.028±3%	.7032 ± .00015	-	-
R-108	54.02	32.5	624.7	0.052±3%	.7031 ± .0003	-	-
R-97	66.22	78.4	34.4	2.279±3%	.7042 ± .0003	.7034±.0004	8.7
R-23	66.55	62.3	6.6	9.44±15%	.7060 ± .0003	.7029±.0005	7.9 <sup>c</sup>
R-29	67.31	77.9	3.6	21.64±15%	.7081 ± .0003	.7017±.0006	7.2
R-88	68.98	85.4	1.2	74.43±20%	.727 ± .0023	.7025±.011	8.0 <sup>c</sup>

a. SiO<sub>2</sub>, Rb, Sr done by X-ray fluorescence spectrometry by M.L. Bevier.

b. Sr<sup>87</sup>/Sr<sup>86</sup> measured on mass spectrometer by M.L. Bevier and K.L. Scott.

c. These ages are estimated on the basis of stratigraphic position.

d. Precision of Rb/Sr based on replicate analyses of Rb and Sr. Error in measured Sr<sup>87</sup>/Sr<sup>86</sup> ratios is 1 σ. Error in calculated Sr<sup>87</sup>/Sr<sup>86</sup> ratios represents the combination of errors in Rb/Sr, Sr<sup>87</sup>/Sr<sup>86</sup>, and dates.

TABLE XII. CALCULATED AND OBSERVED VISCOSITIES ( $\eta$ ).

Temperature	950 <sup>o</sup> C	950 <sup>o</sup> C	1200 <sup>o</sup> C	1200 <sup>o</sup> C	Reference
Water Content (wt. %)	0	1	0	0	
Comenditic trachyte (3) <sup>a</sup>	1.1 x 10 <sup>7</sup>	1.5 x 10 <sup>6</sup>	9.4 x 10 <sup>4</sup>	1.2 x 10 <sup>4</sup>	This study <sup>b</sup>
Comendite (4) <sup>a</sup>	1.5 x 10 <sup>7</sup>	2.0 x 10 <sup>6</sup>	1.2 x 10 <sup>5</sup>	1.7 x 10 <sup>4</sup>	This study <sup>b</sup>
Pantellerite	-	-	-	6.3 x 10 <sup>4</sup>	Scarfe, 1977 <sup>c</sup>
Calc-alkaline rhyolite (10) <sup>a</sup>	7.8 x 10 <sup>8</sup>	4.5 x 10 <sup>7</sup>	3.3 x 10 <sup>6</sup>	4.4 x 10 <sup>5</sup>	Schminke, 1974 <sup>b</sup>
Hawaiian tholeiite	-	-	4 x 10 <sup>2</sup>	-	Shaw et al., 1969 <sup>c</sup>
Ne-bearing alkaline basalt	-	-	4 x 10 <sup>2</sup>	-	Bottinga and Weill, 1972 <sup>c</sup>

a. Number of analyses averaged for calculating viscosities.

b. Calculated using the method of Shaw (1972).

c. Determined experimentally.

TABLE XIII. LEAST-SQUARES MASS BALANCE CALCULATION DERIVING MUGEARITE FROM HAWAIIITE.

	<u>Parent</u>	<u>Observed</u> <u>Daughter</u>	<u>Calculated</u> <u>Daughter</u>	<u>Variable</u>	<u>Wt. Fraction</u>
	R-36	R-99			
SiO <sub>2</sub>	48.92	55.00	54.94	Olivine	15.86
TiO <sub>2</sub>	2.18	1.71	1.68	Plagioclase	65.37
Al <sub>2</sub> O <sub>3</sub>	17.93	15.71	15.72	Augite	8.27
Fe <sub>2</sub> O <sub>3</sub>	12.62	11.53	11.40	Magnetite	7.52
MgO	5.19	2.69	2.70	Ilmenite	2.05
CaO	8.13	5.76	5.77	Apatite	0.92
Na <sub>2</sub> O	3.52	4.58	4.57		
K <sub>2</sub> O	1.15	2.60	2.80		
P <sub>2</sub> O <sub>5</sub>	0.36	0.52	0.44		
		$\Sigma r^2 = 0.0504$			
Rb	15.9	31.1	49.9		
Sr	649.1	468.7	463.1		
Ba	290.0	663.3	705.2		
Ni	39.2	10.9	10.2		
Mass of New Magma Relative to Old = 29.29 weight percent					

TABLE XIV. LEAST-SQUARES MASS BALANCE CALCULATION DERIVING  
COMENDITIC TRACHYTE FROM HAWAIIITE.

	<u>Parent</u>	<u>Observed</u> <u>Daughter</u>	<u>Calculated</u> <u>Daughter</u>	<u>Variable</u>	<u>Wt. Fraction</u>
	R-36	R-97			
SiO <sub>2</sub>	48.92	68.04	67.88	Olivine	14.84
TiO <sub>2</sub>	2.18	0.32	0.28	Plagioclase	63.90
Al <sub>2</sub> O <sub>3</sub>	17.93	14.45	14.45	Augite	9.39
Fe <sub>2</sub> O <sub>3</sub>	12.62	4.61	4.58	Magnetite	8.97
MgO	5.19	0.00	0.00	Ilmenite	1.74
CaO	8.13	0.95	0.96	Apatite	1.15
Na <sub>2</sub> O	3.52	6.58	6.57		
K <sub>2</sub> O	1.15	4.98	5.20		
P <sub>2</sub> O <sub>5</sub>	0.36	0.07	0.02		
		$\Sigma r^2 = 0.0645$			
Rb	15.9	78.4	96.5		
Sr	649.1	34.4	203.4		
Ba	290.0	781.8	1082.3		
Ni	39.2	8.9	3.9		
Mass of New Magma Relative to Old = 14.04 weight percent					

TABLE XV. LEAST-SQUARES MASS BALANCE CALCULATION DERIVING COMENDITE FROM HAWAIIITE.

	<u>Parent</u>	<u>Observed</u> <u>Daughter</u>	<u>Calculated</u> <u>Daughter</u>	<u>Variable</u>	<u>Wt. Fraction</u>
	R-36	R-48			
SiO <sub>2</sub>	48.92	69.08	68.97	Olivine	15.10
TiO <sub>2</sub>	2.18	0.41	0.34	Plagioclase	65.22
Al <sub>2</sub> O <sub>3</sub>	17.93	12.26	12.23	Augite	8.15
Fe <sub>2</sub> O <sub>3</sub>	12.62	7.70	7.64	Magnetite	8.18
MgO	5.19	0.00	-0.01	Ilmenite	2.04
CaO	8.13	0.35	0.36	Apatite	1.31
Na <sub>2</sub> O	3.52	5.32	5.46		
K <sub>2</sub> O	1.15	4.83	5.12		
P <sub>2</sub> O <sub>5</sub>	0.36	0.06	-0.10		
		$\Sigma r^2 = 0.1515$			
Rb	15.9	70.1	103.8		
Sr	649.1	10.5	173.7		
Ba	290.0	15.8	1433.8		
Ni	39.2	8.7	3.9		
Mass of New Magma Relative to Old = 12.90 weight percent					

TABLE XVI. LEAST-SQUARES MASS BALANCE CALCULATION DERIVING COMENDITIC TRACHYTE FROM MUGEARITE.

	<u>Parent</u>	<u>Observed</u> <u>Daughter</u>	<u>Calculated</u> <u>Daughter</u>	<u>Variable</u>	<u>Wt. Fraction</u>
	R-99	R-97			
SiO <sub>2</sub>	55.00	68.04	68.02	Olivine	10.14
TiO <sub>2</sub>	1.71	0.32	0.31	Plagioclase	57.08
Al <sub>2</sub> O <sub>3</sub>	15.71	14.45	14.45	Augite	14.50
Fe <sub>2</sub> O <sub>3</sub>	11.43	4.61	4.60	Magnetite	15.71
MgO	2.69	0.00	0.00	Ilmenite	0.31
CaO	5.76	0.95	0.96	Apatite	2.26
Na <sub>2</sub> O	4.58	6.58	6.58		
K <sub>2</sub> O	2.60	4.98	5.07		
P <sub>2</sub> O <sub>5</sub>	0.52	0.07	0.11		
		$\Sigma r^2 = 0.0101$			
Rb	31.1	78.4	64.3		
Sr	468.7	34.4	517.9		
Ba	663.3	781.8	1204.3		
Ni	10.9	8.9	7.9		
Mass of New Magma Relative to Old = 48.02 weight percent					

TABLE XVII. LEAST-SQUARES MASS BALANCE CALCULATION DERIVING COMENDITE FROM MUGEARITE.

	<u>Parent</u>	<u>Observed</u> <u>Daughter</u>	<u>Calculated</u> <u>Daughter</u>	<u>Variable</u>	<u>Wt. Fraction</u>
	R-99	R-48			
SiO <sub>2</sub>	55.00	69.08	68.89	Olivine	11.89
TiO <sub>2</sub>	1.71	0.41	0.29	Plagioclase	64.60
Al <sub>2</sub> O <sub>3</sub>	15.71	12.26	12.17	Augite	7.30
Fe <sub>2</sub> O <sub>3</sub>	11.43	7.70	7.59	Magnetite	11.07
MgO	2.69	0.00	-0.03	Ilmenite	2.01
CaO	5.76	0.35	0.38	Apatite	3.13
Na <sub>2</sub> O	4.58	5.32	5.84		
K <sub>2</sub> O	2.60	4.83	5.14		
P <sub>2</sub> O <sub>5</sub>	0.52	0.06	-0.22		
		$\Sigma r^2 = 0.5286$			
Rb	31.1	70.1	67.2		
Sr	468.7	10.5	453.8		
Ba	663.3	15.8	1336.8		
Ni	10.9	8.7	8.6		
Mass of New Magma Relative to Old = 44.32 weight percent					

TABLE XVIII. LEAST-SQUARES MASS BALANCE CALCULATION DERIVING COMENDITE FROM COMENDITIC TRACHYTE.

	<u>Parent</u>	<u>Observed Daughter</u>	<u>Calculated Daughter</u>	<u>Variable</u>	<u>Wt. Fraction</u>
	R-97	R-48			
SiO <sub>2</sub>	68.04	69.08	69.07	Anorthoclase	97.80
TiO <sub>2</sub>	0.32	0.41	0.48	Hedenbergite	2.20
Al <sub>2</sub> O <sub>3</sub>	14.45	12.26	11.81		
Fe <sub>2</sub> O <sub>3</sub>	4.61	7.70	7.36		
MgO	0.00	0.00	-0.02		
CaO	0.95	0.35	0.57		
Na <sub>2</sub> O	6.58	5.32	5.54		
K <sub>2</sub> O	4.98	4.83	5.10		
P <sub>2</sub> O <sub>5</sub>	0.07	0.06	0.09		
		$\Sigma r^2 = 0.4973$			
Rb	78.4	70.1	114.9		
Sr	34.4	10.5	26.1		
Ba	781.8	15.8	375.7		
Mass of New Magma Relative to Old = 59.63 weight percent					

TABLE XIX. LEAST-SQUARES MASS BALANCE CALCULATION DERIVING ANAHIM PEAK TRACHYTE FROM ANAHIM PEAK HAWAIIITE.

	<u>Parent</u>	<u>Observed Daughter</u>	<u>Calculated Daughter</u>	<u>Variable</u>	<u>Wt. Fraction</u>
	AP-15	AP-12			
SiO <sub>2</sub>	50.40	61.40	61.39	Olivine	11.17
TiO <sub>2</sub>	2.30	0.64	0.64	Plagioclase	48.01
Al <sub>2</sub> O <sub>3</sub>	16.20	17.33	17.29	Augite	28.33
Fe <sub>2</sub> O <sub>3</sub>	12.86	6.40	6.40	Magnetite	10.66
MgO	4.32	0.56	0.55	Ilmenite	1.79
CaO	8.02	2.83	2.84	Apatite	0.04
Na <sub>2</sub> O	4.16	6.18	6.50		
K <sub>2</sub> O	1.57	4.24	3.99		
P <sub>2</sub> O <sub>5</sub>	0.17	0.42	0.41		
		$\Sigma r^2 = 0.1731$			
Rb	24.9	54.7	58.9		
Sr	568.2	267.9	652.9		
Ba	431.9	1050.9	1050.6		
Ni	47.0	12.6	15.9		
Mass of New Magma Relative to Old = 40.54 weight percent					

REFERENCES

- Abbott, M.J., 1967, Aenigmatite from the groundmass of a peralkaline trachyte. *Amer. Mineralogist* 52, pp. 1895-1901.
- Abbott, M.J., 1969, Petrology of the Nandewar volcano, N.S.W., Australia. *Contrib. Mineral. Petrol.* 20, pp. 115-134.
- Albee, A.L. and Ray, L., 1970, Correction factors for electron microanalysis of silicates, oxides, carbonates, phosphates, and sulfates. *Anal. Chem.* 42, pp. 1408-1414.
- Apland, B., 1977, Reconnaissance survey of the Rainbow Mountains region: west-central British Columbia. Report to National Museum of Canada (in press).
- Armstrong, R.L., Green, N.L., and Watters, B.R., 1977, Sr isotopic study of Late Cenozoic volcanic rocks of the Canadian Cordillera (abst.). *Geol. Assoc. of Canada Prog. with Abst.* 2, p. 5.
- Artemov, Y.M. and Yaroshevskiy, A.A., 1965, The isotopic composition of strontium as an indicator of character and duration of magmatic differentiation. *Geochem. Internat.* 2, pp. 810-813.
- Arth, J.G., 1976, Behavior of trace elements during magmatic processes - a summary of theoretical models and their applications. *J. Res. U.S. Geol. Surv.* 4, pp. 41-47.
- Baer, A.J., 1973, Bella Coola - Laredo Sound map-areas, British Columbia. *Geol. Surv. Can. Mem.* 372, 122 p.
- Bailey, D.K., 1973, Trachytes and feldspar fractionation: a simple phillipic (abst.). *J. Geol. Soc. London Proc.* 129, p. 649.
- Bailey, D.K., 1974, Experimental petrology related to oversaturated peralkaline volcanics: a review. *Bull. Volc.* 38, pp. 637-652.
- Bailey, D.K., Cooper, J.P., Knight, J.L., 1974, Anhydrous melting and crystallization of peralkaline obsidians. *Bull. Volc.* 38, pp. 653-665.
- Bailey, D.K. and Macdonald, R., 1969, Alkali feldspar fractionation trends and the derivation of peralkaline liquids. *Amer. J. Sci.* 267, pp. 242-248.
- Bailey, D.K. and Macdonald, R., 1970, Petrochemical variations among mildly peralkaline (comendite) obsidians from the oceans and continents. *Contrib. Mineral. Petrol.* 28, pp. 340-351.
- Bailey, D.K. and Macdonald, R., 1975, Fluorine and chlorine in peralkaline liquids and the need for magma generation in an open system. *Mineralog. Mag.* 40, pp. 405-414.
- Bailey, D.K. and Schairer, J.F., 1964, Feldspar - liquid equilibria in peralkaline liquids - the orthoclase effect. *Amer. J. Sci.* 262, pp. 1198-1206.

- Bailey, D.K. and Schairer, J.F., 1966, The system  $\text{Na}_2\text{O}-\text{Al}_2\text{O}_3-\text{Fe}_2\text{O}_3-\text{SiO}_2$  at 1 atmosphere, and the petrogenesis of alkaline rocks. *J. Petrol.* 7, pp. 114-170.
- Bailey, D.K., Weaver, S.D., and Sutherland, D.S., 1975, Eburru volcano: a re-appraisal of the previous sample population. *Contrib. Mineral. Petrol.* 50, pp. 47-48.
- Barberi, F., Borsi, S., Ferrari, G., and Innocenti, F., 1969, Strontium isotopic composition of some recent basic volcanites of the southern Tyrrhenian Sea and Sicily Channel. *Contrib. Mineral. Petrol.* 23, pp. 157-172.
- Barberi, F., Santacroce, R., Ferrara, G., Treuil, M., and Varet, J., 1975, A transitional basalt - pantellerite sequence of fractional crystallization, the Boina Centre (Afar Rift, Ethiopia). *J. Petrol.* 16, pp. 22-56.
- Barberi, F., and Varet, J., 1970, The Erta Ale volcanic range (Danakil depression, northern Afar, Ethiopia). *Bull. Volc.* 34, pp. 848-917.
- Barker, D.S., 1977, Northern Trans-Pecos magmatic province: Introduction and comparison with the Kenya rift. *Geol. Soc. Amer. Bull.* 88, pp. 1421-1427.
- Barker, D.S., and Hodges, F.N., 1977, Mineralogy of intrusions in the Diablo Plateau, northern Trans-Pecos magmatic province, Texas and New Mexico. *Geol. Soc. Amer. Bull.* 88, pp. 1428-1436.
- Barker, D.S., Long, L.E., Hoops, G.K., and Hodges, F.N., 1977, Petrology and Rb-Sr isotope geochemistry of intrusions in the Diablo Plateau, northern Trans-Pecos magmatic province, Texas and New Mexico. *Geol. Soc. Amer. Bull.* 88, pp. 1437-1446.
- Barr, S.M., and Chase, R.L., 1974, Geology of the northern end of the Juan de Fuca ridge and sea-floor spreading. *Can. J. Earth Sci.* 11, p. 1384-1406.
- Barth, T.F.W., 1962, Theoretical petrology. John Wiley and Sons, Inc., New York, 416 p.
- Becker, S.W., 1976, Field relations and petrology of the Burro Mesa "Riebeckite" Rhyolite, Big Bend National Park, Texas. Unpublished M.S. Thesis, University of California, Santa Cruz, 116 p.
- Bence, A.E., and Albee, A.L., 1968, Empirical correction factors for the electron micro-analysis of silicates and oxides. *J. Geol.* 76, pp. 382-403.
- Binns, R.A., Duggan, M.B., Wilkinson, J.F.G., and Kalocsai, G.I.Z., 1970, High pressure megacrysts in alkaline lavas from the northeastern New South Wales. *Amer. J. Sci.* 269, pp. 132-168.
- Bottinga, Y. and Weill, D.F., 1972, The viscosity of silicate liquids: a model for calculation. *Amer. J. Sci.* 272, pp. 438-475.

- Boyd, F.R., and England, J.L., 1960, Minerals of the mantle. Carnegie Inst. Wash. Year Book 59, pp. 47-52.
- Boyd, F.R., and England, J.L., 1963, Some effects of pressure on phase relations in the system MgO-Al<sub>2</sub>O<sub>3</sub>-SiO<sub>2</sub>. Carnegie Inst. Wash. Year Book 62, pp. 121-124.
- Bowen, N.L., 1945, Phase equilibria bearing on the origin and differentiation of the alkaline rocks. Amer. J. Sci. 243-A, pp. 75-89.
- Bryan, W.B., 1976, A basalt-pantellerite association from Isla Socorro, Islas Revillagigedo, Mexico. in: Volcanoes and Tectosphere, Aoki, H. and Iizuka, S., ed., Tokai University Press, pp. 75-91.
- Bryan, W.B., Finger, L.W., and Chayes, F., 1969, Estimating proportions in petrographic mixing equations by least squares approximation. Science 163, pp. 926-927.
- Buddington, A.F., and Lindsley, D.H., 1964, Iron-titanium oxide minerals and synthetic equivalents. J. Petrol. 5, pp. 310-357.
- Cannillo, E., Mazzi, F., Fang, J.H., Robinson, P.D., and Ohya, Y., 1971, The crystal structure of aenigmatite. Amer. Mineral. 56, pp. 427-446.
- Carman, M.F., Cameron, M., Gunn, B., Cameron, K.L., and Butler, J.C., 1975, Petrology of Rattlesnake Mountain Sill, Big Bend National Park, Texas. Geol. Soc. Amer. Bull. 86, pp. 177-193.
- Carmichael, I.S.E., 1962, Pantelleritic liquids and their phenocrysts. Mineral. Mag. 33, pp. 86-113.
- Carmichael, I.S.E., 1967, The iron-titanium oxides of salic volcanic rocks and their associated ferromagnesian silicates. Contrib. Mineral. Petrol. 14, pp. 36-64.
- Carmichael, I.S.E., and MacKenzie, W.S., 1963, Feldspar-liquid equilibria in pantellerites: an experimental study. Amer. J. Sci. 261, pp. 382-396.
- Carmichael, I.S.E., Turner, F.J., Verhoogen, J., 1974, Igneous Petrology. McGraw-Hill, Inc., New York, 739 p.
- Chase, R.L., Tiffin, D.L., and Murray, J.W., 1975, The western Canada continental margin. in: Canada's Continental Margins and Offshore Petroleum Exploration, Yorath, C.J., Parker, E.R., and Glass, D.J., ed., Can. Soc. Petrol. Geol. Mem. 4, pp. 701-721.
- Cox, K.G., Gass, I.G., and Mallick, D.I.J., 1970, The peralkaline volcanic suite of Aden and Little Aden, South Arabia. J. Petrol. 11, pp. 433-461.
- Drake, M.J., and Weill, D.F., 1975, Partition of Sr, Ba, Ca, Y, Eu<sup>2+</sup>, Eu<sup>3+</sup>, and other REE between plagioclase feldspar and magmatic liquid: an experimental study. Geochim. Cosmochim. Acta 39, pp. 689-712.

- Ernst, W.G., 1962, Synthesis, stability relations, and occurrence of riebeckite relations, and occurrence of riebeckite and riebeckite-arfvedsonite solid solutions. *J. Geol.* 70, pp. 689-736.
- Eugster, H.P., and Wones, D.R., 1962, Stability relation of the ferruginous biotite, annite. *J. Petrol.* 3, pp. 82-125.
- Ewart, A., Mateen, A., and Ross, J.A., 1976, Review of mineralogy and chemistry of Tertiary central volcanic complexes in southeast Queensland and northeast New South Wales. in: *Volcanism in Australasia*, R.W. Johnson, ed., Elsevier, New York, pp. 21-39.
- Ewart, A., Taylor, S.R., and Capp, A.C., 1968, Geochemistry of the pantellerites of Mayor Island, New Zealand. *Contrib. Mineral. Petrol.* 17, pp. 116-140.
- Ferrara, G., and Treuil, M., 1974, Petrological implications of trace element and Sr isotope distributions in basalt-pantellerite series. *Bull. Volc.* 38, pp. 548-574.
- Fiesinger, D.W. and Nicholls, J., 1977, Petrography and petrology of Quaternary volcanic rocks, Quesnel Lake region, east-central British Columbia. in: *Volcanic Regimes in Canada*, Baragar, W.R.A., Coleman, L.C., Hall, J.M., ed., *Geol. Assoc. Can. Spec. Paper* 16, pp. 25-38.
- Gass, I.G., and Mallick, D.I.J., 1968, Jebel Khariz: an upper Miocene stratovolcano of comenditic affinity on the south Arabian coast. *Bull. Volc.* 32, pp. 33-88.
- Gast, P.W., 1968, Trace element fractionation and the origin of tholeiitic and alkaline magma types. *Geochim. Cosmochim. Acta* 32, pp. 1057-1086.
- Green, D.H. and Hibberson, W.D., 1970, Experimental duplication of conditions of precipitation of high-pressure phenocrysts in a basaltic magma. *Phys. Earth Planet. Interiors* 3, pp. 247-254.
- Green, D.H., and Ringwood, A.E., 1967, The genesis of basaltic magmas. *Contrib. Mineral. Petrol.* 15, pp. 103-190.
- Green, N.L., 1977, Multistage andesite genesis in the Garibaldi Lake area, southwestern British Columbia. Unpublished Ph.D. Thesis, University of British Columbia, 246 p.
- Hawkins, J.W.Jr., and Natland, J.H., 1975, Nephelinites and basanites of the Samoan linear volcanic chain: their possible tectonic significance. *Earth Planet. Sci. Lett.* 24, pp. 427-439.
- Hirayama, C., and Camp, F.E., 1969, The effect of fluorine and chlorine substitution on the viscosity and fining of soda-lime and potassium-barium glass. *Glass Tech.* 10, pp. 123-127.
- Irvine, T.N., and Baragar, W.R.A., 1971, A guide to the chemical classification of the common volcanic rocks. *Can. J. Earth Sci.* 8, 523-548.

- Irving, A.J., 1974, Megacrysts from the Newer basalts and other basaltic rocks of southeastern Australia. *Geol. Soc. Amer. Bull.* 85, pp. 1503-1514.
- Korringa, M., and Noble, D.C., 1972, Genetic significance of chemical, isotopic, and petrographic features of some peralkaline salic rocks from the island of Pantelleria. *Earth Planet. Sci. Lett.* 17, pp. 258-262.
- Lacroix, A., 1927, Les rhyolites et les trachytes hyperalcalins quartzifères, à propos de ceux de la Corée. *Compt. Rend. Acad. Sci. Paris* 185, pp. 1410-1415.
- Larsen, L.M., 1976, Clinopyroxenes and coexisting mafic minerals from the alkaline Ilimaussag intrusion, South Greenland. *J. Petrol.* 17, pp. 258-290.
- Lindsley, D.H., 1971, Synthesis and preliminary results on the stability of aenigmatite ( $\text{Na}_2\text{Fe}_5\text{TiSi}_6\text{O}_{20}$ ). *Carnegie Inst. Wash. Year Book* 69, pp. 188-190.
- Lindsley, D.H., Haggerty, S.E., and Smith, D., 1971, Petrography and mineral chemistry of a differentiated flow of Picture Gorge basalt near Spray, Oregon. *Carnegie Inst. Wash. Year Book* 69, pp. 264-285.
- Lipman, P.W., 1965, Chemical comparison of glassy and crystalline volcanic rocks. *U.S. Geol. Surv. Bull.* 1201-D, pp. D1-D24.
- Macdonald, R., 1974, Nomenclature and petrochemistry of the peralkaline oversaturated extrusive rocks. *Bull. Volc.* 38, pp. 498-516.
- Macdonald, R. and Bailey, D.K., 1973, Data of geochemistry, Sixth Ed. Ch. N. *Chemistry of Igneous Rocks. Part 1. The chemistry of the peralkaline oversaturated obsidians.* *U.S. Geol. Surv. Prof. Paper* 440-N-1, pp. N1-N37.
- Marsh, J.S., 1975, Aenigmatite stability in silica-undersaturated rocks. *Contrib. Mineral. Petrol.* 50, pp. 135-144.
- Martin, R.F., 1974, Role of water in pantellerite genesis. *Bull. Volc.* 38, pp. 666-679.
- Minster, J.B., Jordan, T.H., Molnar, P., and Haines, E., 1974, Numerical modelling of instantaneous plate tectonics. *Geophys. Jour. R. Astr. Soc.* 36, pp. 541-576.
- Murase, T., and McBirney, A.R., 1973, Properties of some common igneous rocks and their melts at high temperatures. *Geol. Soc. Amer. Bull.* 84, pp. 3563-3592.
- Nash, W.P., Carmichael, I.S.E., Johnson, R.W., 1969, The mineralogy and petrology of Mount Suswa, Kenya. *J. Petrol.* 10, pp. 409-439.
- Nicholls, J., and Carmichael, I.S.E., 1969, Peralkaline acid liquids: a petrological study. *Contr. Mineral. Petrol.* 20, pp. 268-294.

- Nicholls, J., Stout, M.Z., and Ghent, E.D., 1976, Petrology of basanite and trachybasalt lavas, western British Columbia, Canada (abst.). EOS, Trans. Amer. Geophys. Union 57, p. 1018.
- Noble, D.C., 1965, Gold Flat Member of the Thirsty Canyon Tuff - a pantellerite ash-flow sheet in southern Nevada. U.S. Geol. Surv. Prof. Paper 525-B, pp. B85-B90.
- Noble, D.C., 1966, Comenditic volcanic rocks in the western United States (abst.). Geol. Soc. Amer. Spec. Paper 87, pp. 117-118.
- Noble, D.C., 1968, Systematic variation of major elements in comendite and pantellerite glasses. Earth Planet. Sci. Lett. 4, pp. 167-172.
- Noble, D.C., 1970, Loss of sodium from crystallized comendite welded tuffs of the Miocene Grouse Canyon Member of the Belted Range Tuff, Nevada. Geol. Soc. Amer. Bull. 81, pp. 2677-2688.
- Noble, D.C., and Haffty, J., 1969, Minor-element and revised major-element contents of some Mediterranean pantellerites and comendites. J. Petrol. 10, pp. 502-509.
- Noble, D.C., Haffty, J., and Hedge, C.E., 1969, Strontium and magnesium contents of some natural peralkaline silicic glasses and their petrogenetic significance. Amer. J. Sci. 267, pp. 598-608.
- Noble, D.C., and Hedge, C.E., 1969,  $^{87}\text{Sr}/^{86}\text{Sr}$  variations within individual ash-flow sheets. U.S. Geol. Surv. Prof. Paper 650C, pp. C133-C139.
- Noble, D.C., Smith, V.C., Peck, L.C., 1967, Loss of halogens from crystallized and glassy silicic volcanic rocks. Geochim. Cosmochim. Acta 31, pp. 215-223.
- Nockolds, S.R., 1954, Average chemical compositions of some igneous rocks. Geol. Soc. Amer. Bull. 65, pp. 1007-1032.
- Norrish, K., and Hutton, J.T., 1969, An accurate x-ray spectrographic method for the analysis of a wide range of geological samples. Geochim. Cosmochim. Acta 33, pp. 431-453.
- Orville, P.M., 1963, Alkali ion exchange between vapor and feldspar phases. Amer. J. Sci. 261, pp. 201-237.
- Papike, J.J., Cameron, K.L., and Baldwin, K., 1974, Amphiboles and pyroxenes: characterization of other than quadrilateral components and estimation of ferric iron from microprobe data. Geol. Soc. Amer. Abst. with Prog. 6, pp. 1053-1054.
- Riddihough, R.P., 1977, A model for recent plate interactions off Canada's west coast. Can. J. Earth Sci. 14, pp. 384-396.
- Riddihough, R.P. and Hyndman, R.D., 1976, Canada's active western margin - the case for subduction. Geoscience Canada 3, pp. 269-278.

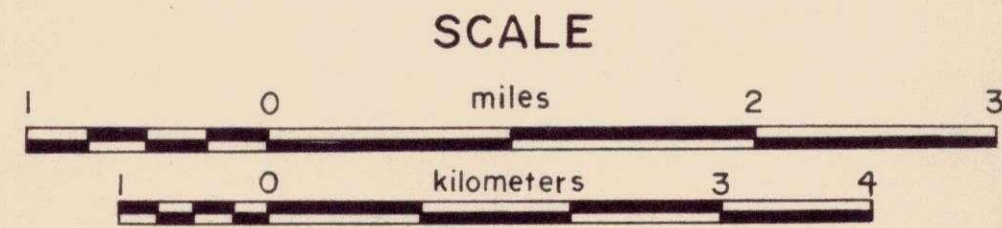
- Ringwood, A.E., 1955, The principles governing trace element behavior during magmatic crystallization, Part II: The role of complex formation. *Geochim. Cosmochim. Acta* 7, pp. 242-254.
- Ringwood, A.E., 1975, Composition and petrology of the earth's mantle. McGraw-Hill, Inc., New York, 618 p.
- Roux, J., and Varet, J., 1975, Alkali feldspar liquid equilibrium relationships in peralkaline oversaturated systems and volcanic rocks. *Contrib. Mineral. Petrol.* 49, pp. 67-81.
- Scarfe, C.M., 1977, Viscosity of a pantellerite melt at one atmosphere. *Can. Mineral.* 15, pp. 185-189.
- Schmincke, H.-U., 1974, Volcanological aspects of peralkaline silicic welded ash-flow tuffs. *Bull. Volc.* 38, pp. 594-636.
- Schmincke, H.-U., and Swanson, D.A., 1967, Laminar viscous flowage structures in ash-flow tuffs from Gran Canaria, Canary Islands. *J. Geol.* 75, pp. 641-664.
- Self, S., and Gunn, B.M., 1976, Petrology, volume, and age relations of alkaline and saturated peralkaline volcanics from Terceira, Azores. *Contrib. Mineral. Petrol.* 54, pp. 293-313.
- Shand, H.S., 1951, Eruptive rocks, 4th ed. John Wiley and Sons, New York, 488 p.
- Shaw, H.R., 1963, Obsidian-H<sub>2</sub>O viscosities at 1000 and 2000 bars in the temperature range 700°-900°C. *J. Geophys. Res.* 68, pp. 6337-6343.
- Shaw, H.R., 1965, Comments on viscosity, crystal settling, and convection in granitic magmas. *Amer. J. Sci.* 263, pp. 120-152.
- Shaw, H.R., 1969, Rheology of basalt in the melting range. *J. Petrol.* 10, pp. 510-535.
- Shaw, H.R., 1972, Viscosities of magmatic silicate liquids: an empirical method of prediction. *Amer. J. Sci.* 272, pp. 870-893.
- Shaw, H.R., Wright, T.L., Peck, D.L., and Okamura, R., 1969, The viscosity of basaltic magma: an analysis of field measurements in Makaopuhi lava lake, Hawaii. *Amer. J. Sci.* 266, pp. 225-264.
- Souther, J.G., 1970, Volcanism and its relationship to recent crustal movements in the Canadian Cordillera. *Can. J. Earth Sci.* 7, pp. 553-568.
- Souther, J.G., 1977, Volcanism and tectonic environments in the Canadian Cordillera - a second look. in: *Volcanic Regimes in Canada*, Baragar, W.R.A., Coleman, L.C., Hall, J.M., ed., *Geol. Assoc. Can. Spec. Paper* 16, pp. 3-24.
- Souther, J.G., 1977, Late Cenozoic volcanism and tectonics of the west central Cordillera of North America. *Geol. Soc. Amer. Abst. with Prog.* 9, p. 1185.

- Souther, J.G., and Symons, D.T.A., 1974, Stratigraphy and paleomagnetism of Mount Edziza volcanic complex, northwestern British Columbia. Geol. Surv. Can. Paper 73-32, 48 p.
- Sutherland, D.S., 1974, Petrography and mineralogy of the peralkaline silicic rocks. Bull. Volc. 38, pp. 517-547.
- Thompson, R.N., Esson, J., and Dunham, A.C., 1972, Major element chemical variation in the Eocene lavas of the Isle of Skye, Scotland. J. Petrol. 13, pp. 219-253.
- Thompson, R.N., and MacKenzie, W.S., 1967, Feldspar-liquid equilibria in peralkaline acid liquids. Amer. J. Sci. 265, pp. 714-734.
- Thornton, C.P., and Tuttle, O.F., 1960, Chemistry of igneous rocks: I. Differentiation Index. Amer. J. Sci. 258, pp. 664-684.
- Tipper, H.W., 1957, Anahim Lake Map-area. Geol. Surv. Can. Map 10-1957.
- Tipper, H.W., 1963, Taseko Lakes Map-area. Geol. Surv. Can. Map 29-1963.
- Tipper, H.W., 1969, Anahim Lake Map-area, British Columbia. Geol. Surv. Can. Map 1202A.
- Troll, G. and Gilbert, M.C., 1974, Stability of fluorine tremolite (abst.). Trans. Amer. Geophys. Union 55, p. 481.
- Villari, L., 1970, Studio petrologico di alcuni campioni dei pozzi Bagno dele'Acqua e Gadir (Isola di Pantelleria). Rend. Soc. It. Miner. Petr. 26, pp. 353-376.
- Walker, G.W., and Swanson, D.A., 1968, Laminar flowage in a Pliocene soda rhyolite ash-flow tuff, Lake and Harney Counties, Oregon. U.S. Geol. Surv. Prof. Paper 600-B, pp. B37-B47.
- Watters, B.R., 1976, XRF Manual, Part II. Department of Geological Sciences, University of British Columbia, Vancouver, Canada.
- Webb, P.K., and Weaver, S.D., 1975, Trachyte shield volcanoes: a new volcanic form from South Turkana, Kenya. Bull. Volc. 39, pp. 294-312.
- Wones, D.R., and Gilbert, M.C., 1968, The stability of fayalite. Ann. Rept. Geophys. Lab. Yearbook 66, pp. 402-403.
- Yagi, K., and Souther, J.G., 1974, Aenigmatite from Mt. Edziza, British Columbia, Canada. Amer. Mineralogist 59, pp. 820-829.
- Yoder, H.S., 1973, Contemporaneous basaltic and rhyolitic magmas. Amer. Mineralogist 58, pp. 153-171.
- York, D., 1967, The best isochron. Earth Planet. Sci. Lett. 2, pp. 479-482.

LE 3  
B7  
1978  
A67  
B49  
C-1

# PLATE I. GEOLOGY OF THE NORTH FLANK OF THE RAINBOW RANGE AND ANAHIM PEAK, BRITISH COLUMBIA

Geology by M.L. Bevier, 1976

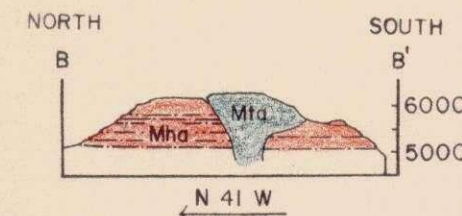
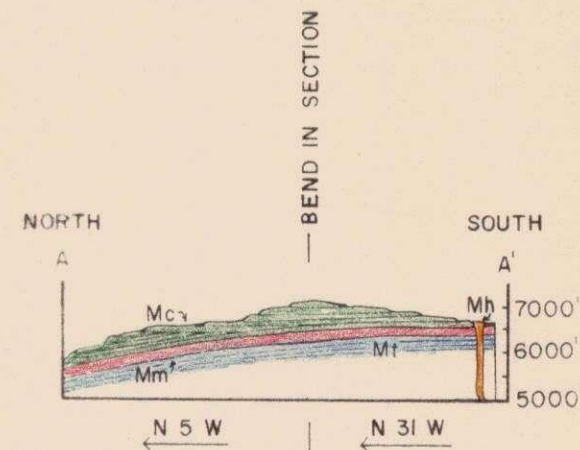
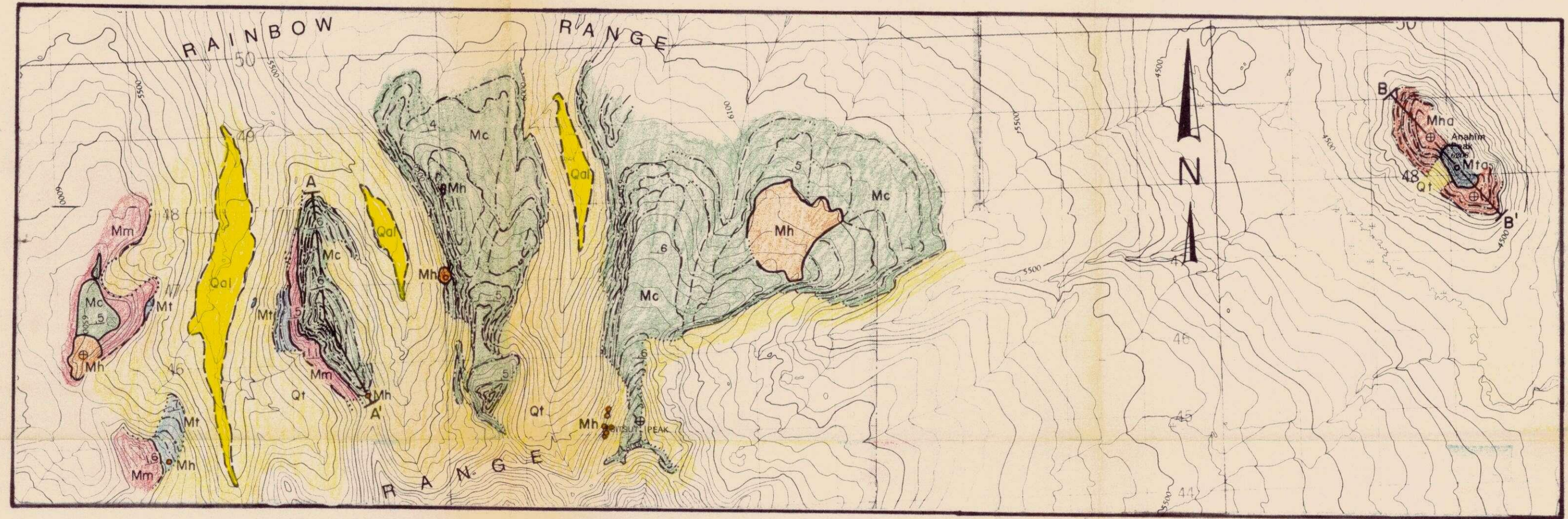


**LEGEND**

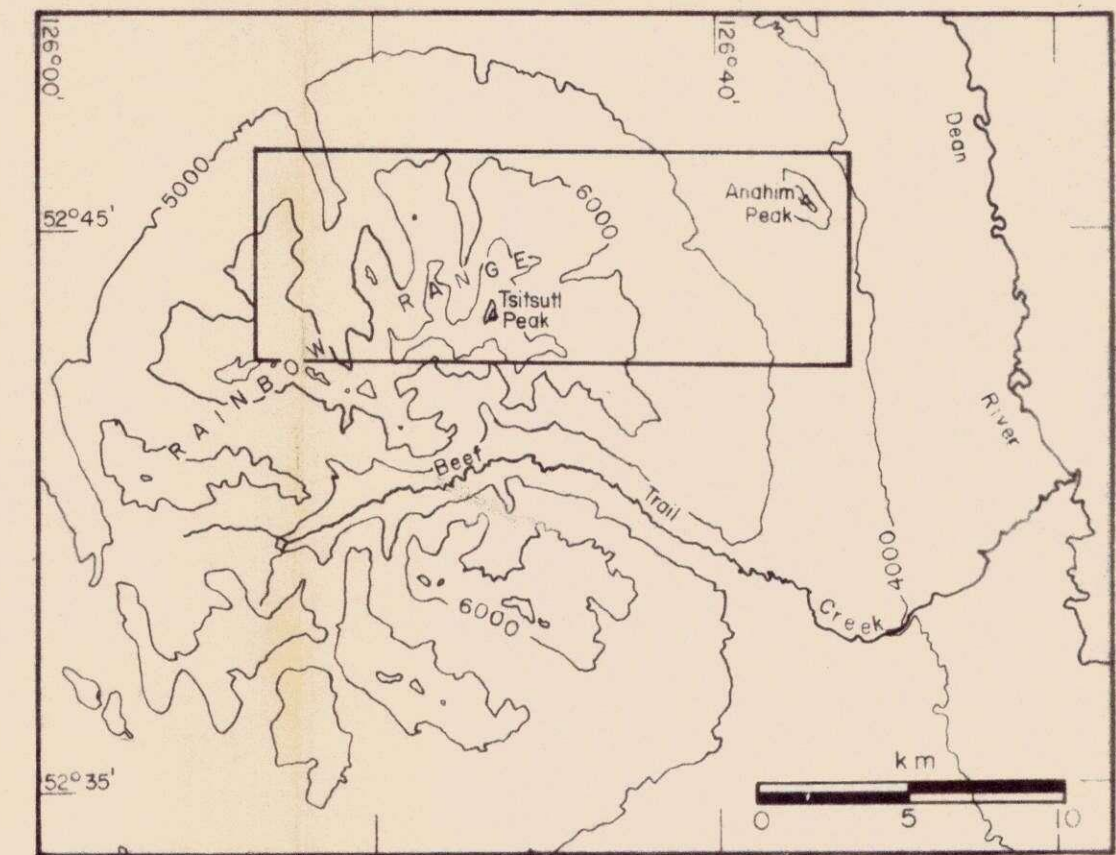
- QUATERNARY**
- Qal** Alluvium, till
  - Qt** Talus, snowfields
- Late Miocene**
- Mta** Trachyte of Anahim Peak
  - Mha** Hawaiiite of Anahim Peak
- TERTIARY**
- Mh** Hawaiiite Unit
  - Mc** Comendite Unit
  - Mm** Mugearite Unit
  - Mt** Comenditic Trachyte Unit

**SYMBOLS**

- Lithologic contact (defined, approximate, inferred)
- Contact between flows (not shown in Mm)
- Bedding (inclined, vertical, horizontal)
- Hawaiiite vent



**INDEX MAP**



LE3  
B7  
1978  
A67  
B49  
C-1

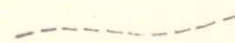
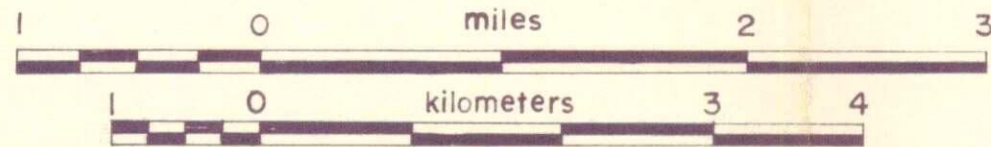
# PLATE II. MAP OF SAMPLE LOCALITIES

Geologic units colored as in Plate I.

Lithologic contact  
(defined, approximate, inferred)

23● Sample locality (Prefixes R-  
and AP-not shown on map)

SCALE



Limits of outcrop area

